ABSTRACT

Title of Dissertation: CHARACTERIZATION OF TOBACCO MOSAIC VIRUS DIRECTED REPROGRAMMING OF PHLOEM GENE EXPRESSION TO PROMOTE VIRAL PHLOEM LOADING AND SYSTMEIC MOVEMENT

Tamara Diane Collum
Doctor of Philosophy, 2016

Dissertation directed by: Dr. James N. Culver
Department of Plant Science and Landscape Architecture

Vascular phloem loading has long been recognized as an essential step in the establishment of a systemic virus infection. Yet little is known about this process and the mechanisms that control it. In this study, an interaction between the replication protein of *Tobacco mosaic virus* (TMV) and phloem specific auxin/indole acetic acid (Aux/IAA) transcriptional regulators was found to modulate virus phloem loading. Promoter expression studies show TMV 126/183 kDa interacting Aux/IAAs predominantly express and accumulate within the nuclei of phloem companion cells (CC). Furthermore, CC Aux/IAA nuclear localization is disrupted upon infection

with an interacting virus but not during infection with a non-interacting virus. *In situ* analysis of virus spread shows the inability of TMV variants to disrupt Aux/IAA CC nuclear localization correlates with a reduced ability to load into the vascular tissue. Subsequent systemic movement assays also demonstrate that a virus capable of disrupting Aux/IAA localization is significantly more competitive at systemic movement than a non-interacting virus. Similarly, CC expression and over-accumulation of a degradation-resistant-interacting Aux/IAA protein was found to selectively inhibit TMV accumulation and phloem loading. Transcriptional expression studies demonstrate a role for interacting Aux/IAA proteins in the regulation of salicylic acid and jasmonic acid dependent host defense responses as well as virus specific movement factors including pectin methylesterase that are involved in regulating plasmodesmata size exclusion limits and promoting virus cell-to-cell movement. Further characterization of the phloem environment was done using two phloem specific promoters (pSUC2 and pSULTR2;2) to generate epitope-tagged polysomal-RNA complexes. Immuno-purification using the epitope tag allowed us to obtain mRNAs bound to polysomes (the translatome) specifically in phloem tissue. We found the phloem translatome is uniquely altered during TMV infection with 90% and 88% of genes down regulated in the pSUC2 and pSULTR2;2 phloem translatomes, compared to 31% of genes down regulated in the whole plant p35S translatome. Transcripts down regulated in phloem include genes involved in callose deposition at plasmodesmata, host defense responses, and RNA silencing. Combined, these findings indicate TMV reprograms gene expression within the vascular phloem as a means to enhance phloem loading and systemic spread.

CHARACTERIZATION OF TOBACCO MOSAIC VIRUS DIRECTED REPROGRAMMING OF PHLOEM GENE EXPRESSION TO PROMOTE VIRAL PHLOEM LOADING AND SYSTMEIC MOVEMENT

by

Tamara Diane Collum

Dissertation submitted to the Faculty of the Graduate School of the
University of Maryland, College Park, in partial fulfillment
of the requirements for the degree of
Doctor of Philosophy
2016

Advisory Committee:
Professor James N. Culver, Chair
Dr. Chris Dardick
Professor Siba Samal
Professor Anne Simon
Dr. Shunyuan Xiao

Dedication

I would like to dedicate this work to my husband, Jonathan. Thank you for all your love, encouragement and support throughout my research career.

Acknowledgements

I would like to thank my advisor, Dr. Jim Culver, who has been a great mentor. I am thankful for his support and guidance though out my research. He was always available when I needed him and I thank him for his investment in my professional growth. I thank my committee members who have been helpful and encouraging throughout the years. They have provided me with ideas for experiments and constructive criticisms, which allowed me to improve both my research and scientific communication skills.

I would like to thank the past and present lab members of the Culver lab for all their help and support throughout my time in the lab. Thank you to Meenu Padamanabhan who began to characterize the interaction between TMV and IAA26. She created the pIAA26:GUS plant lines used in my research and set the foundation for much of my project. Thank you to Yi-Chen Hsieh for his contribution to this project and providing the images shown in Fig. 2.6B. Thank to you to Adam Brown and Rena Shimizu for the camaraderie and all the times you helped me keep my experiments going by watering my plants. Thank you to Xiao Wang and Sabrina Krammer who provided a lot of help and guidance training me when I first joined the lab.

Special thanks to my family. My parents have always supported and encouraged me in all that I do. Thank you to my husband, Jonathan who has been with me through all the ups and downs of graduate student life.

Table of Contents

List of Tables

List of Figures

List of Abbreviations

ABA	Abscisic Acid
ARF	Auxin Responsive Factor
ARR	Age-Related Resistance
Aux	Auxin
Aux/IAA	Auxin/Indole Acetic Acid
AuxRE	Auxin Responsive Element
BP	Base Pair
BR	Brassinosteroids
BTH	benzothiadiazole S-methylester
CaMV	*Cauliflower mosaic virus*
CC	Companion Cell
cDNA	Complementary DNA
CgCP	Coat Protein from crucifer-infecting TMV
CK	Cytokinin
CP	Coat Protein
dRNA	Defective RNA
ER	Endoplasmic Reticulum
Et	Ethylene
GA	Gibberellin
GFP	Green Fluorescent Protein
GRP	Glycine-Rich Protein
GUS	*β*-glucuronidase

HEL	Helicase
HR	Hypersensitive Response
IR	Intervening Region
JA	Jasmonic Acid
MP	Movement Protein
MT	Methyltransferase
OAS	Origin of Assembly
ORF	Open Reading Frame
PD	Plasmodesmata
PNRSV	*Prunus necrotic ringspot virus*
PPU	Plasmodesmata Pore Unit
POL	Polymerase
PPV	*Plum pox virus*
PVX	*Potato virus X*
R	Resistance
RDV	*Rice dwarf virus*
RF	Replicative Form
RI	Replicative Intermediate
RSS	RNA Silencing Suppressor
SA	Salicylic Acid
SAR	Systemic Acquired Resistance
SE	Sieve Element
SEL	Size Exclusion Limit

TLS	t-RNA Like Structure
TMGMV	*Tobacco mild green mosaic virus*
TMGMV	*Tobacco mild green mosaic virus*
TMV	*Tobacco mosaic virus*
TOM1	Tobamovirus multiplication 1
ToMV	*Tomato mosaic virus*
ToRSV	*Tomato ringspot virus*
TRV	*Tobacco rattle virus*
TuMV	*Turnip mosaic virus*
TVCV	*Turnip vein clearing virus*
UTR	Untranslated Region
VRC	Viral Replication Complex
vRNA	Viral RNA
vRNP	Viral RNA-Protein Complex

Chapter 1: General Introduction

1.1 Rationale and Significance

Plant viruses are responsible for huge losses in crop production and quality throughout the world (1, 2). For example, *Plum pox virus* (PPV) causes Sharka disease which has devastated stone fruit crops (3). The combined costs of Sharka disease and control efforts have been more than 10 billion dollars over the past 30 years worldwide (4). In East and Central Africa, *African cassava mosaic virus* and related species have caused severe hardship with annual losses estimated at 1.9 to 2.7 billion dollars (2). Viruses are obligate parasites that rely on a host to survive. Viral-host interactions contribute to viral replication, spread and the development of disease. Understanding how viruses interact with their hosts is essential for the development of viral control strategies to protect crops.

To establish disease, a plant virus must spread from the initially infected cell and gain access to vascular tissues to reach distal areas of the plant. The vast majority of plant viruses travel systemically through the vascular phloem, with a few rare exceptions traveling in the xylem (5-7). Unfortunately, little is known about the molecular mechanisms involved in viral phloem loading or the host components and gene networks that contribute to this process. This lack of knowledge is partially due to the technical difficultly of many phloem sampling techniques. For example, methods such as collecting phloem exudate from insect stylets and phloem bleeding can be challenging, and are also likely to introduce contaminants (8).

The goal of this study is to use a model virus, *Tobacco mosaic virus* (TMV), to identify host genes and pathways involved in phloem loading and viral systemic movement. Specifically, cell biology and transcriptome studies have been used to characterize an interaction between TMV and host phloem expressed transcriptional regulators. Additionally, a new phloem sampling technique relying on the immunopurificaiton of tagged ribosomes was used to characterize alterations to the phloem translatome in response to TMV infection. The identification of host factors and gene pathways involved in viral phloem loading and viral systemic movement provides greater insight into this important pathway in plants and provides new targets for viral control strategies.

1.2 Tobacco Mosaic Virus

TMV is the type member of the genus Tobamovirus (9) and was the first infectious agent identified as a virus (10). TMV has a wide host range including tobacco, tomato and pepper (11). TMV infection can result in disease symptoms including mosaic, mottling, necrosis, stunting, leaf curling, yellowing and plant death (Fig. 1.1) (12). In tomato, TMV infection can also result in poor yield or distorted fruits. Since its discovery TMV has been studied extensively as a model plant virus. The TMV genome has been characterized (13), full length infectious cDNA clones are available (14), and there is high-resolution crystallographic data on the TMV virion structure (15). Additionally, a great deal is known about TMV biology and replication strategies (16-20). These properties make TMV an ideal system to study long distance viral movement through the vascular phloem.

1.2.1 Genome Characteristics

TMV has a monopartite single-stranded positive sense RNA genome. The genome is 6395 nucleotides long and encodes for at least four proteins - two viral replication proteins (126 and 183 kDa), a 30 kDa movement protein (MP) and a 17.5 kDa coat protein (CP) (13) (Fig 1.2). The 5′ end of the genome has a methyl guanosine cap and the 3′ terminus folds into a t-RNA like structure (TLS) (21-23). Both the 5′ and 3′ untranslated regions (UTRs) are required for viral replication (24, 25). The 5′ UTR, also called omega (Ω), is 68 nucleotides long and acts as a translation enhancer (24, 26). The host heat shock protein HSP101 binds the Ω sequence, which ultimately leads to the recruitment of eukaryotic translation initiation factor 4F (eIF4F) for efficient translation (27, 28).

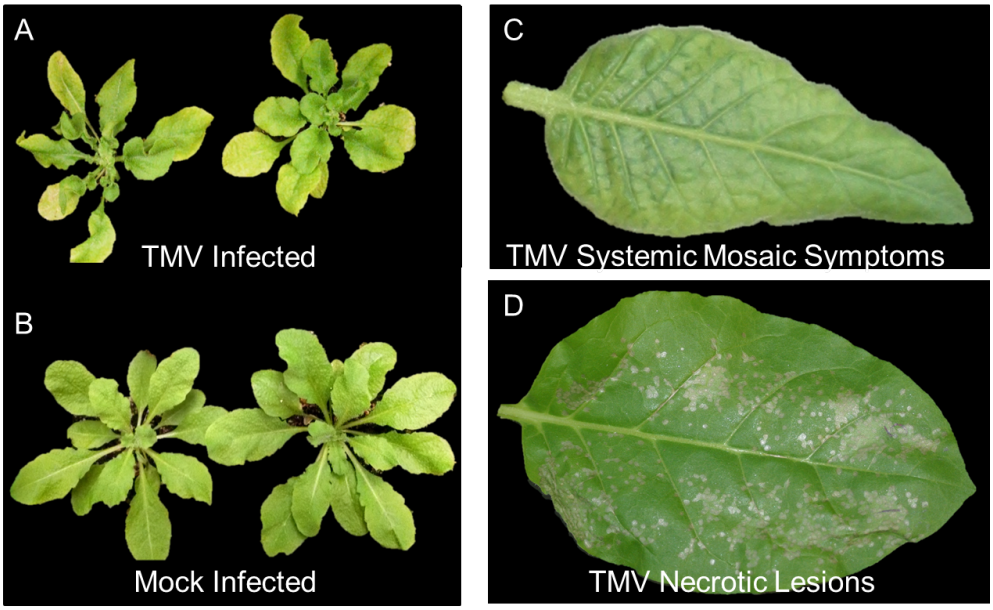

Fig. 1.1. TMV Disease Symptoms. *A. thaliana* ecotype Shahdara infected with TMV (A) or mock infected (B). (C) Systemic mosaic disease symptoms in permissive tobacco. (D) Necrotic lesions in *N* gene resistant tobacco.

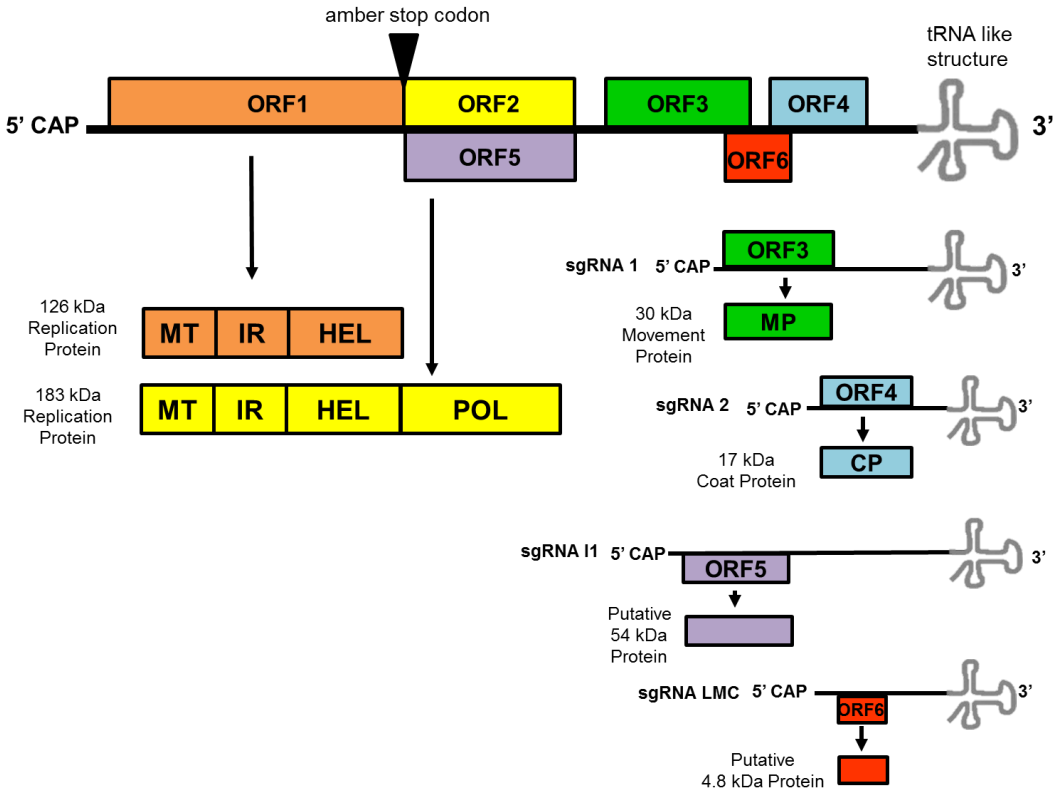

Fig. 1.2. TMV Genome Organization. TMV has a single stranded RNA genome with a 5' cap and 3' tRNA like structure. The genome encodes for at least four proteins. The triangle indicates the position of a leaky amber stop codon at the end of ORF1. The two replication proteins 126 kDa in orange and 183 kDa in yellow are translated directly from the genomic RNA. Domains within the replication proteins include a methyl transferase (MT), intervening region (IR), helicase (HEL) and in the 183 kDa replication protein a polymerase (POL) domain. sgRNA represents sub genomic RNA. The 30 kDA movement protein (MP) shown in green is translated from subgenomic RNA 1. The 17 kDa coat protein (CP) shown in blue is translated from subgenoic RNA 2. sgRNA I1 corresponds to the POL domain and it contains ORF5 encoding for a putative 54 kDa protein shown in purple. sgRNA LMC contains ORF6 encoding for a putative 4.8 kDa protein shown in red.

The 3′ UTR contains three conserved pseudoknots followed by a TLS (22, 23, 29). The TLS can be aminoacylated by histidine aminoacyl-tRNA synthetases and in that state can interact with eukaryotic translation elongation factor 1A (eEF1A) with high affinity (30). During viral replication the 3′ UTR also acts as a promoter for initiation of minus strand synthesis (25, 31, 32).

1.2.2 126 and 183 kDa Replication Proteins

The TMV replication proteins are the first viral proteins translated, and they contain multiple domains and are responsible for multiple functions (20). The 183 kDa protein is produced by read through of a leaky amber stop codon of the 126 kDa open reading frame (ORF). Both 126 and 183 kDa proteins have a methyltransferase domain (MT), an intervening region (IR) and a helicase domain (HEL) (Fig 1.2). The 183 kDa protein additionally contains the RNA-dependent RNA polymerase (POL) domain (33).

The MT domain possesses virus-specific methyltransferase and guanylytransferase activities and is responsible for viral RNA (vRNA) capping. The 5' cap protects the vRNA from cellular exonucleases and is also involved in cap-dependent translation. The HEL domain is able to unwind double-stranded RNAs in vitro and also plays multiple roles in mediating virus infection and host responses (34-36). There is also a possible role for the IR region in symptom modulation (37).

The 126 kDa replication protein is expressed 10-fold higher than the 183 kDa protein (38, 39). Disruption of this ratio results in an impairment of viral replication. When the amber stop codon is changed to a hard stop codon to produce only the 126 kDa protein, the virus is unable to replicate. If the amber stop codon is mutated to a

tyrosine, only the 183 kDa replication protein is made and viral replication efficiency is reduced to 20% of wild-type levels. Thus, both proteins are required for efficient TMV replication (38, 40). Both the 126 and 183 kDa replication proteins can be detected in membrane-associated complexes isolated from TMV-infected plant tissues (39). Additionally, when antibodies against various portions of the 126 kDa or the POL domain of the 183 kDa protein are added RNA synthesis activities are greatly inhibited, providing further evidence both proteins are actively involved in replication (18). The TMV 126 kDa protein, but not the 183 kDa protein has been shown to bind the vRNA 3′ terminal region in an *in vitro* cross-linking study (41). This study suggests that the 126 kDa replication protein may act as a bridge connecting the 183 kDa protein which contains the POL domain to the vRNA template.

Beyond their replication activities, the 126 and 183 kDa replication proteins have also been shown to be involved in virus cell-to-cell movement (35, 36, 42-44). vRNAs that cannot produce the 126 and 183 kDa proteins also fail to disassemble in the 3′ to 5′ direction, suggesting an essential role for the replication proteins in viral particle disassembly (45). Additionally, the 126 kDa replication protein is a RNA silencing suppressor (RSS) (46).

1.2.3 30 kDa Movement Protein

The 30 kDa MP is produced from subgenomic RNA 1. The MP is not required for viral replication, but is essential for viral cell-to-cell movement through plasmodesmata (PD) (47). During infection MP localizes to PD where it dilates the PD increasing its size exclusion limit (SEL) (48-52). This change in the PD SEL is

relatively fast (3 to 5 min), suggesting TMV usurps a pathway that is already in place for host molecule transport (52). Gating of the PD by MP is restricted to the cells at the infection front (53).

MP is able to bind single-stranded RNA in a sequence-independent manner (54, 55). TMV travels cell-to-cell through PD as a viral RNA-protein complex (vRNP) that includes vRNA, MP and the 126 kDa replication protein (20). In electron microscopy studies vRNP complexes were observed to have thin extended structures which may be better suited for transport through PD (55). The TMV MP has been shown to complement the movement of MP-deficient virus and supports movement of other viruses (47, 56-61). Additionally, TMV MP has been shown to enhance the spread of RNA silencing (61).

The TMV MP is also present in viral replication complexes (62, 63) and is likely involved in intracellular transport of viral replication complexes to PD though interactions with the plant cytoskeleton (20). TMV MP has been reported to bind to actin in protoplasts and exhibits actin-severing activity in vitro (64, 65). Additionally, stabilization of actin filaments by treatment with the drug Phalloidin prevented MP from increasing PD SEL in vivo (65). However, other in vivo studies in leaves have argued against an MP and actin interaction (66) and it remains unclear if MP can sever actin in vivo. There is evidence for MP binding to microtubules, tublin and microtubule-associated factors (63, 64, 67-74).

During infection, phosphorylation of MP by a PD-associated protein kinase is likely one mechanism of regulation (75-79). MP may also be regulated by ubiquitination (80). MP has predicted hydrophobic transmembrane domains that are

involved in endoplasmic reticulum (ER) membrane association (81). However, in this model the MP domains required for other activities such as RNA binding, interaction with microtubules, chaperones, and cell wall-associated proteins are buried in the membrane. Thus, either this model is incorrect or additional protein folds must exist.

1.2.4 17 kDa Coat Protein

The 17 kDa CP of TMV is produced from subgenomic RNA 2. Translation of CP from a subgenomic RNA ensures that CP is produced later after the replication cycle is already established. This may help prevent premature particle assembly. Historically plant viral CPs have been predominately associated with structural function during virion assembly, but it is becoming clear that CPs are multifunctional and are involved in several aspects of viral infection (82, 83).

The TMV mature virion is composed of a single plus-sense genomic RNA surrounded by 2130 subunits of the CP stacked in a helix to form a rigid rod shape (18 nm x 300 nm). The CP assembles with both C- and N- termini exposed to the outside of the virion, while the interior channel is formed around the vRNA (84). Depending upon the environmental conditions, TMV CP can exist in several aggregate forms including a 4S form which is a trimer/pentamer/monomer mixture, the 20S disk or helix composed of approximately 38 subunits, and an extended virion like-rod (84-86). Virion assembly is initiated when the 20S aggregate, which is the predominant CP aggregate under cellular conditions, associates with the RNA origin of assembly (OAS), near the 3′ end of the viral genomic RNA (87). Virion elongation occurs in both the 5′ and 3′ directions (84, 88). Assembly in the 5′

direction is quicker and involves subsequent additions of 20S aggregates, while assembly in the 3′ direction is slower and thought to include incorporation of smaller CP aggregates (87).

Disassembly of the virion is directed by the molecular interactions of CP subunits and is triggered by changes in pH and Ca2+ concentration (89, 90). Disassembly begins at the 5′ RNA end, where CP interactions with the vRNA are weakest due to the lack of guanine residues. Once the 5′ end of the vRNA is exposed, ribosomes bind and additional CP subunits are pushed off as the vRNA is translated in a process called cotranslational disassembly (91, 92). Once the replication proteins are made, they may bind to the 3′ end to initiate replication of the vRNA and assist disassembly in the 3′ to 5′ direction in a process called coreplicational disassembly (45).

TMV does not require its CP for replication, but CP has been found in replication complexes and its expression leads to a more rapid appearance of viral replication complexes (VRCs) and increased VRC size (62, 93, 94). Additionally, experiments with CP mutants that cannot assemble resulted in viruses that could move cell to cell, but were inefficient in long distance movement through the phloem vascular tissue (93, 95, 96). Similarly, a study with a closely related Tobamovirus, *Cucumber green mottle mosaic virus*, found that only virions but not viral RNAs could be detected in infected phloem (97). Together these results suggest TMV moves as an assembled virion through the phloem vascular tissue and CP is required for systemic movement.

TMV CP also plays a role in the appearance of disease symptoms and defense responses. Accumulation of CP in chloroplasts correlates with chlorotic symptoms (98). Additionally, transgenic plants expressing TMV CP show resistance towards TMV and closely related tobamoviruses as well as a delay in symptom appearance (99, 100). This is known as coat protein-mediated resistance (CP-MR) (101). Accumulation of CP but not CP non-translated mRNA confers resistance (102). This resistance is overcome when plants are infected with TMV RNA, suggesting CP may block an early infection step and could interfere with proper disassembly of viral particles (100, 101). TMV CP also confers a heterologous CP-mediated resistance to *Potato virus X* (PVX) in protoplasts. This resistance is dependent on CP quaternary structure, as CP mutants that could not aggregate or produce pseudovirions did not reduce PVX replication (103). The TMV CP is also the elicitor of a gene specific hypersensitive response (HR) in host plants that contain the resistance (R) gene N' (104, 105). More recently expression of the CP from crucifer-infecting TMV (CgCP) has been shown to stabilize DELLA proteins leading to negative modulation of salicylic acid (SA) mediated defense pathways without altering SA and jasmonic acid (JA) levels (106). Expression of CgCP also lead to reduced plant growth and delayed timing of floral transition (106).

1.2.5 Putative 54 kDa protein and 4.8 kDa proteins

In TMV-infected tobacco tissues, a subgenomic RNA, termed I1 RNA, has been detected. I1 RNA corresponds to the polymerase domain and it contains an ORF encoding for a putative 54 kDa protein (107). The expression of this protein has never been detected in vivo, but double-stranded RNA with a size corresponding to

the duplex I1 subgenomic RNA has been observed (108, 109). Additionally, plants expressing the plus-sense 54 kDa gene, but not its antisense RNA, are completely resistant to TMV infection (110).

A sixth ORF encoding a putative 4.8 kDa protein has also been described (111, 112). This small ORF overlaps the C terminus of the MP and the N terminus of the CP. In vitro, the 4.8 kDa protein of *Tomato mosaic virus* (ToMV) strain L (L-ORF6) has been shown to strongly bind to eukaryotic elongation factor 1α (113). Mutations blocking the translation of ORF6 in an infectious clone of TMV U1 resulted in attenuated disease symptoms in *N. benthamiana* plants. Conversely, expression of TMV U1-ORF6 from either PVX or *Tobacco rattle virus* (TRV) enhanced the virulence of both viruses in *N. benthamiana*. However, when *N. tobacum* plants were similarly infected with U1-ORF6 expressed from PVX or TRV there was no effect on symptom development. Additionally, expression of U1-ORF6 did not alter the level of accumulation of PVX or TRV in any of these experiments (112). More recently it has been shown that L-ORF6 causes mild necrotic symptoms in *N. benthamiana* when expressed from TRV, while U1-ORF6 causes severe symptoms including death of the plant apex (114). Experiments using site-specific mutations of ORF6 and hybrid ORF6 proteins showed that this difference in symptoms was associated with the C-terminal region of L-ORF6, which directed the protein to the ER, whereas U1-ORF6 was directed to the nucleus with subsequent relocalization to mitochondria (114). Together, these experiments suggest a possible role for the 4.8 kDa protein in symptom development in certain host plants, however the protein has yet to be detected during a natural TMV infection.

1.3 TMV Life Cycle

TMV uses viral proteins and host factors to accumulate and spread in the host. For a successful infection TMV must gain entry, replicate and accumulate in the first cell, move to neighboring cells, and then spread systemically throughout the whole plant via the vascular phloem tissue (Fig. 1.3).

1.3.1 TMV Initial Infection

TMV has no known vector and enters cells through mechanical wounds that either temporarily open the plasma membrane or allow for pinocytosis (115, 116). Although TMV particles are highly stable outside the cell, disassembly begins rapidly (within 3 min) after entry (20). Compared to the outside environment, the host cytoplasm has a higher pH and relatively low Ca^{2+} concentration. These changes result in the depletion of Ca^{2+} ions and protons from carboxyl-carboxylate and carboxyl-phosphate pairs between adjacent CP subunits and between CP and viral RNA. The mutual repulsion of carboxylate groups within amino acids from neighboring CP subunits now destabilizes the virus particle and drives disassembly (90, 117). Interaction between CP subunits and genomic RNA at the 5' end is relatively weaker due to the lack of guanine residues in the 69-nucleotide 5' leader sequence, resulting in disassembly starting from the 5' end of the TMV genome (118). Uncoating of the 5' leader sequence exposes the first start codon within the viral RNA, allowing cellular ribosomes to bind to the exposed end and initiate translation of the positive sense genomic RNA. Ribosome binding to and scanning through the viral RNA dislodges more CP units at a 5′ to 3′ direction.

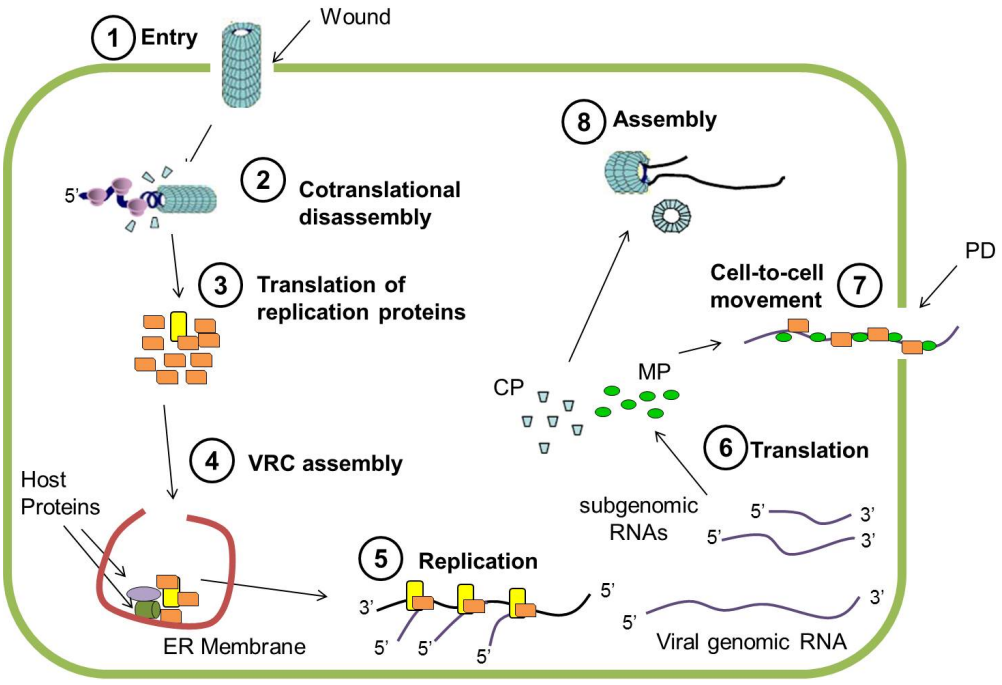

Fig. 1.3. TMV Life Cycle. TMV enters the cell through a wound in the cell wall (1). The change in pH and calcium ion concentration causes the CP subunits to repel and expose the 5' end of the viral genomic RNA. Ribosomes bind to the exposed 5' end and displace additional CP subunits via cotranslational disassembly (2). Translation of the genomic RNA produces the 126 and 183 kDa replication proteins (3), which along with host proteins are important for the assembly VRCs which are likely associated with the ER (4). The replication proteins interact with the 3' end of the viral genomic RNA and begin the synthesis of minus-sense genomic RNA. The minus-sense RNA then serves as a template for the synthesis of plus-sense genomic RNA and subgenomics RNAs (5). Translation of subgenomic RNAs produce viral MPs and CPs (6). MPs bind the viral genomic RNA and along with the replication protein form a RNP that travels to neighboring cells through PD (7). CP subunits encapsidate the viral plus-sense genomic RNA. TMV moves systemically through the vascular phloem as an assembled virion to distal tissues (8).

This process of uncoating promoted by ribosome binding to RNA is referred to as cotranslational disassembly (91). 5′ to 3′ disassembly stops when ribosomes reach the termination codons of the 126 and 183 kDa replication proteins. The newly translated replication proteins then bind to the 3′ end TLS of viral RNA to begin synthesis of the negative-strand genomic RNA and initiate uncoating of the remaining CP units in a 3′ to 5′ direction (45, 119). This process is called coreplicational disassembly. This bidirectional disassembly of the TMV virion protects the viral RNA until it can be accessed for either translation or replication.

1.3.2 TMV Replication

The replication proteins associate with the 3' end of the viral RNA and synthesize complementary negative strands which serve as templates for synthesis of full-length positive strands and subgenomic mRNAs (120, 121). The 183 kDa protein can replicate the genome, but the 126 kDa protein is necessary for maximum replication (38, 40). Minus-strand synthesis stops a few hours after inoculation, while plus-strand synthesis continues throughout virus infection (122). This leads to a hundred fold excess of plus-strand over minus-strand RNAs, similar to observations for other positive-stranded RNA viruses (123). In TMV infected plants during viral replication viral RNA is found in two prominent structures, the replicative form (RF) and the replicative intermediate (RI) (124, 125). RF RNA is double stranded and genomic length while RI RNA is partly double-stranded and partly single-stranded. The 5′ and 3′ UTRs are important for TMV replication. The 5′ 69-nucleotide leader sequence, Ω, serves as a translational enhancer (26) and small deletions in this region abolish virus replication (24). The 3′ UTR contains a TLS and three upstream

pseudoknot domains that function as a cis-acting element for virus replication (25, 31, 32). Deletion or disruption of the pseudoknot just upstream of the TLS completely abolishes synthesis of viral genomic RNAs (25). Subgenomic RNAs are synthesized when replication proteins bind to internal promoters on negative-strand RNA template (126). MP is expressed at the early stage of infection, while CP is expressed late. The internal promoters are thought to drive this difference in expression timing. This is supported by an experiment where expression of the MP was put under the control of the CP subgenomic promoter, resulting in late expression of MP (127).

Replication occurs in a membrane-associated complex containing replication proteins, MP, vRNA, and host proteins (20, 63, 121, 128, 129). While not required for replication, CP has also been detected in replication complexes (62, 93). CP expression can result in earlier appearance of VRCs and increased VRC size (62). The ER has been implicated as the site for TMV replication. Evidence for this comes from co-localization studies where an ER marker, BiP, co-localizes with MP tagged with green fluorescent protein (GFP). MP-GFP in turn co-localizes with the replication proteins (63, 129). Additionally, in transgenic plants expressing an ER-targeted GFP, dramatic morphological changes to the ER are observed during TMV infection (130). Early in infection large cortical aggregates form and there are fewer membrane tubules. After replication ends, the ER returns to a normal tubular like structure (130). Conversely, later studies with ToMV using fluorescence microscopy and biochemical fractionation methods suggest the replication proteins are predominately associated with the vacuolar membrane, although they also show some localization with other less defined membrane fractions including the ER (128).

However, ToMV has also been shown to replicate in cells that are vacuole-diminished (131). While it is clear host membranes are required for TMV VRC formation, additional work is needed to clarify the role of ER and vacuolar membranes.

Interestingly, VRCs formed by tobamoviruses are not all uniform. TMV forms X-bodies, while ToMV and *Tobacco mild green mosaic virus* (TMGMV) form virus bundles (132). Differences in VRCs correlate with differences in replication protein sequences (133, 134). For TMV the size of the VRCs can also vary, and the size of VRCs has been positively correlated with the level of disease observed (133, 135). However, a more recent study found that silencing the expression of the gamma subunit of ATP synthase, a nuclear-encoded chloroplast protein, resulted in smaller but more numerous VRCs and severe disease symptoms (136). Thus size of VRCs may not be the only factor that influences the disease phenotype.

Host proteins are also likely involved in VRC assembly. Tobamovirus multiplication 1 (TOM1) is a predicted multipass transmembrane protein required for tobamovirus accumulation (137, 138). TOM1 has been shown to interact with the HEL domain of the TMV replication protein in yeast (138, 139) and can be co-fractioned with membrane-bound replication proteins (128). It is hypothesized that TOM1 forms a link between the host membrane and tobamovirus replication proteins and is important for VRC formation.

1.3.4 TMV Intracellular Movement

For a virus infection to spread from the initially infected cell, viruses must first move within the cell from the site of replication to the PD. This intracellular movement is thought to be mediated by viral protein interactions with the host cytoskeleton. Early work identified that the TMV MP associated with microtubules (64, 67, 68). MP has since been shown to strongly bind to microtubules and contains motifs characteristic of tubulin (69). MP can also interact with microtubule assembly factors, such as GFP-fused EB1 (73) and γ-tubulin (74). Consistent with a role for microtubules in intracellular movement, tobacco mutants that are defective in microtubule dynamics are less susceptible to TMV infection (140). Additionally, inhibiting microtubule polymerization using a pharmacological treatment reduces intracellular movement of TMV MP (74). These studies suggest a model where microtubule dynamics at the leading edge of infection drive movement of MP, possibly in association with viral RNA, to the PD.

However, there are also reports that dispute the significance of the MP-microtubule association for TMV movement (43, 141)(71)(142). In some studies, disruption of microtubule structure and/or polymerization by pharmacological treatments or by silencing the tubulin gene had no negative effect on TMV spread (43, 141). Additionally, mutations in TMV MP that reduced affinity form microtubules had no effect on TMV spread (141). It has also been observed that late in infection TMV MP localizes to microtubules but it does not move (71, 142). It is possible that this could be part of a degradation pathway (71).

Actin microfilaments have also been implicated in TMV intracellular movement. In some studies intact microfilaments have been reported to be required for TMV intracellular spread (43, 134). However, a conflicting report found that microfilaments were not required for TMV spread (66). Myosin proteins may also be required for viral trafficking along microfilaments. Silencing of myosin XI-2 inhibited movement of TMV but not PVX, *Tomato bushy stunt virus*, or *Turnip vein clearing virus* (TVCV) (134). This study suggests that different viruses may use different myosins for trafficking. TMV VRCs have been observed to localize and traffic along microfilaments (133), and TMV VRCs have also been observed at the cell periphery adjacent to PD (43). Together these studies suggest that TMV VRCs move intracellularly associated with microfilaments to the PD and vRNA may transport through the PD within a VRC. Alternatively, VRCs may become anchored to PD and direct vRNA through PD in a process termed coreplicational insertion (143). Supporting this model for virus movement, PVX encoded TGB2 and TGB3 have PD targeting activity and form peripheral bodies consisting of reorganized ER membranes that cap the PD and contain PVX replication sites (143). The linking of viral replication and movement at PD entrances could maximize the efficiency of vRNA delivery to PD and be a conserved mechanism used by many plant viruses (143).

1.3.5 TMV Cell-to-Cell Movement

TMV moves cell-to-cell through specialized pores known as PD. PD have continuous ER (known as the desmotubule) and cytoplasm and are tightly regulated by the plant (Fig. 1.4). PD are structurally diverse and can be classified as simple, twinned or branched. Simple PD have a single linear channel, twinned PD have two channels, and branched PD can have multiple channels. Simple PD predominate in young tissues, while twinned and branched PD predominate in mature tissues (144). The SEL of PD can also depend on the tissue age and type. Generally open PD are considered to allow movement of solutes less than 1 kDa, but in growing tissue PD SELs between 30 and 50 kDa have been reported (79, 145). Additionally, PD connecting CCs to SE in the phloem have a much higher SEL of > 67 kDa (146). While SEL is usually reported in terms of kDa, it is important to note that the size and shape not just weight impacts movement of molecules. Thus, molecules of the same kDa may be different in their ability to cross PDs (145).

The TMV MP has been shown to increase the PD SEL to allow for the movement of cytoplasmic probes (50). This discovery was followed by similar discoveries for many other viral MPs (147). KNOTTED1 (KN1) was the first endogenous host protein shown to traffic via PD in a targeted manner (148). Additional endogenous proteins that move though PD have now been discovered although no universal trafficking signal has been identified (149, 150). Thus, viruses usurp an existing host pathway to promote viral cell-to-cell movement.

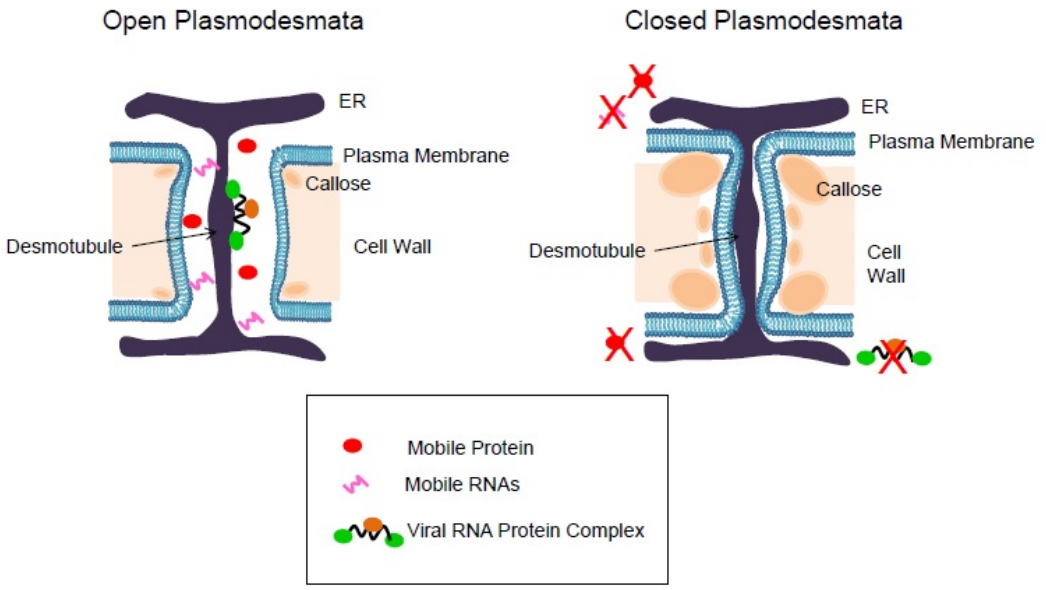

Fig. 1.4. Plasmodesmata. Specialized pores connecting neighboring plant cells are called plasmodesmata (PD). PD have continuous plasma membrane and a compressed endoplasmic reticulum (ER) called a desmotubule. Molecules such as mobile proteins, RNAs and viruses can move cell to cell via the cytoplasmic sleeve or along the ER membrane. Small molecules may also move via the ER lumen. Callose deposition at the neck region regulates the PD size exclusion limit (SEL) to control the trafficking of molecules.

TMV does not require its CP for cell-to-cell movement and moves through the PD as a ribo-nucleoprotein complex formed from the virus genomic RNA, MP, and replication protein. Conversely, other plant viruses such as *Cowpea mosaic virus* and *Grapevine fanleaf virus* require their CP for cell-to-cell movement and travel in an encapsidated form. These viruses form tubules that displace the desmotubule (151-153).

In addition to viral proteins, host factors are also involved in viral trafficking through PD. Callose, a β-1,3-glucan polymer, is deposited at the PD and is a key regulator of PD permeability. Callose acts as a physical barrier that localizes to the neck region of the PD reducing the SEL (154-158). The plant uses a balance of β-1,3-glucan synthases (also called callose synthases) and β-1,3-glucanases that degrade callose to regulate callose deposition at the PD (157, 159). Expression of a β-1,3-glucanase from the TMV genome increases viral spread (158).

In addition to callose synthases and glucanases, other families of host proteins have also been proposed to function in the regulation of callose deposition at PD. PD callose-binding proteins (PDCBs) localize to the PD neck region and can bind callose *in vitro* (160). Increased PDCB1 expression leads to increased callose accumulation and reduction of GFP movement (160). Thus, PDCBs may function to stabilize callose at the PD. Another group of proteins found to associate with PD are the reversibly glycosylated polypeptides (RGPs) class 1 members (161). Transgenic tobacco expressing RGP2-GFP have reduced PD permeability, which may be related to callose deposition as mutants overexpressing RGP2 have excessive callose at the PD. However, the underlying mechanism remains unclear (162). Additionally, PD

located proteins (PDLP) are a family of membrane associated proteins that localize to the PD. Plants overexpressing PDLP1 showed a dramatic reduction in GFP movement, whereas in combined knockout lines of several PDLP family members GFP movement is increased (163). Additionally, PDLP5 has been shown to act as an inhibitor of PD trafficking, likely by enhancing callose deposition at the PD. In contrast with PDLP1, downregulation of PDLP5 alone is sufficient to enhance PD permeability (164). Interestingly, in the *pdlp* knockout lines unlike GFP movement which is enhanced, virus movement is inhibited (165). It was found that PDLPs can bind to the MPs of some tubule-forming viruses and this interaction can mediate viral cell-to-cell movement (165).

Actin filaments also may play a role in regulating PD SEL (166). Immunolabeling studies have shown that actin and myosin localize to the PD (154, 167, 168). Both TMV and CMV MPs have been shown to inhibit actin polymerization and sever actin filaments *in vitro* (65). This microfilament-severing activity may be a mechanism by which MPs are able to increase the PD SEL, although MP actin severing activity has yet to be demonstrated *in vivo*. Consistent with this hypothesis, when microfilaments are stabilized or MP mutants without severing activity are used there is no significant increase in PD SEL (65). There also is an emerging role for lipid rafts at the PD. Some raft-associated proteins have been found at the PD, suggesting that PD might have similar properties to rafts (145). Thus, studies of the lipid composition at the PD may provide greater insight into PD structure and regulation.

1.3.6 TMV Assembly and Systemic Movement

TMV, like the vast majority of plant viruses, travels long distances through the vascular phloem. To reach the phloem tissue, TMV continues to move cell-to-cell via PD through the bundle sheath cells, phloem parenchyma cells, companion cells (CC) and sieve elements (SE) (169) (Fig. 1.5). The PD connecting CC and SE's is specialized and branched and has a higher SEL (146). TMV entry can occur in all vein classes of source leaves, while TMV exit is limited to the major veins of sink tissues (170-172), suggesting these two processes are different.

Plant viruses have been described to move systemically in two transport forms, assembled virions and vRNP complexes which may or may not include a functional CP. In assembled virions the viral genome is protected by a shell formed by the CP while in vRNP complexes the viral genome is associated with viral and/or host proteins. TMV requires a functional CP for long distance movement and is thought to travel as an assembled virion (96, 166).

A common theme in virus systemic movement is the requirement of a functional CP, but this requirement is not universal. Additionally, there are some viruses such as *Potato mop-top virus* (Pomovirus) that can move simultaneously in the form of RNP complexes and virions (173-175). Virus long distance transport forms may also depend on the host. For example *Bean golden mosaic virus* (Begomovirus) travels in a CP-dependent manner, likely as an assembled virion, in *N. benthamiana* and its natural host *P. vulgaris*, but can also be transported in bean, although less efficiently, as CP-independent RNP complexes (176).

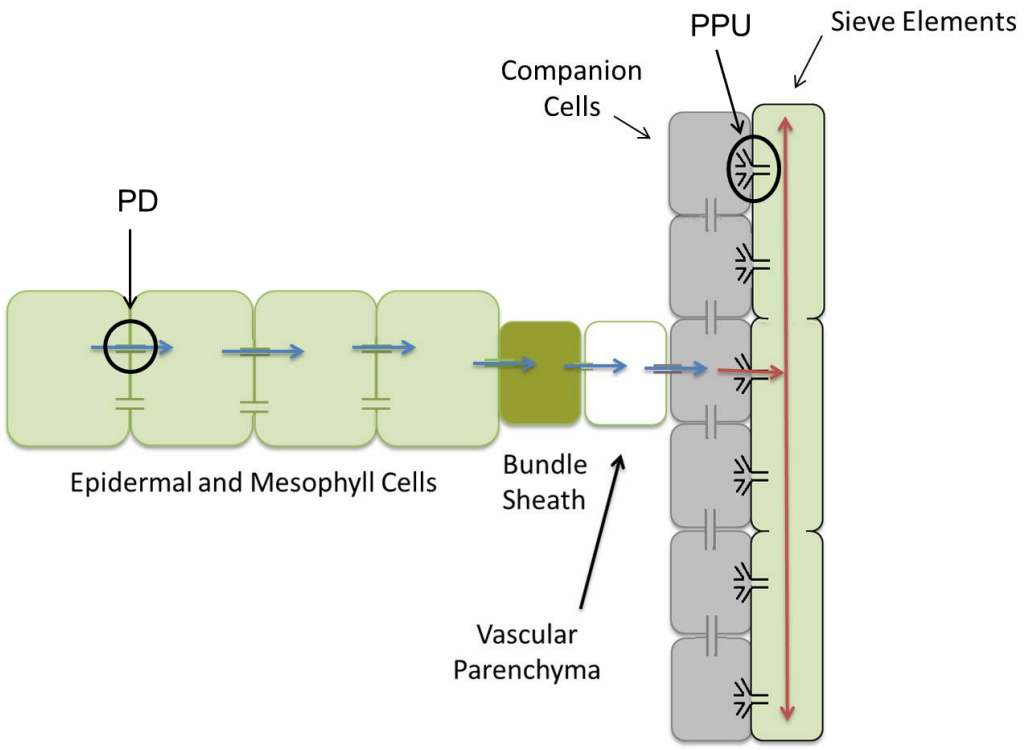

Fig 1.5. Virus Cell-to-Cell and Long Distance Movement. TMV moves cell to cell through plasmodesmata (PD). To reach the vascular phloem, TMV must cross multiple cell types including, epidermal, mesophyll, bundle sheath, vascular parenchyma, and companion cells. Cell to cell movement is depicted by blue arrows. Specialized branched PD called pore plasmodesmata units (PPU) connect companion cells and sieve elements. TMV travels systemically as an assembled virion and is loaded into the sieve elements for long distance movement. Long distance movement is depicted by red arrows. Figure adapted from (169).

Viral encapsidation was thought to protect vRNA from the potential harshness of the phloem environment. However, RNase activity has yet to be detected in the phloem (177, 178) while in contrast the entire machinery for a functional 26S proteasome was identified in pumpkin sap exudates (179). Proteome studies also identified aminopeptidases and proteases in sieve tube sap of pumpkin and *A. thaliana* (179, 180). These studies suggest viruses may actually need protection from proteolytic enzymes not RNases. The recruitment of cellular factors to protect their virion or RNP complexes may be one strategy viruses use to survive movement within the phloem environment.

Virion assembly is thought to occur in the SEs (181), however this has yet to be conclusively demonstrated for TMV. During assembly, TMV CP subunits interact with each other to form 20S disc-like aggregates (88, 182). Virus assembly originates at the OAS (nts 5444-5518). The RNA in this region is highly structured and forms three loops (183, 184). Mutations disrupting the TMV OAS suppress encapsidation of vRNA and virus systemic movement (96). Once the virus is assembled inside the SEs the virions move along the flow of photosimillates from source to sink tissue (185). Long distance movement is much faster than cell-to-cell movement with reported values between 1.5 cms/h to 2.5 cms/h (169, 186). Once TMV reaches distil sink tissue, it must egress from the vascular tissue and continue spreading cell-to-cell.

Besides the TMV CP, the TMV replication protein is also important for TMV systemic movement (187, 188). There are two roles for the TMV replication protein in systemic movement. One depends on its activity as a RSS (46, 189) while another is independent of its RSS function and likely affects cell-to-cell transport of the virus

within minor veins although is not fully understood. Evidence for this second role comes from an experiment where defective TMV RNA (dRNA) was found to be capable of replication and systemic movement in the presence of a helper TMV genome (190, 191). The N-terminal portion of the replication protein encoded by dRNAs was found to determine the ability of the dRNA to move systemically. Function of the dRNA-encoded replication protein fragments operated *in cis* and could not be influenced by the full length replication protein provided by the helper virus (191). Thus, the activity of the replication protein as an RSS is unlikely to be responsible for the observed *in cis* effects of dRNA-encoded replication protein fragments.

Some host factors have been identified as playing a role in tobamovirus systemic movement, but the molecular mechanisms remain largely unknown. A screen of EMS treated *A. thaliana* plants identified a mutant named *vsm1* (virus systemic movement 1) in which TVCV entry into the vascular tissue is inhibited (192). TMV, also a tobamovirus, is affected by the *vsm1* mutation, but the carmovirus *Turnip crinkle virus* is not affected (192). This suggests the effect is specific to tobamoviruses. *vsm1* is a recessive mutation at a single locus that has yet to be mapped. It is hypothesized that VSM1 could assist tobamovirus phloem loading (192). *DSTM1* (Delayed Systemic Tobamovirus Movement 1) is a recessive resistance gene to TMV-U1 that was identified in *A. thaliana* Col-0 (193). In mutant plants, virus particles observed in the vascular tissue displayed curved virions unlike the rigid rods observed in mesophyll cells or in susceptible plants (194). Thus, *DSTM1* may encode a phloem protein required for proper virion assembly, virus

stability or virus transport in the phloem. However, this gene has also yet to be precisely mapped.

Pectin methylesterase (PME) is a cell wall enzyme that has been shown to interact with the TMV MP and may play a role in viral systemic movement and egress. Tobacco plants with reduced PME expression in the vasculature showed significant delays in viral movement into sink tissue (195). Another protein, IP-L, was identified in a yeast two-hybrid screen using ToMV CP as bait. It is an elicitor responsive protein and is also related to senescence. Repression of IP-L by virus induced gene silencing led to a delay in virus accumulation in non-inoculated leaves (196). However, the molecular mechanism remains unknown.

In tobacco plants treated with low but not with high concentrations of cadmium, systemic movement of TMV and TVCV is reduced. Using cDNA library subtraction experiments, a glycine-rich protein (GRP) that was specifically expressed at low cadmium levels was identified and named Cadmium-ion-induced GRP protein (cdiGRP). This protein localized to the cell wall of SE and CC. Reduction of cdiGRP expression allowed systemic movement of TVCV. Conversely, over-expression of cdiGRP reduces TVCV systemic movement by preventing the exit of virions from vascular bundles. The blocking capacity of cdiGRP may be explained by callose deposition in the cell wall of phloem cells after constitutive expression of cdiGRP (197).

Another growing theme in viral systemic movement is the reprogramming of the host cell. TVCV MP was recently found to localize to the nucleus, in addition to the typical localization in the ER and PD (198). In the nucleus TVCV MP

accumulated in F-actin-containing filaments that were associated with chromatin (198). Mutations in the nuclear localization signal of the TVCV MP blocked nuclear localization and also suppressed and delayed TVCV systemic transport in *N. benthamiana* and *A. thaliana*. This suggests TVCV MP may reprogram transcription of host genes in favor of virus systemic movement (198). Additionally the MP of ToMV has been shown to interact with plant transcriptional coactivator KELP (199). Together these studies suggest viral MPs may have an additional function regulating host gene expression.

Furthermore, TMV-cg infection suppresses WRKY8 binding to the ABI4 promoter, reducing ABI4 activation and reducing abscisic acid (ABA) signaling (200). WRKY8-mediated suppression of ABA signaling seems to work to promote virus systemic movement. TMV-cg systemic movement is accelerated in the *wrky8* mutant of *A. thaliana.* Accelerated TMV-cg systemic transport correlated with activation of ethylene biosynthesis pathway. Plants treated with an ethylene precursor had accelerated viral systemic transport whereas in *acs6* mutant plants viral systemic transport was delayed (200). Virus-activated signaling via the ethylene pathways could be required for efficient RSS activity, which is in turn needed for systemic movement of the virus (201).

1.4 The Impact of Phytohormones on Virus Infection and Disease

Viruses utilize a variety of strategies to reprogram their host's cellular environment to one that is more conducive to replication and spread. As a consequence virus infections can directly or indirectly disrupt phytohormone accumulation and signaling pathways. Within plants there are an array of plant hormone pathways that contribute to nearly all aspects of plant physiology including growth, development and reproduction (202). SA, JA and ethylene (Et) are primarily involved in defense mechanisms (203). Auxin (Aux), gibberellins (GA) cytokinins (CK), brassinosteroids (BR) and ABA also contribute to defense but play key roles in plant development and physiological processes (204, 205). In addition, there are extensive interactions or "cross-talk" between the different phytohormone pathways, providing a means for the plant to finely regulate responses to environmental cues or pathogen attack (204, 206, 207). Here we discuss the role of phytohormones in the development of disease symptoms, the modulation of host defenses and enhancement of virus replication and movement. We focus primarily on specific virus-host interactions that have been linked to alterations in phytohormone synthesis and signaling and the role these interactions play in infection and disease. The phytohormone Aux will be discussed in greater detail in the following section 1.5. This section has been published in Current Opinion in Virology (208).

1.4.1 Phytohormones and Symptom Development

Some of the most common symptoms produced by plant viruses include stunting, leaf curling and chlorosis. These types of symptoms have long been

associated with disruptions in plant hormone production, accumulation and sensing (209, 210). Yet despite these associations our understanding of the viral components and interactions that affect phytohormone pathways and their role in symptom development is limited. Recently several interactions between viral and host components involved in phytohormone pathways have been identified and linked to symptom development. These interactions provide the first mechanistic explanation for how viruses modulate phytohormone regulatory systems within their hosts and how those modulations lead to symptom development. One phytohormone system that is directly disrupted by viral components is Aux. Disruption of Aux signaling has been linked to developmental phenotypes with Aux biosynthesis or signaling mutants resembling viral disease symptoms such as stunting, leaf curling, and loss of apical dominance (211). The TMV 126 kDa replication protein has been shown to disrupt Aux signaling via an interaction with select Aux/IAA family members (212, 213). These Aux/IAA proteins function as negative regulators of ARF and control their ability to modulate genes involved in a range of plant processes (214) (see section 1.5.3 for a in depth review of Aux signaling). Interaction with the TMV 126 kDa protein disrupts the nuclear localization of interacting Aux/IAA proteins and correlates with the development of leaf curling and developmental disease symptoms. In contrast, a mutant, TMV-V1087I or related virus, TMGMV, do not interact with these Aux/IAA family members and produce attenuated disease symptoms even though these viruses replicate to wild-type TMV levels (213). Thus the TMV – Aux/IAA interaction appears to be an important determinant in the development of disease.

The activity of viral silencing suppressors has also been linked to alterations in Aux signaling and the development of disease symptoms. Specifically, transgenic Arabidopsis plants constitutively expressing the TuMV silencing suppressor HC-Pro display leaf developmental abnormalities similar to those that occur during virus infection (215). Overexpression of HC-Pro was found to increase accumulations of several miRNAs, including ones targeting Aux responsive transcription factors. Furthermore, increased levels of these miRNAs corresponded with enhanced cleavage of their target mRNAs (215). The authors conclude that expression of viral suppressor proteins interferes with miRNA regulated pathways including those under the control of Aux and that disruption of these pathways accounts for many of the developmental symptoms induced during virus infection.

Disruption of the GA biosynthesis pathway has also been linked to viral disease symptoms. GA is involved in cell division and elongation. *Rice dwarf virus* (RDV) induces stunting and leaf darkening, symptoms that are characteristic of GA-deficient rice mutants. An interaction between the RDV outer capsid P2 protein and the rice *ent*-kaurene oxidase has been identified (216). *Ent*-kaurene oxidases are key components in the synthesis of GA and have been linked to dwarfing in rice (217, 218). Treatments of RDV infected plants with exogenous GA restored the non-dwarf phenotype but not treatments with Aux (216). It was speculated that the virus directed disruption of *ent*-kaurene oxidase activity was responsible for symptom development but could also potentially interfere with the synthesis of antimicrobial phytoalexins, leaving the plant more susceptible to infection.

Another example of a viral component linked to symptom development is the P6 protein of *Cauliflower mosaic virus* (CaMV). P6 is a multifunctional viral protein involved in virus replication, movement and suppression of RNAi (134, 219). Transgene expression of P6 induces stunting, chlorosis and vein banding (220). P6 expression has been shown to interfere in the ethylene response pathway as P6 transgenic Arabidopsis plants display an ethylene-insensitive phenotype (221, 222). It was suggested that P6 may interfere with ethylene signaling leading to the observed symptoms (222). However, a direct interaction between P6 and a component of the ethylene pathway has not been identified.

1.4.2 Phytohormones and Plant Defense Responses

SA is a key virus defense phytohormone involved in *R* gene mediated resistance, systemic acquired resistance (SAR) and basal defense processes (223-226). Activation of SA biosynthesis and signaling can lead to the accumulation of reactive oxygen species, pathogenesis-related (PR) proteins, callose deposition and induction of HR (223, 224, 227, 228). SA is also required for SAR activation in tissues distal from the site of infection (225). SA and JA / ET mediated defense pathways are generally antagonistic, with SA largely responsible for defense against biotrophic pathogens such as viruses and JA / ET largely responsible for defense against necrotrophic pathogens and insects (229-231). However, examples of synergism between these pathways do exist (232-234).

In many studies, depletion of endogenous SA or disruption of SA signaling leads to an impairment of defense response and susceptibility to viral infections (235-239). For example, reducing the accumulation of SA through the use of a salicylate

hydrolase (NahG) transgene negates resistance conferred by the potato *Ny-1 R* gene against *Potato virus Y* (240). Thus inhibition of SA synthesis or SA dependent defenses is one strategy viruses may use to enhance infection. Virus interactions that impact the SA pathway include the TMV replication protein**,** which was found to target the proteasome degradation of a NAC domain transcription factor, ATAF2, involved in the regulation of host basal defenses (241). *ATAF2* knockout or repressor lines displayed reduced levels of the SA marker gene *PR1* when treated with SA. In addition, *PR1* is not induced upon SA treatment of systemically infected leaf tissues, indicating that host defense responses become attenuated as TMV moves systemic. These findings suggest that TMV targeted degradation of ATAF2 is involved in the suppression of SA mediated defenses.

In another example, the CaMV P6 protein has been shown to inhibit SA dependent defenses by altering the expression and localization of the SA receptor NPR1 (242, 243). Plants expressing P6 display the miss-localization of an inactive form of NPR1 to the nucleus, effectively disrupting SA signaling (243). As a result plants expressing P6 are more susceptible to SA sensitive pathogens but more resistant to JA sensitive pathogens (243). Additionally, a recent study with TMV-Cg, crucifer strain, has shown the virus coat protein (CgCP) can also suppress SA signaling by stabilizing DELLA proteins without altering SA or JA levels (106). DELLA proteins are negative regulators of GA signaling and have been shown to repress SA defense responses, possibly by modulating the antagonistic cross-talk between SA and JA pathways (204, 244). In addition, CgCP expression also reduces

plant growth and delays the timing of floral transition, potentially linking this interaction to symptom development.

JA - SA antagonism appears to be a recurring factor in mediating virus defense processes. In *N* gene resistant tobacco, exogenously applied methyl jasmonate reduced resistance to TMV and conferred systemic viral movement (245). Additionally, silencing of the JA receptor *COI1* or a JA biosynthetic enzyme, allene oxide synthase, resulted in increased SA accumulation and reduced TMV accumulations in *N* gene tobacco (245). Antagonistic interactions between SA and JA signaling have also been implicated in defense gene expression and the activation of *RCY*1 resistance to *Cucumber mosaic virus* where a mutant allele of *COI1,* the JA receptor, restored resistance in plants blocked in SA accumulation (236). Thus, antagonism between JA and SA pathways represents an important mechanism in regulating *R* gene mediated resistance to these viruses. However, increased JA accumulation is not always favorable for viral infection. Endogenous JA levels have been reported to increase in incompatible plant-virus interactions in tobacco and potato (246, 247). Additionally, exogenous application of JA disrupts geminivirus infection (248). Furthermore, the geminivirus C2 protein has been found to interact with the catalytic subunit of the COP9 signalosome, compromising SCF ubiquitin ligase activity and altering its ability to regulate JA activity. C2 targeting of SCF ubiquination thus provides a mechanism for this virus to modulate host resistance.

Phytohormones also appear to modulate the general virus defense mechanism of RNA silencing. Plants that contain mutations in RNA silencing pathway components including *HEN1*, *DCL1* and *AGO1* are hypersensitive to ABA (249-251),

while increased *AGO1* levels lead to ABA hyposensitivity (250, 251). Additionally, miR168 which regulates *AGO1* contains ABA-responsive elements in its promoter region and is up regulated by ABA (251). There is also evidence for cross-talk between SA and silencing defense pathways (252-255). It was found that plants expressing *NahG*, for reduced accumulations of SA, produce lower levels of siRNAs when infected with *Plum pox virus* (PPV). Furthermore, overexpression of the potyvirus silencing suppressor protein HC-Pro reduced SA-mediated defenses against PPV (253). Combined these findings suggest a strong connection between virus defense responses and phytohormone signaling.

1.4.3 Phytohormones and Virus Replication

Only recently has evidence emerged linking specific phytohormone systems directly to virus replication. In one system SA was shown to inhibit the replication of *Tomato bushy stunt virus* (TBSV) by competitively binding cytosolic Glyceraldehyde 3-phosphate dehydrogenase (GAPDH) (256). Cytosolic GAPDH binds the negative RNA strand of TBSV and is required for replication (257, 258). When SA accumulates it can directly bind to GAPDH, preventing its interaction with virus RNA and leading to suppression of TBSV replication (256). In another system, a mutation in the ABA biosynthesis gene *ABA2* resulted in decreased *Bamboo mosaic virus* titers and a dramatic reduction of negative sense virus RNA (259). Similarly, *Cucumber mosaic virus* (CMV) also failed to replicate in the *aba2-1* mutant. The authors propose the product of *ABA2* may be an essential component of the virus replication or translation complexes or that ABA2 negatively regulates host defense

responses. Based on these findings it is clear phytohormones and their associated components can directly impact virus replication.

1.4.4 Phytohormones and Virus Movement

The movement of viruses from cell-to-cell as well as into the vascular phloem occurs via intercellular PD connections. Mounting evidence indicates that several phytohormones play a role in regulating PD connections. For example, ABA can limit virus spread through inhibition of β-1,3-glucanase, which degrades callose (157, 260, 261). Deposition of callose at PD is known to decrease viral cell-to-cell movement (157, 262, 263). Furthermore, exogenous application of ABA has been shown to increase plant resistance to viruses such as TMV and *Tobacco necrosis virus* by limiting virus movement (264, 265). SA is another phytohormone linked to PD closure. Specifically, exogenous application of SA results in callose deposition within PD and reduced intercellular movement of a fluorescent marker dye (228). This SA mediated PD closure requires the SA signaling pathway as well as a regulator of PD gating, PDLP5 (164). SA has also been tied to the inhibition of virus movement and replication via a process linked to the mitochondrial alternative oxidase pathway (AOX) (239). Specifically, inhibition of AOX functions to counter SA induced resistance against TMV, PVX and CMV. It would be interesting to determine if AOX can contribute to the regulation of PD.

The plant-to-plant movement of viruses via their insect vectors represents another aspect of virus biology impacted by phytohormones. In particular, JA, the primary hormone involved in plant insect defenses appears to be a key target in vector transmission. For example, *Tomato spotted wilt virus* (TSWV) is vectored by the

western flower thrip, which prefers to feed on infected tissues (266). Plants infected with TSWV have increased SA levels and decreased levels of JA (230, 266). However, it remains to be determined if TSWV directly targets these pathways in order to enhance insect transmission. In another example, the 2b silencing suppressor from CMV was found to interfere in the JA signaling pathway as a means to promote its own transmission by its vector Myzus persicae. CMV infected plants or transgenic plants expressing 2b display reduced levels of JA signaling (267). In addition, aphid survival increases on tobacco infected with CMV but decreases on tobacco plants infected with CMV strain lacking 2b (268). Finally, NIa-Pro (Nuclear Inclusion - Protease domain) from TuMV has been shown to alter Et responses, suppressing aphid-induced callose defenses. NIa-Pro is highly conserved among Potyviruses and the authors propose this interaction could represent a conserved mechanism for increasing aphid transmission of this important group of viruses (269).

1.4.5 Summary and Remaining Questions

From these studies it is clear that phytohormones play a significant role in many aspects of virus infection and disease. Alterations in phytohormone levels have been repeatedly linked to changes in virus accumulation. Furthermore, in a few systems we are beginning to understand the molecular mechanism whereby viruses target and modulate plant hormone synthesis and sensing systems to avoid host defenses and enhance their own infection and movement (summarized in Table 1.1). It is also becoming increasingly clear that cross-talk between phytohormone pathways is essential to the regulation of virus defense responses as well as a target for viruses to exploit during infection (summarized in Fig. 1.6). However, despite these

advances we still lack specific information on the phytohormone regulated genes and pathways that directly impact virus biology. What Aux regulated genes are involved in symptom development or what SA mediated processes directly impact virus accumulation are just a few of the questions that when answered will provide a greater understanding of the interactions between viruses and their plant hosts.

Table 1.1
Specific virus-host interactions that impact phytohormone pathways.

Phytohormone Pathway	Virus	Viral Protein	Host Component	Result	Reference
Increases Aux signaling	TMV	126 kDa	IAA26 IAA27 IAA18	Enhanced phloem loading and viral systemic movement, symptom development	(212, 213)
	TuMV	HC-Pro	miR167 (targets ARF8)	Symptom development	(215)
Alters ET responses	TuMV	NIA-Pro	unknown	Suppresses callose formation to promote transmission by insect vector	(269)
	CaMV	P6	unknown	Symptom development	(221, 222)
Inhibits GA synthesis	RDV	P2	ent-Kaurene oxidase	Enhanced susceptibility, symptom development	(216)
Inhibits GA signaling, inhibits SA mediated defense	TMV-Cg	CgCP	DELLA proteins	Enhanced viral accumulation	(106)
Reduces SA defense responses	TMV	126 kDa	ATAF2	Enhanced viral accumulation	(241)
Inhibits SA signaling, enhances JA signaling	CaMV	P6	NPR1	Enhanced susceptibility	(270)
Increases SA signaling, Inhibits JA signaling	TSWV	unknown	unknown	Promotes insect vector feeding	(266)
Inhibits JA signaling	Geminivirus	C2	CSN5	Enhanced viral replication	(248)
Decreases JA signaling	CMV	2b	unknown	Promotes insect vector feeding	(271)

Fig. 1.6. Virus and phytohormone pathway interactions. Phytohormones shown in blue generally have positive effects on plant defense against viruses, while phytohormones shown in red generally have negative effects. SA and JA / ET are the phytohormones primarily involved in defense responses, while Aux, GA, CK, BR and ABA also contribute to defense but play key roles in plant development and physiological processes (203-205). The ABA and JA pathways have positive effects on defense against herbivorous insects that can act as viral vectors (230). JA also promotes defense against Geminiviruses (248). Viruses boxed in red inhibit SA mediated defense responses either through inhibition of the GA and SA pathways (106, 216, 241, 243) or through activation of the antagonistic phytohormone Aux (213, 215). Viruses boxed in blue inhibit JA and ABA mediated defense responses against their insect vector either directly (268) or through activation of the SA or ET pathways which can both be antagonistic to ABA (266, 269). Geminiviruses boxed in green inhibit JA signaling (248). SA and ABA are also linked to the general virus defense mechanism of RNA silencing (251, 254). SA, salicylic acid; JA, jasmonic acid; ET, ethylene; Aux, auxin; GA, gibberellins; CK, cytokinins; BR, brassinosteroids; ABA, abscisic acid; TMV, *Tobacco mosaic virus*; RDV, *Rice dwarf virus*; CaMV, *Cauliflower mosaic virus*; TSWV, *Tomato spotted wilt virus*; TuMV, *Turnip mosaic virus*; CMV, *Cucumber mosaic virus*.

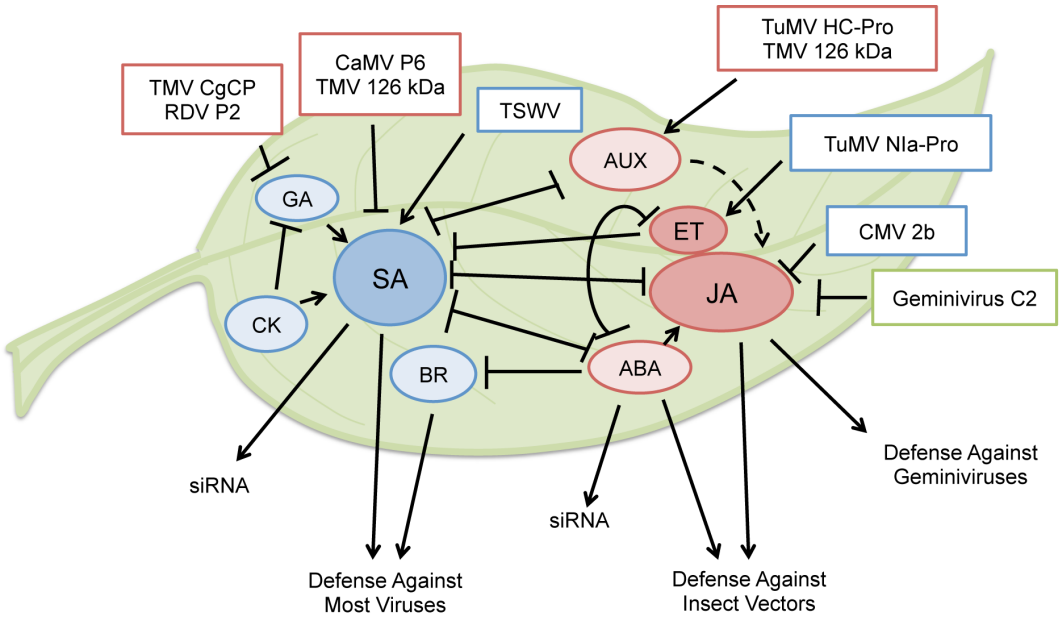
TuMV HC-Pro
TMV 126 kDa
CaMV P6
TMV 126 kDa
TMV CgCP
RDV P2
TSWV
AUX
TuMV NIa-Pro
GA
ET
CMV 2b
SA
JA
Geminivirus C2
CK
BR
ABA
siRNA
Defense Against
Geminiviruses
siRNA
Defense Against
Most Viruses
Defense Against
Insect Vectors

1.5 Auxin

Aux is an important phytohormone that is involved in many aspects of plant growth and development. The term "auxin" is derived from the Greek word "auxein" meaning "to grow". Aux is involved in regulating plant responses such as embryogenesis, tropism, organogenesis, root development, leaf patterning, apical dominance, fruit development and more recently has also been associated with plant defense (211, 272-276). The study presented in Chapter 2 focuses on an interaction between the TMV replication protein and select Aux/IAA family members. Aux/IAA proteins are key regulators involved in Aux signaling. To study the impact this interaction has on virus and host biology it is important to first understand how Aux normally functions in the host plant. This section will focuses on what is known about Aux biosynthesis, transport, signal transduction and role in plant defense responses.

1.5.1 Auxin Biosynthesis

The major naturally occurring Aux in plants is indole-3-acetic acid (IAA) (277). Plants can use multiple pathways to synthesize IAA(278, 279), but tryptophan dependent synthesis of IAA through the IAA precursor indole-3-pyruvic acid (IPyA) is the main IAA biosynthetic pathway (278-280). The tryptophan aminotransferase of Arabidopsis (TAA) family of enzymes converts tryptophan to IPyA (281, 282) and the YUCCA (YUC) family of enzymes converts IPyA to IAA (283, 284). IAA may be present in the cell in free active forms or in conjugated inactive storage forms including methyl ester IAA (MeIAA), IAA-glucose, IAA-amino acid (IAA-AA) and

indole-3-butryic acid (IBA). The conjugated inactive forms can be rapidly converted to free IAA to regulate Aux homeostasis (278). The roles of Aux derived from these conjugated storage molecules are only beginning to be understood. Experiments where conversion of specific IAA conjugates to free IAA were blocked resulted in various developmental defects (285-290) and blocking conversion of multiple storage forms to free IAA resulted in increased activity of the IPyA biosynthesis pathway (291). Further studies are needed to better understand the conditions in which plants use de novo Aux biosynthesis as opposed to conversion of specific storage forms.

1.5.2 Auxin Transport

Aux is transported cell-to-cell by specialized membrane-localized transport proteins. Members of the pin-formed (PIN) and ATP-binding cassette subfamily B (ABCB) protein families are responsible for the efflux of IAA. Auxin resistant 1 (AUX1) and Like AUX1 (LAX) family members are responsible for IAA uptake (292, 293). AUX1/LAX family members differ in the natural and synthetic Aux compounds they are able to uptake and these transport specificities may contribute to Aux response differences (294).

PIN proteins are unique to plants and mediate Aux efflux. There are eight PIN family members in Arabidopsis that are divided into “long” and “short” PIN categories (294). Long PIN proteins include PIN1, PIN2, PIN3, PIN4 and PIN7 which have a polar localization pattern on the plasma membrane and are involved in polar transport of IAA (292, 294). The location of these PIN proteins is dynamic and they can be rearranged in response to external stimuli such as gravity and light (295-298). Long PIN proteins are additionally endogenously regulated by phytohormones

including Aux, CK, strigolactone, GA and SA (298-304). Aux regulation of long PIN expression and subcellular polarization provides a mechanism for Aux to regulate its own transport (298). Aux can have a stabilizing effect on long PINs by inhibiting endocytosis (305, 306). However, both prolonged elevation and reduction of Aux levels can lead to long PIN degradation (306). Thus, an optimal level of Aux is required for stabilization of long PINs at the plasma membrane. CK has been shown to promote degradation of long PINs (300). Additionally, strigolactone causes depletion of PIN1 from the plasma membrane in stem xylem parenchyma cells (304). Conversely, GA has a stabilizing effect on plasma membrane-localized PINs (301, 302). SA also can play a role in stabilizing long PINs by affecting endocytosis as part of a general inhibitory effect on clathrin-mediated endocytosis (303).

Short PIN proteins include PIN5, PIN6 and PIN8. Unlike long PINs involved in the polar cell-to-cell transport of IAA, short PINs are localized to the ER and transport IAA from the cytoplasm into the ER (307-310). While it is still unclear if IAA plays a role inside the ER, this is likely a mechanism to regulate cytoplasmic levels of free IAA (294). Additional proteins called PIN-LIKES also transport Aux into the ER and may also have a role in regulating cytoplasmic free Aux levels (311).

In addition to PINs, several ABCB transporters are required for IAA efflux including ABCB1, ABCB4, ABCB19 and ABCB21 (312). Interestingly, ABCB4 and ABCB21 may be able to switch from Aux efflux to Aux influx depending on the Aux concentration (313-315). Plants lacking ABCB family members show developmental phenotypes, suggesting a role for these Aux transporters in plant development (293).

1.5.3 Auxin Signal Transduction

Transcriptional responses to Aux are controlled by the TIR1/AFB Aux signaling pathway. At low Aux concentrations, Aux/IAA proteins accumulate and interact with ARFs (214). ARFs are then either prevented from binding efficiently to AuxRE in the promoter region of Aux responsive genes or Aux/IAA proteins recruit co-repressors TOPLESS (TPL) or TOPLESS RELATED (TPR) (214, 316). TPL/TPRs can mediate transcriptional repression by recruiting histone deacetylases (HDACs) (317-319). When Aux levels are high, an Aux/IAA protein and a TIR1/AFB F-box protein come together to form an Aux coreceptor and directly bind Aux (320-322). Aux acts as "molecular glue" holding these molecules together (214, 323). The TIR1/AFB F-box protein, which is part of a Skp1-Cullin-F-box (SCF) E3 ubiquitin ligase complex, then polyubiquitylates the Aux/IAA protein and it is targeted for degradation by the 26S proteosome (214, 294). Degradation of Aux/IAA proteins leaves ARF proteins free to regulate target Aux responsive genes (214, 294) (Fig. 1.7).

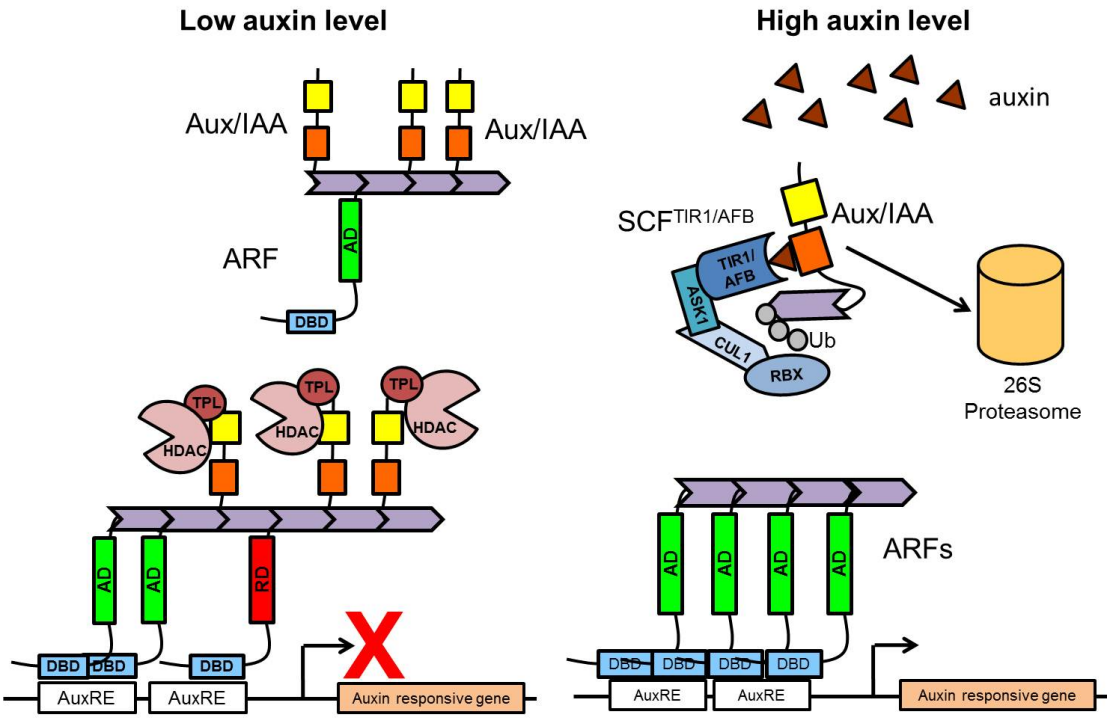

Fig. 1.7. A Model for Auxin Mediated Gene Regulation. When there are low levels of auxin (Aux), Aux/IAA proteins and ARFs form oligomers through front to back interactions of their PB1 domains. Aux/IAAs in the oligomers either block ARFs from efficient binding to AuxREs upstream of Aux responsive genes or recruit co-repressor complexes, which are composed of TPL/TPRs and HDACs. The general result is repression of the transcription of Aux responsive genes. When Aux levels are high, Aux promotes an interaction between Aux/IAA and the E3 ubiquitin ligase, $SCF^{TIR/AFB}$. This leads to ubiquitination and degradation of Aux/IAAs via the 26S proteasome. ARFs are now free to form dimers or oligomers and bind to AuxRE, generally resulting in the transcription of Aux responsive genes. Figure adapted from (294).

1.5.4 TIR1/AFBs - Aux/IAA Auxin Co-Receptors

In Arabidopsis there are six TIR1/AFBs referred to as TIR1 and AFB1-5 (320) and 29 Aux/IAAs referred to as IAA1-20 and IAA26-34 (324) that could participate in forming Aux coreceptor pairs. TIR1 shares 50-70% sequence identity with AFB1-5. In mutants lacking TIR1 and AFB1-3, the binding of radiolabeled IAA was reduced providing evidence these proteins act as Aux receptors (320). Single loss-of-function mutants for *tir1* or *afb* do not cause dramatic developmental defects suggesting they have some redundant functions (320). However, combining *tir1 and afb1*-3 mutations leads to a severely reduced Aux response and a variety of Aux-related developmental defects (320). Additionally, loss of *AFB5* results in resistance to the synthetic Aux picloram (325).

The variation in sequence identity among Arabidopsis Aux/IAA family members is high and can range from 36% to 87% (326). Despite this variation, single loss-of-function Aux/IAA mutants rarely show strong phenotypes (274, 327, 328) suggesting that Aux/IAAs have some redundant functions. Most Aux/IAA proteins share three conserved motifs referred to as domains I, II, and PB1 (Phox and Bern1, formerly referred to as domain III/IV or domain III and domain IV) (Fig. 1.8A). Domain I and II contain a bipartite nuclear localization motif (326). Domain I is additionally required for transcriptional repression and recruits TPL/TPR co-repressor proteins (214, 316). Domain II destabilizes Aux/IAA proteins through direct interactions with Aux and TIR1/AFBs. Domain II has been demonstrated to act as a transferable protein degradation signal when fused to luciferase (329). Different Aux/IAA proteins exhibit different degradation rates primarily due to variations in

Domain II (214). Aux/IAA proteins lacking Domain II have extended lifetimes (330). The PB1 domain plays a role in interactions with other Aux/IAA proteins or ARFs.

Different combinations of Aux/IAA – TIR1/AFB pairings display different affinities for one another and for different auxins (331, 332). Differences in binding affinities to Aux appear to be determined primarily by the Domain II sequence of the Aux/IAA proteins, although other sequences may also contribute (331). These differences provide a possible mechanism for the plant to fine tune responses to Aux to regulate different aspects of plant development.

1.5.5 Aux/IAA - ARF Interactions

Combinations of Aux/IAA and ARF proteins function in a complex system to regulate gene expression. In Arabidopsis 23 ARF family members have been identified (333). ARF proteins have a DNA-binding domain and a PB1 domain (Fig. 1.8A). ARFs bind to the AuxRE, TGTCTC, in the promoter region of Aux responsive genes (334, 335). The first four bases in the TGTCTC sequence are absolutely required for binding, while more variation is tolerated in the last two bases (333, 336). Protoplast studies characterized ARFs as transcriptional activators or repressors. ARF5, 6, 7, 8 and 19 have a glutamine-rich variable middle region and are considered activators. All the remaining ARFs except for ARF23 have a middle region rich in serine, proline or leucine/glycine and are thought to act as repressors (333). However, this repressor activity has not been experimentally tested for every ARF protein in this group. ARF23 consists of a truncated DNA-binding domain only (333).

Fig 1.8. Diagrams of ARF and Aux/IAA Interactions. (A) ARF proteins are approximately 110 kDa in size and contain a N-terminal DNA binding domain (blue), either an activation domain (AD, green) or repressor domain (RD, red), and a C-terminal PB1 domain (previously referred to as Domain III/IV, purple). Some ARFs with RDs lack the PB1 domain. Aux/IAA proteins are approximately 30 kDa and contain an N-terminal repression domain I (yellow), followed by a conserved degron called domain II (orange) and a C-terminal PB1 domain (purple) that is related to the PB1 domain in ARF proteins. PB1 domains are shown as arrows with a N-terminal basic amino acid region (+) and a C-terminal acidic region (-) which are required to form dimers or oligomers. **(**B) The most common PB1 domain interactions occur between Aux/IAA-Aux/IAA and Aux/IAA-ARF activators (276) and are shown with black double-headed arrows. The gray double-headed arrows indicate the less common interactions reported between Aux/IAA-ARF repressors and ARF-ARF proteins. These interactions include ARF5-ARF5, ARF7-ARF7, and IAA10 and repressor ARF9 (337-339) Figure adapted from (340).

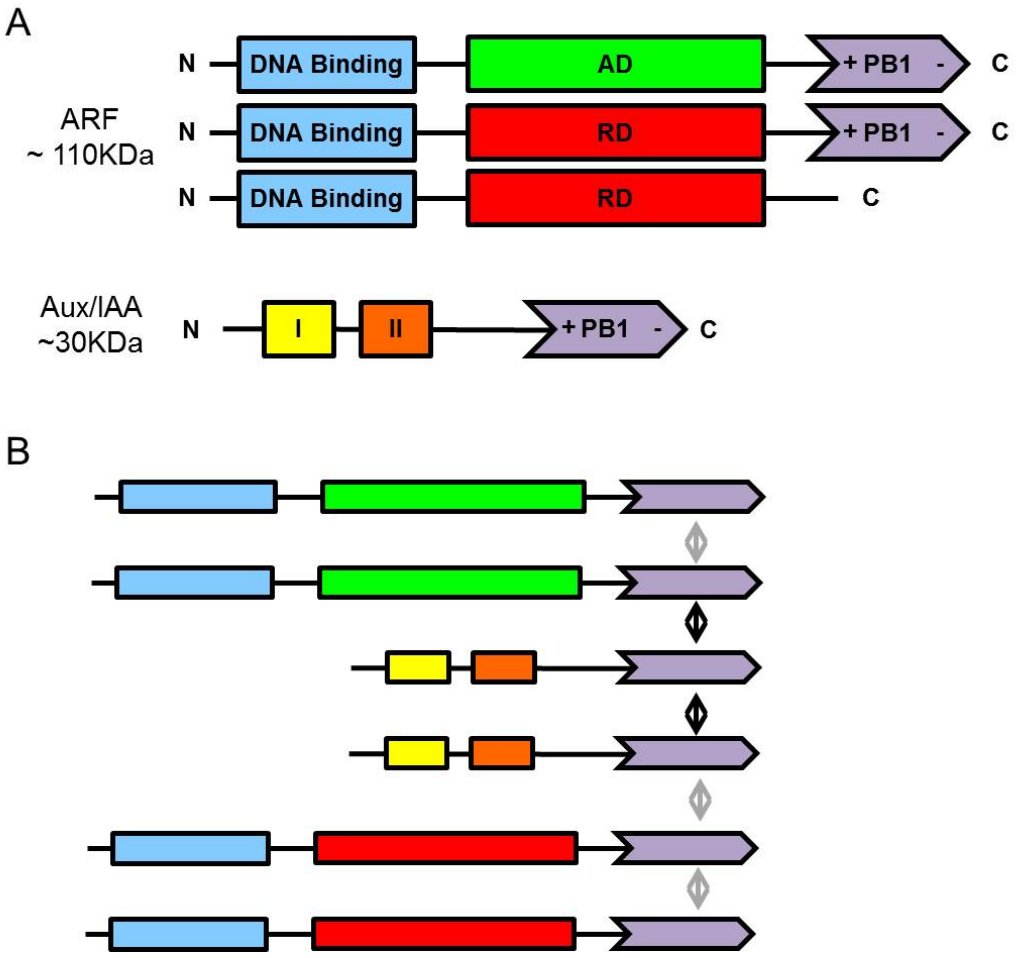
A
ARF
~ 110KDa
N
DNA Binding
AD
+ PB1 -
C
N
DNA Binding
RD
+ PB1 -
C
N
DNA Binding
RD
C
Aux/IAA
~30KDa
N
I
II
+ PB1 -
C
B

While characterization of ARFs as activators or repressors in protoplasts provides some understanding of ARF activities, it is important to keep in mind that ARF behavior in plants may be more complex.

Analysis of ARF loss-of-function mutants has given some insight into developmental processes specific ARFs may be involved in (341-348). Similarly, analysis of gain-of-function Aux/IAA mutations have been used to try to understand processes Aux/IAA proteins are involved in (349-351). The comparison of ARF loss-of-function mutant phenotypes to Aux/IAA gain-of-function mutant phenotypes has provided some evidence that specific pairs of Aux/IAA and ARF proteins may preferentially bind. For example, stabilization of IAA12 or loss-of-function of ARF5 both result in a rootless phenotype (344, 352, 353). More recently, a large-scale analysis of Aux/IAA and ARFs interactions was done using systemic large-scale yeast two-hybrid assays and bimolecular fluorescence complementation assays. The main conclusion of this study is that Aux/IAA-Aux/IAA and Aux/IAA-activator ARF interactions are common, whereas interactions between ARFs or between Aux/IAAs and repressor ARFs are less common (276) (Fig. 1.8B). The authors further propose that if ARF-ARF and Aux/IAA-ARF repressor interactions do occur they are weaker and/or more specific than Aux/IAA-Aux/IAA and Aux/IAA-ARF activator interactions. However, recent crystallographic studies provide evidence for ARF5-ARF5 and ARF7-ARF7 interactions (337, 338). Additionally, there is genetic evidence for an interaction between ARF9, characterized as a repressor ARF, and IAA10 (339). Despite numerous studies using yeast two hybrids and other protein-protein interaction assays to try to identify Aux/IAA and ARF binding partners,

results remain controversial and have been inconsistent (354). Furthermore, interaction studies often express ARF and Aux/IAA proteins at higher levels than those that occur in the cell which can lead to false positives. Additionally, proteins that bind in interaction studies may not be expressed in the same place at the same time in the plant.

Even further complicating this system, recent discoveries suggest that ARF and Aux/IAA proteins may form oligomers through front to back interactions between the + and – face of PB1 domains, rather than simply forming dimers (337, 338). A conserved lysine in the N-terminal end of the PB1 domain and a conserved acidic motif in the C-terminal end of the PB1 domain promote electrostatic and hydrogen-bonding interactions (340). PB1 domains that contain both the conserved lysine and acidic motif residues are referred to as type I/II, while type I PB1 domains contain only the conserved acidic motif and type II PB1 domains contain only the conserved lysine (Fig. 1.9A). Different types of PB1 domains can interact to form dimers or oligomers (Fig. 1.9B) (340). In general, Aux/IAA and ARF proteins are predicted to have a type I/II PB1 domain (340) and crystal structures have confirmed this type I/II PB1 domain for ARF5 (337) and ARF7 (338). However, a few Aux/IAA and ARF proteins appear to have type I or type II PB1 domains. The IAA33 PB1 domain lacks the conserved lysine residue and might be classified as type I. Conversely, IAA29, IAA31, IAA32 , ARF1, ARF10, ARF14, ARF15, ARF20 and ARF21 lack one or more conserved acidic residues and might be classified as having type II PB1 domains (340).

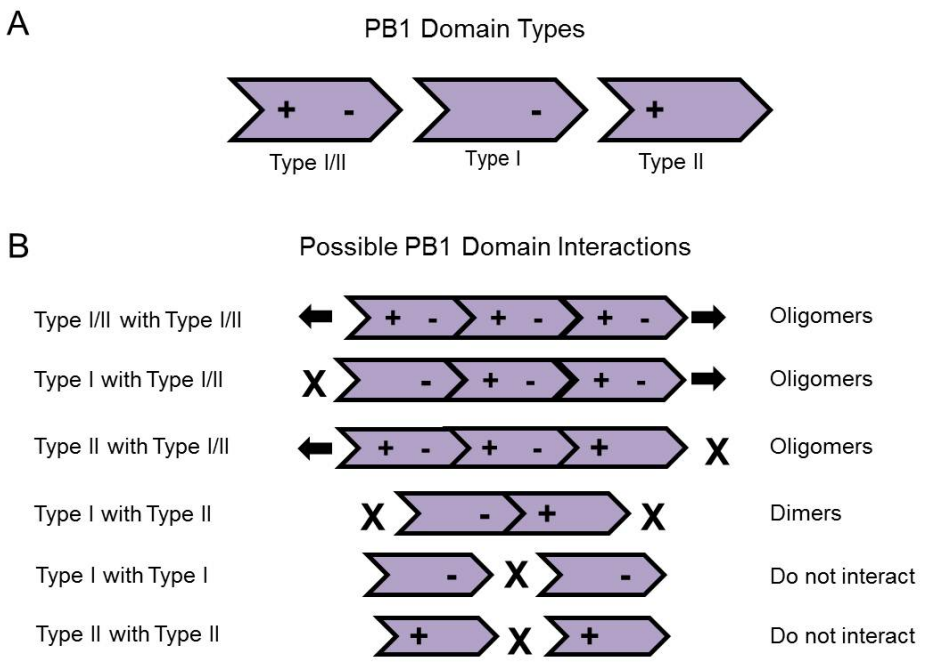

Fig. 1.9. PB1 Domain Types Front to Back Interactions. (A) Type I/II PB1 domains have a conserved N-terminal basic amino acid region (+) and a C-terminal acidic region (-). Type I PB1 domains lack the N-terminal basic amino acid region (+), while Type II PBI domains lack the C-terminal acidic region (-). (B) Front to back interactions between PB1 domains occur through the + and – face. Type I/II PB1 domains facilitate the formation of homo- and heterodimers or oligomers. Type I and type II PB1 domains can interact with type I/II domains to form dimers, and oligomerization is possible through additional binding to the type I/II domain. An arrow indicates that additional PB1 domains can be added, while a X indicates the loss of either the + face or the – face, which is required for an interaction to occur. Type I PB1 domains can interact with type II PB1 domains to form dimers but oligomerization cannot occur. Type I PB1 domains cannot interact with one another, and type II PB1 domains cannot interact with one another. Figure adapted from (340).

Although, it is currently unknown if one amino acid substitution is sufficient to disrupt the type I PB1 domain. PB1 domains can also be highly specific or promiscuous in interactions with other PB1 domains (355).

A remaining question is if the PB1 domains in ARF and Aux/IAA proteins may also interact with other PB1 domain proteins in plants. PB1 domain interactions could allow for multiple different ARFs and Aux/IAA proteins or even additional PB1 containing proteins to be part of the ARF-Aux/IAA complex to further fine tune Aux responses. This complexity may explain how the Aux signaling pathway regulates such a diverse array of developmental processes.

1.5.6 Regulatory Loops in Auxin Signaling

The Aux/IAA genes were first identified because some family members are rapidly induced in response to Aux. Increasing the expression of *Aux/IAAs* in response to Aux creates a negative feedback loop which allows Aux signaling to be rapidly dampened by increased production of Aux/IAA transcriptional repressors. However, the kinetics of the Aux regulation of *Aux/IAAs* are complex with different family members having different responses to Aux, and some *Aux/IAAs* such as *IAA28* in Arabidopsis are not Aux induced (356).

An additional regulatory loop occurs through Aux/IAA and ARF regulation of members of the PIN family (357). In root apical meristem, application of Aux leads to rearrangements in the subcellular localization of PIN proteins (358). This provides a mechanism for Aux to act as a polarizing cue to regulate its own transport. Additionally, *PIN* gene transcription is influenced by Aux signaling. Multiple *PIN* genes are upregulated in response to Aux in a tissue and PIN specific manner (357).

For example in the roots, the CK response factor ARR1 activates transcription of *SHY2/IAA3*. The IAA3 protein then represses transcription of *PIN1* resulting in a change in Aux distribution that promotes cell differentiation (359).

1.5.7 Auxin and Plant Defense

While traditionally Aux has been associated with plant growth and development, there is increasing evidence that Aux is also involved in plant defense responses through cross-talk with the SA and JA signaling pathways. Treatment of *Arabidopsis thaliana* with the SA analog, benzothiadiazole S-methylester (BTH) results in an overall reduction of Aux responses (360). SA may inhibit Aux signaling through transcriptional repression of *TIR1/AFB* genes, leading to reduced degradation of Aux/IAA proteins and thus repression of Aux responsive genes. Consistent with this mechanism is the observation that *TIR1* and *AFB1* are both down regulated in response to BTH treatment and detection of Aux/IAA proteins is enhanced after SA treatment (360). Additionally, when the amino terminus of AXR3/IAA17 is fused to the reporter gene β-glucuronidase (GUS), SA has a stabilizing effect (360). Conversely, activation of Aux signaling leads to the suppression of SA biosynthesis and signaling (361). It has also been reported that Aux triggers induction of genes involved in JA biosynthesis (362). Furthermore, ARF6 and ARF8 have been linked to positive regulation of JA biosynthesis (363). Together these studies suggest a possible role for Aux as a negative regulator of the SA pathway, perhaps via activation of JA signaling.

Stabilization of Aux/IAA proteins has been linked to plant resistance to bacterial pathogens. Transgenic plants producing a nondegradable form of

AXR2/IAA7 had a 10-fold reduction in *Pseudomonas syringae* growth (360). Furthermore, in transgenic plants expressing both nondegradable ARX/IAA7 and the *NahG* gene which encodes a bacterial salicylate hydroxylase that degrades endogenous SA, bacterial growth was drastically reduced compared to plants expressing only *NahG* which are highly susceptible to *P. syringae* (360). Conversely, increased degradation of Aux/IAA proteins by over-expressing the Aux receptor *AFB1* resulted in increased growth of *P. syringae* pv. *tomato* and enhanced disease symptoms (364). Thus, alterations in Aux signaling can contribute to plant defense against pathogens.

1.6 Research Objective

A plant virus's ability to establish a successful infection is often correlated with the virus's ability to gain access to the vascular tissue and travel systemically to reach distil part of the plant. A great number of studies have focused on identifying viral and host factors required for virus cell-to-cell movement through the PD, but comparatively little is known about viral systemic movement (7, 169). The work presented in this dissertation is aimed at understanding how the phloem environment is altered during viral infection and how the reprogramming of the phloem promotes viral phloem loading and systemic movement. Studies were conducted using TMV and *Arabidopsis thaliana* as model systems. *A. thaliana* ecotype Shahdara is extremely susceptible to TMV infection. Levels of viral accumulation, rate of cell-to-cell spread, rate of long distance movement through the phloem, and display of disease symptoms in Shahdara were similar to other highly susceptible hosts such as

tobacco, pepper and tomato (365). *A. thaliana* also has the advantage of a mapped and annotated genome and a wealth of genetic information available (366, 367). Thus, the TMV-Shahdara system is ideal to study virus induced changes to phloem gene expression.

Previous work identified an interaction between the TMV replication protein and select Aux/IAA proteins (212, 213). My initial studies identified that all three interacting Aux/IAAs are expressed in the phloem vascular tissue. Further studies focused on IAA26 because it is the highest expressed and has the greatest degree of interaction with the TMV replication protein. Results from these studies showed the interaction between TMV with IAA26 occurs in phloem CCs and the TMV-IAA26 interaction promotes viral phloem loading and systemic movement. Additionally, since IAA26 is a transcriptional regulator my objective was to identify potential downstream target genes using RNAseq transcriptome analysis. Plant lines expressing Aux degradation resistant IAA26-P108H from the IAA26 native promoter were compared to control non-transformed plant lines to identify potential downstream targets of IAA26 regulation. Results from this study identified alterations in genes involved in callose deposition at the PD viral movement, and SA and JA mediated defense responses. The experiments described in this first objective are presented in Chapter 2 and have been submitted to PNAS for publication. Meenu Padmanabhan created the pIAA26::GUS plant lines and provided the stem cross section image shown for pIAA26::GUS in Fig. 2.1. The experiment shown in Fig. 2.6B was done by Yi-Chen Hsieh.

My second objective was to characterize the effects of virus infection on the phloem cellular environment. This objective focuses on identifying the phloem specific genes and pathways that are altered during TMV infection. The expression of FLAG-tagged ribosomal proteins from two phloem specific promoters was used to isolate the population of ribosome bound mRNAs termed the translatome. FLAG-tagged ribosomal proteins were also expressed from the CaMV 35S promoter as a control. RNAseq analysis of the translatome populations identified phloem expressed transcripts that are altered during TMV infection. The genes and pathways identified represent candidates that may be important for the movement of macromolecules, such as the TMV virion, through the phloem vascular tissue. This study is being prepared for publication and will be submitted to Molecular Plant-Microbe Interactions journal.

Chapter 2: Tobacco Mosaic Virus Directed Reprogramming of Auxin/Indole Acetic Acid Protein Transcriptional Responses Enhances Phloem Loading

2.1 Introduction

To establish a systemic infection, plant viruses must access their host's vascular phloem. The first step in this process involves cell-to-cell movement through intercellular cytoplasmic and endo-membrane connections called plasmodesmata (PD). Virus movement through the PD is facilitated by viral movement proteins (MP) that function to modulate the size exclusion limits (SEL) of the PD allowing virus transport forms composed of either nucleoprotein complexes or virions to pass between cells (201, 368). For systemic movement viruses must "load" into the vascular phloem. Phloem loading requires passage through specialized branched PD connections known as pore units that occur between companion cells (CC) and phloem sieve elements (SE) (369). Once in the anucleate SEs, viruses move following the source to sink path of photoassimilates to distal plant tissues. In addition to the transport of photoassimilates, the vascular phloem also serves as a conduit for the movement of numerous host components including proteins, mRNA, micro-RNAs and small molecules involved in a range of plant responses including development and flowering as well as abiotic and biotic stress responses (370-372). It is clear that the vascular phloem functions as a gatekeeper between distal plant tissues, controlling the passage of numerous molecules that affect many aspects of plant physiology as well as responses to outside stimuli. Thus, to establish a systemic

infection, plant viruses must usurp this gateway. However, how plant viruses appropriate the vascular phloem remains a fundamental question in plant virology.

There have been a number of virus and host components shown to impact virus systemic movement (7, 201). For *Tobacco mosaic virus* (TMV) systemic transport via the phloem involves the viral coat protein (CP), P30 MP and 126/183 kDa replication proteins. Both the MP and replication protein are required for cell-to-cell movement via the PD (20). Phloem loading and systemic movement also involves the MP and replication protein, as transit via PD is necessary to access the SEs. In addition, a functional virus CP is also required for TMV systemic movement. Mutations that disrupt CP expression or its ability to form virions are known to inhibit systemic movement (95, 105, 166). Furthermore, chimeric TMV recombinants encoding the MP or CP of the orchid infecting Tobamovirus *Ondontoglossum ringspot virus* display impaired systemic movement in tobacco despite replication levels and virion assembly rates that are similar to TMV (93, 373). Similarly, virus movement assays involving CP and MP chimeric recombinants derived from another Tobamovirus, *Sun-hemp mosaic virus,* also demonstrate a role for the viral replication proteins in vascular movement (187). Combined these findings suggest a host selective gating mechanism involving multiple virus – host interactions as essential factors in TMV phloem loading.

Several host components have also been found to impact the systemic spread of TMV. Many of these host factors affect PD gating and have been reviewed in detail (7, 20, 201)**.** However, there is an emerging link between virus systemic movement and transcriptional reprograming. For example, the crucifer strain of

TMV-cg has been shown to modulate the expression of a WRKY8 transcription factor while the P30 protein from *Tomato mosaic virus* (ToMV) associates *in vivo* with the transcriptional co-activator KELP (199, 200). WRKY transcription factors are associated with basal defense responses and suppression of WRKY8 during infection correlates with enhanced TMV-cg systemic accumulation (200). Similarly, overexpression of KELP resulted in the partial relocation of P30 to the nucleus and prevented ToMV cell-to-cell and systemic movement. Furthermore, the P30 protein from the Tobamovirus *Turnip vein clearing virus* (TVCV) encodes a unique nuclear localization signal required for both cell-to-cell and systemic virus movement (198). Within the nucleus the TVCV P30 accumulated in chromatin associated F-actin containing filaments. These P30 associated chromatin structures were speculated to alter gene expression as a means to promote virus infection (198). These studies provide evidence that virus interactions with host associated transcriptional regulators can modulate systemic virus movement. However, the mechanisms behind this reprogramming and its impact on virus systemic movement have not been identified.

In our previous studies we identified an interaction between the 126/183 kDa replication protein of TMV and specific auxin/indole acetic acid (Aux/IAA) host transcriptional regulators (212, 213, 374). These studies show that the helicase domain present within the virus replication protein strongly interacts with Aux/IAA member IAA26 and more weakly with IAA27 and IAA18 in Arabidopsis as well as an IAA26 homologue in tomato. Members of the Aux/IAA family encode short-lived nuclear proteins that mediate Aux dependent gene expression (375-377). Based on current evidence, Aux/IAA proteins interact with Aux responsive transcription factors

(ARFs) that in turn regulate numerous Aux responsive genes (322, 340). Within Arabidopsis there are 29 Aux/IAA family members and 23 ARF members capable of forming an array of hetero- and homo-complexes from which to orchestrate Aux signaling (337, 338, 378). Within the plant, Aux binds TIR1/AFB F-box proteins of the SCF E3 ubiquitin ligase complex, promoting their association with Aux/IAA proteins (320-322, 376). Ubiquitination of Aux/IAA results in targeted degradation via the 26S proteasome (322, 379). The plants Aux gradient thus provides a spatially sensitive means to regulate Aux/IAA activity via targeted proteolysis.

Cellular localization studies demonstrate the nuclear localization of interacting Aux/IAA proteins to be disrupted during TMV infection (212, 213). In contrast, Aux/IAA proteins remain nuclear localized during infection by non-interacting viruses. Subsequent analysis indicates that viruses with reduced abilities to interact with Aux/IAA proteins are compromised in the ability to accumulate and move in inoculated tissue (374). Interestingly, effects on virus accumulation are observed only in mature tissues and not in younger immature tissues (374). This developmental relationship corresponds to the accumulation of Aux/IAA proteins in mature tissues and is consistent with the lower Aux levels and reduced Aux mediated degradation found in older plant tissues (374, 380). Evidence from these studies suggests that TMV targeted disruption of Aux/IAA proteins functions to reprogram the transcriptome of mature host tissues to enhance virus infection.

In this study the mechanism through which the TMV - Aux/IAA interactions affect virus accumulation and spread was investigated. Results indicate that interacting Aux/IAA proteins are predominantly expressed in the CC of mature

vascular phloem tissues. The ability to disrupt the nuclear localization of these Aux/IAAs was found to correlate with enhanced virus phloem loading and movement within the vascular tissues. As a result, TMV with the ability to interact with Aux/IAA proteins gains a significant advantage in systemic movement over a virus defective in this interaction. Transcriptome analysis of plant genes under the control of an interacting Aux/IAA protein identified an array of host genes linked to plant defense responses, virus cell-to-cell movement and PD regulation. Many of these genes have been previously shown to affect virus movement including pectin methylesterase and callose binding proteins. In addition, genes associated with salicylic acid (SA) and jasmonic acid (JA) defense pathways also show significant alterations in expression. Based on these studies we propose that TMV selectively targets phloem expressed Aux/IAA proteins in order to reprogram functions of the CC-SE complex that contribute to phloem loading.

2.2 Results

2.2.1 Interacting Aux/IAA Factors are Expressed and Localize within the Nucleus of Phloem Companion Cells

To define the importance of the Aux/IAA interaction on TMV accumulation, we first examined the expression patterns of three known interacting Arabidopsis Aux/IAA proteins. Previously IAA26, IAA27 and IAA18 were identified as interacting with and displaying varying levels of cytoplasmic co-localization with the TMV 126 kDa replication protein (212). The strength of the interaction corresponded to the level of cytoplasmic co-localization. IAA26 confers the strongest interaction

with the virus 126 kDa protein and shows the greatest disruption in nuclear localization, followed by IAA27 and IAA18. These past studies utilized only the *Cauliflower mosaic virus* 35S constitutive promoter to drive the expression of green fluorescent protein (GFP) tagged IAA proteins in whole leaf tissues. However, Aux/IAA family members are known to be differentially expressed and to confer tissue specific functions (376, 381). To determine the expression pattern of the three TMV126/183 kDa interacting Aux/IAAs, promoter sequences upstream of their translation start codons (2000 nt for *IAA26*, 1500 nt for *IAA27* and 2000 nt for *IAA18*) were all cloned in front of the *β*-glucuronidase (GUS) open reading frame (ORF) to create *pIAA26::GUS*, *pIAA27::GUS*, and *pIAA18::GUS*. All three promoter-reporter constructs were transformed into the systemic TMV host *Arabidopsis thaliana* ecotype Shahdara (365). Fully expanded leaves from T2 generation plants were histochemically stained for GUS activity. Results from three to four independent plant lines for each of the three interacting Aux/IAAs consistently showed the predominant GUS activity in vascular tissues however with distinct expression patterns (Fig. 2.1). *pIAA26::GUS* displayed the most robust expression with strong levels of GUS staining in all vein classes I, II, III and IV of the leaves. Conversely, *pIAA27::GUS* was predominately expressed in vein class I of the petiole. Like *pIAA26::GUS*, *pIAA18::GUS* expression was observed in the all vein classes, but at a markedly lower level, indicating that in leaf tissue *IAA18* is not as highly expressed as *IAA26* (Fig. 2.1A).

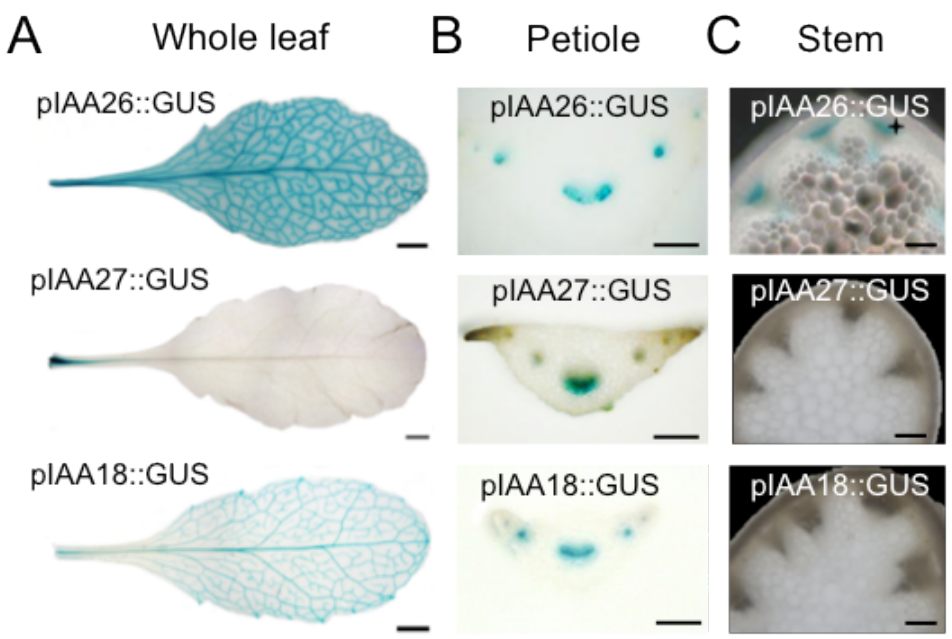

Fig. 2.1. Histochemical analysis of pIAA26::GUS, pIAA27::GUS and pIAA18::GUS expression in *A. thaliana* Shahdara leaves, petioles and stems. (A) GUS expression in seven week old leaves after staining overnight. Bars are 2 mm. (B) Petiole cross-sections. Bars are 200 µm. (C) Stem cross sections. Bars are 100 µm.

Petiole cross-sections of pIAA26::GUS, pIAA27::GUS, and pIAA18::GUS lines showed GUS staining predominantly localized to the phloem for all three interacting Aux/IAA family members (Fig. 2.1B). *pIAA26::GUS* expression was also observed in stem and root vascular phloem (Fig. 2.1C and Appendix A). In contrast *pIAA27::GUS* expression was not observed in stem or root vascular tissues but at the sites of lateral root formation (Appendix A). *pIAA18::GUS* expression was not observed in either stem or roots (Fig. 2.1C and Appendix A).

To further investigate the localization of Aux/IAA proteins we focused on IAA26 since it displays by far the strongest interaction with the TMV 126 kDa protein and as described above is the most abundantly expressed in leaf and root vascular tissues. However, Aux/IAA proteins are rapidly turned over, which can make detecting or visualizing Aux/IAA proteins difficult. To address this issue, we chose to use a previously generated IAA26 mutant allele, IAA26-P108H, which is resistant to Aux mediated degradation but is not altered in its ability to interact with the TMV 126/183 kDa protein (212). The native IAA26 promoter (2000 nt upstream of the start codon) was cloned in front of the IAA26-P108H ORF and fused to GFP, creating *pIAA26::IAA26-P108H-GFP*. This construct was used to transform *A. thaliana* ecotype Shahdara. Transgenic pIAA26::IAA26-P108H-GFP plant lines grew and developed similarly to non-transformed Shahdara (Fig. 2.2A). In addition, qRT-PCR analysis for the endogenous *IAA26* and transgene *IAA26-P108H-GFP* mRNAs show a similar expression pattern of increasing transcripts in older plant tissues (Fig. 2.2B).

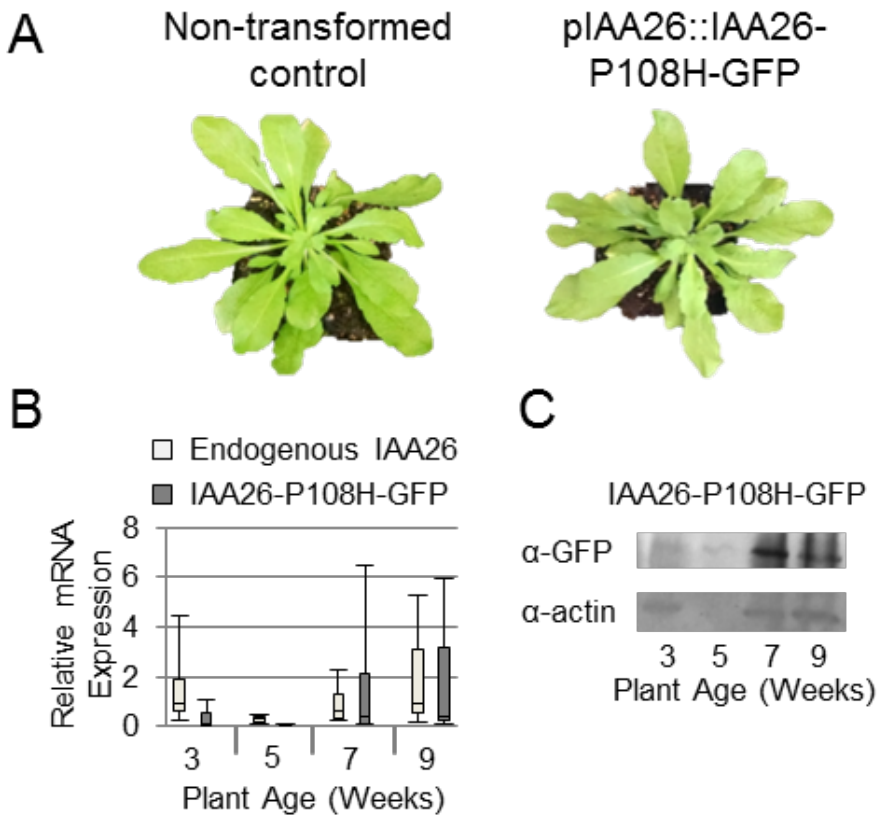

Fig. 2.2. Characterization of pIAA26::IAA26-P108H-GFP transgenic plant lines. (A) Representative image of seven week old non-transformed control Shahdara plant and pIAA26::IAA26-P108H-GFP transgenic Shahdara plant. (B) Relative mRNA expression of endogenous *IAA26* mRNA in control plants or *IAA26-P108H-GFP* mRNA expressed from the pIAA26::IAA26-P108H-GFP transgene in three to nine week old plants as measured by qRT-PCR. Total RNA was isolated from the leaves of four plants from two independent pIAA26::IAA26-P108H-GFP plant lines or non-transformed controls and pooled for each of three biological replicates. 18S RNA was used as an internal control for normalization. (C) Western immunoblot detection of IAA26-P108H-GFP protein levels in three to nine week old pIAA26::IAA26-P108H-GFP transgenic plants as probed with anti-GFP antibody. Actin levels were used as a loading control.

Thus, transgenic pIAA26::IAA26-P108H-GFP plants express *IAA26-P108H-GFP* mRNA in a manner similar to the endogenous *IAA26* gene. Consistent with the mRNA expression analysis the IAA26-P108H-GFP protein is predominantly detectable by western immunoblot in seven to nine week old tissues (Fig. 2.2C). Subsequent petiole cross-sections from T2 generation plant lines showed IAA26-P108H-GFP fluorescence specifically expressed and localized to the nuclei of phloem-associated CCs (Fig. 2.3). Similar to immunoblot studies, detection of IAA26-P108H-GFP fluorescence occurred only in seven to eleven-week-old tissues. From these studies it is clear that interacting IAA26 is primarily expressed within older leaf and stem phloem CCs.

2.2.2 TMV Disrupts the Nuclear Localization of Interacting IAA26 within Phloem Companion Cells

To examine pIAA26::IAA26-P108H-GFP nuclear localization in response to TMV infection, nine to eleven-week-old T2 plants from two independent lines were infected with TMV and observed for IAA26-P108H-GFP fluorescence at 12 days post inoculation (dpi). Within TMV infected tissues the number of phloem cells displaying IAA26-P108H-GFP derived nuclear fluorescence was reduced seven-fold in comparison to mock-inoculated tissues (Fig. 2.4A and C). In contrast, tissues infected with TMV-V1087I, a mutant virus able to replicate in protoplasts at levels similar to TMV but that does not interact with IAA26 did not disrupt the nuclear localization of IAA26-P108H-GFP in CCs (188, 213) (Fig. 2.4A and B). Thus, TMV disrupts the nuclear localization of an interacting Aux/IAA protein expressed within its native CC environment.

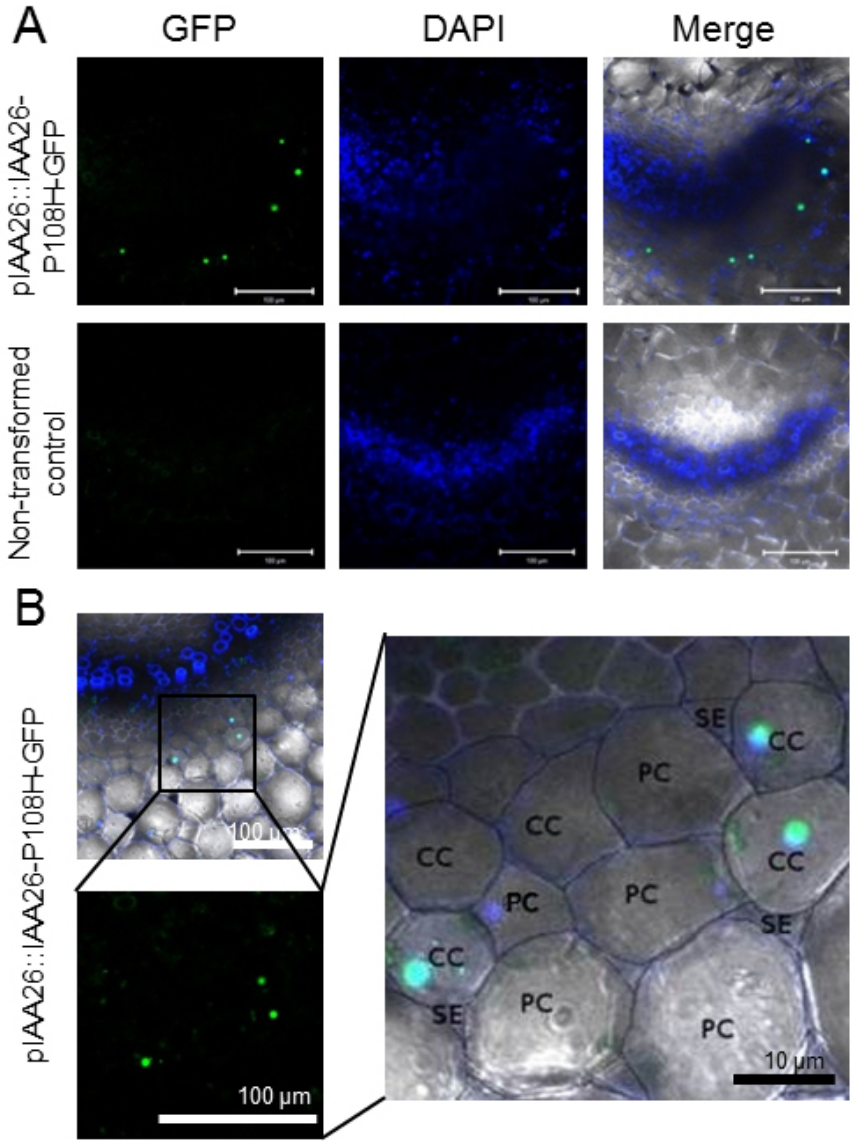

Fig. 2.3. Localization of IAA26-P108H-GFP expressed from the *IAA26* native promoter in *A. thaliana* Shahdara petioles. (A) Representative fluorescent images of cells expressing IAA26-P108H-GFP from the *IAA26* native promoter or non-transformed controls. Petioles from nine to eleven week old T2 generation plants were hand sectioned for imaging. Green - GFP, Blue - DAPI. Bars are 100 µm. (B) Localization of IAA26-P108H-GFP in companion cell nuclei. CC companion cells, SE sieve elements, PC phloem parenchyma cells.

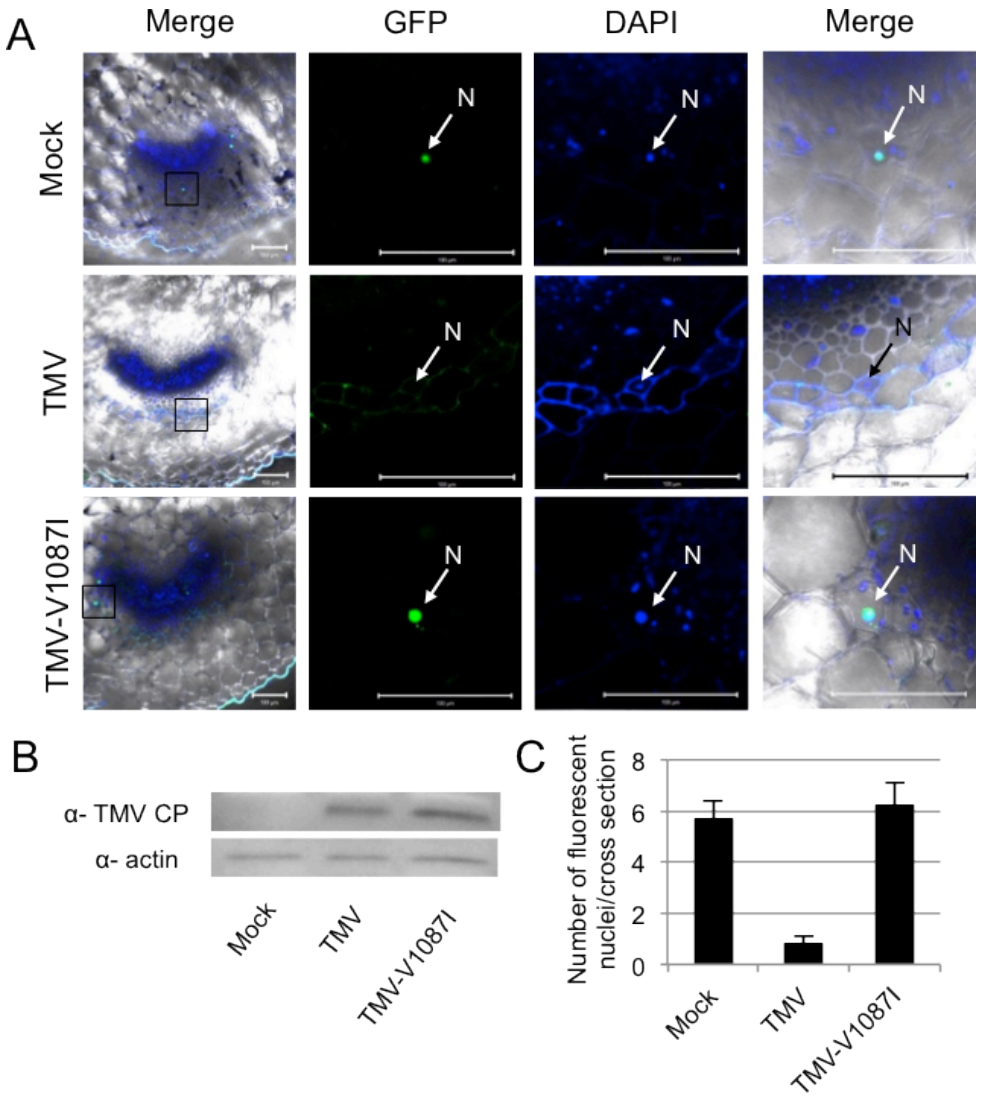

Fig. 2.4. Localization of IAA26-P108H-GFP in virus infected tissue.

(A) Representative fluorescent images of cells expressing IAA26-P108H-GFP in mock infected, TMV infected or TMV-V1087I infected phloem tissue. Inoculated leaf petioles were hand sectioned and imaged 12 dpi. Bars are 100 μm. N indicates nucleus. (B) Western immunoblot for the detection of the TMV CP present in the investigated cross-sections of pIAA26::IAA26-P108H-GFP plants at 12 dpi using actin levels as a loading control. (C) Quantification of cell nuclei with GFP fluorescence averaged from ten petiole cross sections ± standard error.

2.2.3 Stabilization of IAA26 Expressed From its Native Phloem Promoter Inhibits TMV Accumulation

A. thaliana ecotype Shahdara lines transformed with *pIAA26::IAA26-P108H-GFP* were used to assess the effect of IAA26 accumulation on TMV infection. We hypothesized that stabilization of IAA26 within the phloem CCs, resulting in greater accumulation of the protein prior to virus infection, would significantly impact the ability of both TMV and the non-interacting TMV-V1087I to accumulate in leaf tissues. Studies above indicated that IAA26-P108H-GFP protein accumulation is consistently detectable by seven weeks in transformed Shahdara (Fig. 2.2C). TMV and TMV-V1087I infections were subsequently monitored in both seven and nine-week-old plants using two independent lines expressing IAA26-P108H-GFP from the native IAA26 promoter or in non-transformed control plants at three, six and nine dpi. Virus accumulation was measured by western immunoblot analysis using an antibody specific for the TMV CP. In seven week old non-transformed plants, both TMV and TMV-V1087I accumulate to similar levels. Conversely, in seven-week-old pIAA26::IAA26-P108H-GFP plants TMV-V1087I accumulated to significantly lower levels ($p = 0.014$, student t-test) than TMV (Fig. 2.5A). Thus, stabilization and over accumulation of IAA26 in younger seven-week-old tissues significantly impacts the ability of this non-Aux/IAA interacting virus to accumulate.

In nine-week-old non-transformed plants TMV-V1087I accumulated to significantly lower levels ($p = 0.006$, student t-test) than TMV (Fig. 2.5B). This is consistent with our previous findings that demonstrated reduced accumulation of the non-Aux/IAA interacting TMV-V1087I occurred only in older leaf tissues (374).

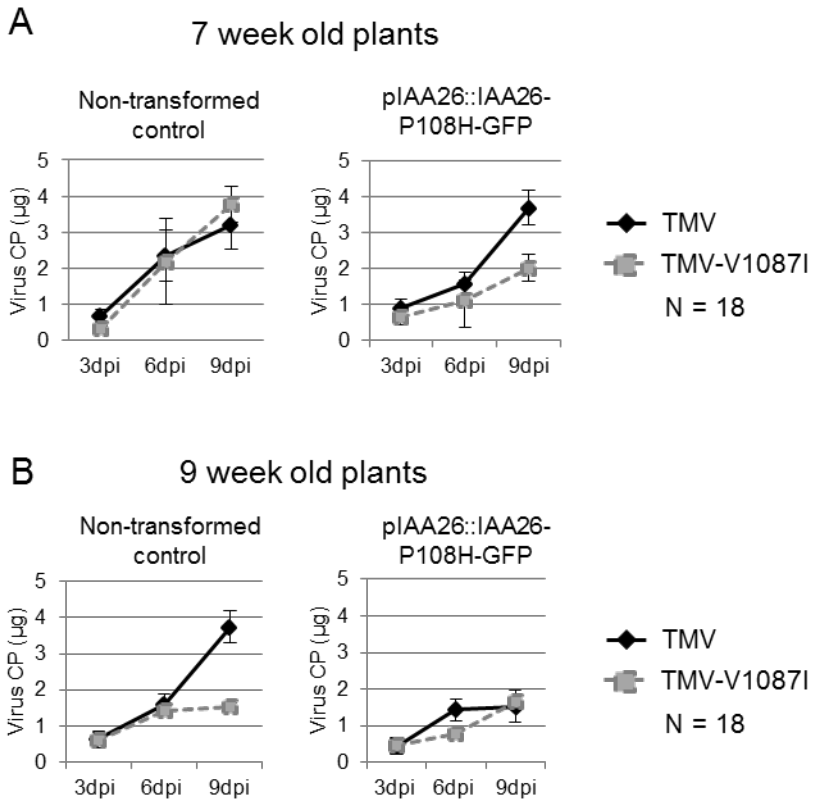

Fig. 2.5. Accumulation of TMV and TMV-V1087I in pIAA26::IAA26-P108H-GFP and non-transformed control *A. thaliana* Shahdara leaf tissue. (A) Virus accumulation in seven week old inoculated leaves at three, six and nine dpi. (B) Virus accumulation in nine week old inoculated leaves at three, six and nine dpi. Each data point represents the average and standard error derived from 18 independent leaves each inoculated with ten µg of TMV or TMV-V1087I. Virus infection was monitored for accumulation of TMV CP by western immunoblotting and quantified using known CP standards. Actin was used as a loading control.

However, in nine-week-old pIAA26::IAA26-P108H-GFP plants TMV accumulated at significantly lower levels than in non-transformed control plants ($p = 0.046$, student t-test) and at a level similar to the non-interacting TMV-V1087I (Fig. 2.5B). Together these findings indicate that the accumulation of IAA26-P108H-GFP prior to infection creates a cellular environment that is not conducive to infection and cannot be overcome by the TMV – Aux/IAA interaction.

2.2.4 Aux/IAA Interaction Enhances TMV Phloem Loading and Accumulation

To identify the mechanism through which IAAs disrupt TMV accumulation, we investigated the ability of both interacting TMV and non-interacting TMV-V1087I to spread within inoculated leaves. For this approach we first developed a tobacco system for the *in situ* detection of TMV and tobacco IAA26. Previously we identified TMV 126/183 kDa interacting Aux/IAA genes in both Arabidopsis and tomato (213, 374). In this study we cloned the corresponding *Nicotiana benthamiana* *Nb*IAA26 and found it shares sequence identity and similarity of 96% and 97% to *Nicotiana tabaccum Nt*IAA26 and 51% and 64% to *Arabidopsis thaliana At*IAA26, respectively (Appendix B). Similar to our previous studies with the Arabidopsis and tomato IAA26 homologues, yeast two-hybrid analysis demonstrated the *Nb*IAA26 protein interacts with the TMV 126/183 kDa helicase domain but not with the TMV-V1087I helicase domain (Appendix C). In addition, localization studies using a transiently expressed *Nb*IAA26 fused to GFP also demonstrated that in the presence of the interacting TMV, *Nb*IAA26 relocalizes from the nucleus to the cytoplasm but is unaffected by infection with the non-interacting TMV-V1087I (Appendix C). We also examined the cellular expression pattern of *Nb*IAA26 mRNA using *in situ*

hybridization. These experiments were performed on fixed stem tissue using a digoxigenin labeled probe specific for the *Nb*IAA26 sequence. Results clearly indicate that *Nb*IAA26 mRNA is predominantly expressed in the vascular tissues of *N. benthamiana* stem sections (Appendix C). Thus, as in Arabidopsis, TMV appears to be targeting similar vascular expressed tobacco Aux/IAAs.

To examine the effect of the *Nb*IAA26 interaction on the cellular movement of TMV, *in situ* hybridization was used for analyzing the accumulation of TMV and TMV-V1087I (non-IAA interacting) in inoculated leaves of *N. benthamiana*. Previous protoplasts studies comparing TMV and TMV-V1087I revealed no significant differences in the replication of these viruses in single cells (188). However, consistent with our previous findings in Arabidopsis, the non-interacting TMV-V1087I virus accumulates to significantly lower levels ($p = 0.004$, student t-test) in mature tissues than those observed for TMV (Fig. 2.6A). For this study mature *N. benthamiana* leaves were inoculated with either TMV or TMV-V1087I, harvested at four and seven dpi and subjected to *in situ* immuno detection for the TMV CP. Results indicate that at four dpi both TMV and TMV-V1087I show defined infection foci that are similar in size and appearance (Fig. 2.6B). In contrast, at seven dpi TMV shows significant accumulation along the veins and vascular networks of the leaf while TMV-V1087I shows continued cell-to-cell spread but limited accumulation within the vascular networks. These findings indicate that a non-Aux/IAA interacting virus is reduced in its ability to load into the vascular network.

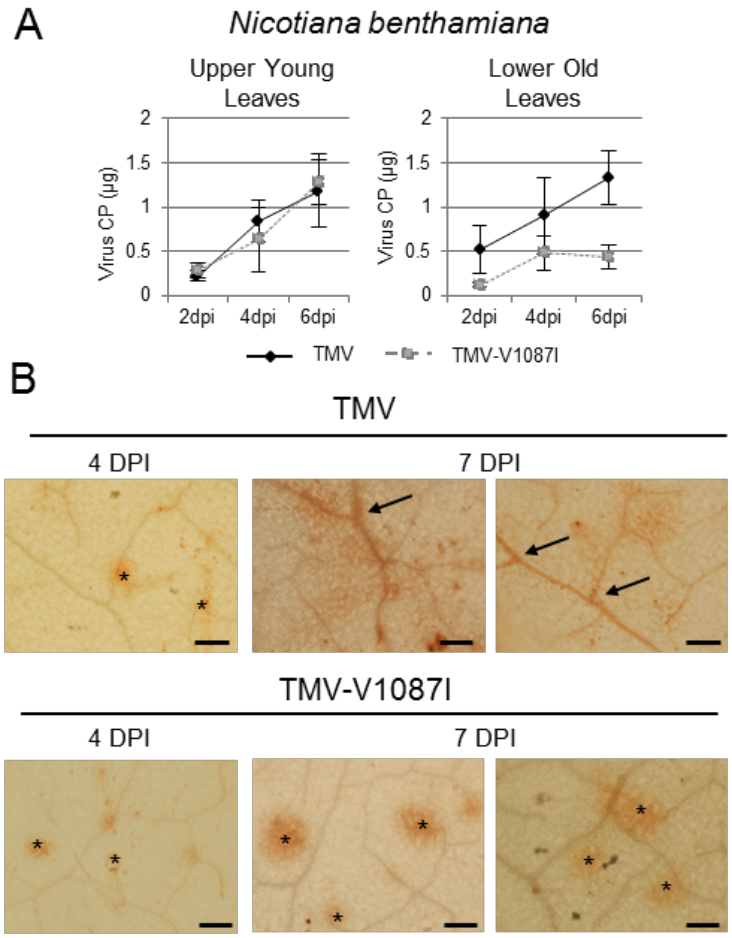

Fig. 2.6. Accumulation and phloem loading of TMV and TMV-V1087I in *N. benthamiana* leaves. (A) Virus accumulation in upper young and lower old inoculated leaves at two, four and six dpi. Each data point represents the average and standard error derived from six independent leaves inoculated with five µg of TMV or TMV-V1087I. Virus infection was monitored for accumulation of TMV CP by western immunoblotting and quantified using CP standards. (B) *In situ* immunolocalization for the accumulation of TMV CP using anti-CP antibody. A positive response for the TMV CP is visualized as a brown stain in the cleared *N. benthamiana* leaves. Arrows denote TMV accumulation in vascular tissue. Asterisks denote TMV accumulation in mesophyll. Bars are 3 mm.

To further investigate the role of the interacting Aux/IAA proteins on TMV phloem loading, we performed similar *in situ* immuno detection for TMV in transgenic *A. thaliana* Shahdara pIAA26::IAA26-P108H-GFP plants. We reasoned that in nine week old plants the cumulative effects of IAA26-P108H-GFP over accumulation would lead to threshold alterations in vascular traits that are restrictive to TMV phloem loading. For these experiments leaves from nine week old plants were harvested for analysis at nine dpi. Results indicate that TMV shows significant accumulation within the vascular tissues of non-transformed control plants (Fig. 2.7A). In contrast, in plants expressing IAA26-P108H-GFP, TMV produces detectable viral accumulation at initial infection foci but little accumulation within the vascular tissues (Fig. 2.7B). This finding confirms that accumulation of IAA26-P108H-GFP prior to infection leads to reduced vascular loading of TMV. These findings are also consistent with the *in situ* virus studies done above in *N. benthamiana* (Fig. 2.6B) and explain the observed reduced accumulation of TMV in older nine week old pIAA26::IAA26-P108H-GFP plants (Fig. 2.5B). Combined these findings indicate that the ability to disrupt the nuclear localization of specific CC expressed Aux/IAA proteins contributes to TMV phloem loading and vascular movement. To address specificity of observed phloem loading restrictions we utilized a fluorescent dye based cell to cell movement and phloem loading assay. Several studies have demonstrated that changes in plasmodesmata SEL and vascular movement can be monitored using 5(6)-carboxyfluorescein diacetate, a membrane permeable non-fluorescent dye that upon cell entry is cleaved by esterases to produce

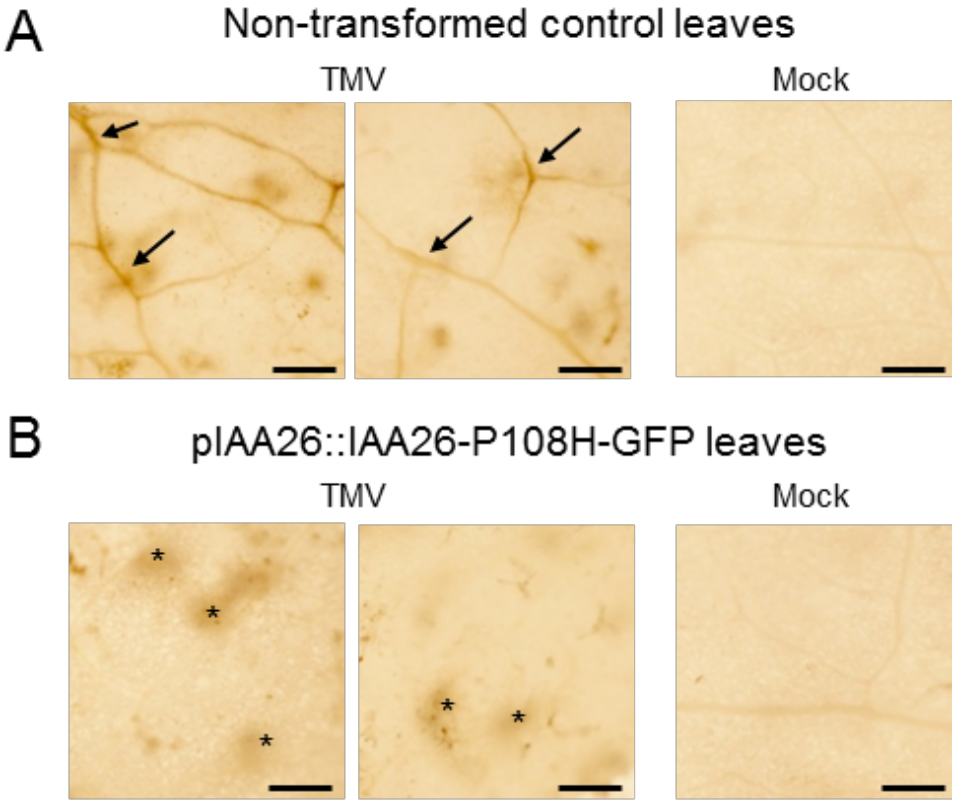

Fig. 2.7. *In situ* immunolocalization for the TMV CP in pIAA26::IAA26-P108H-GFP *A. thaliana* Shahdara leaves at nine dpi infected with ten µg of TMV.

(A) Immunolocalization in nine week old non-transformed control leaf tissue infected with TMV, two representative panels, or mock infected, one representative panel. (B) Similar immunolocalization panels for TMV CP in nine week old leaf tissue from pIAA26::IAA26-P108H-GFP plants similarly infected with TMV or mock infected. Arrows denote TMV accumulation in the veins visualized as a brown stain. Asterisks denote TMV accumulation in mesophyll. Bars are 1 mm.

5(6)-carboxyfluorescein (CF), a non-membrane permeable fluorescent dye (171, 228, 382). In these experiments we compared CF mobility in nine-week-old non-transformed control and pIAA26::IAA26-P108H-GFP plants. CF mobility showed no difference between IAA26-P108H-GFP and the control plants (Appendix D). Consistent with previous studies, treatment of these plants with SA 24 hrs prior to CF application produced significant reductions in fluorescence movement (Appendix D). Reduced CF movement after SA treatment has been attributed to the deposition of callose at the PD (228). The inability of pIAA26::IAA26-P108H-GFP plants to affect CF movement indicates that the observed restriction in TMV phloem loading is not the result of non-specific effects on PD gating. Thus, effects on phloem loading directed by IAA26-P108H-GFP are likely to be specific to TMV or other large macromolecules.

2.2.5 Aux/IAA Interactions Confer a Competitive Advantage

To determine the impact of Aux/IAA interactions on TMV systemic movement we performed mixed infection assays for the accumulation of TMV and TMV-V1087I in systemic non-inoculated leaf tissues. For these assays a single lower leaf of *N. tabaccum* plants with at least six fully expanded leaves was inoculated with TMV, TMV-V1087I or 1:1, 1:5 or 1:10 ratio of TMV to TMV-V1087I. At ten dpi symptomatic systemic leaf tissue was harvested and cDNA generated from total RNA. Quantitative sequencing for the V1087I mutation was used to determine the relative concentrations of each virus in the systemic tissue (383). Results indicated that inoculation ratios of greater than five times TMV-V1087I to TMV were required for TMV-V1087I to be the predominant systemic virus (Fig. 2.8).

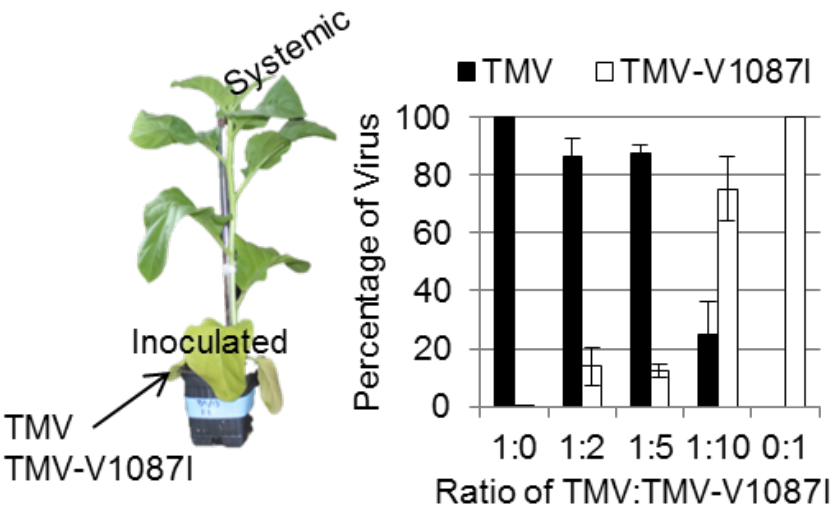

Fig. 2.8. Competitive accumulation of Aux/IAA interacting TMV vs the non-Aux/IAA interacting TMV-V1087I. In this assay the lower leaves of *N. tabaccum* cv. Xanthi plants were inoculated with one of five inoculation treatments: single inoculation with either TMV or TMV-V1087I and simultaneous inoculations with either 1:1, 1:5 or 1:10 ratios of TMV to TMV-V1087I. The infectivity of TMV and TMV-V1087I inoculum was determined by local lesion assays on *N. tabaccum* cv. Xanthi-NC and standardized to insure an equal infection potential. RNA was isolated from systemic leaves upon appearance of mosaic disease symptoms at ten dpi. The relative amount of each virus was determined by quantitative sequencing (383). Each bar represents the average of three independent plants ± standard error.

As a control, plants inoculated with only TMV-V1087I did not yield reversions to the TMV sequence, demonstrating that this mutation is stable. Together these results suggest that interaction with Aux/IAA proteins significantly enhances the ability of TMV to load into the vascular tissue and move systemically.

2.2.6 IAA26 Directed Transcriptional Reprogramming

To identify genes regulated by IAA26 we compared the transcriptome of seven week old pIAA26::IAA26-P108H-GFP transgenic plants to non-transformed control plants. These plants were selected for analysis because at this age IAA26-P108H-GFP protein accumulates to high levels and induces a significant reduction in the accumulation of TMV-V1087I (Figs. 2.2C and 2.5A). For transcriptome analysis, mRNA from three biological replicates, each composed of leaves from four to six plants combined from two independent T2 generation pIAA26::IAA26-P108H-GFP plant lines or similarly grown non-transformed control plants, were used to construct cDNA libraries for RNAseq analysis. Results showed 1,228 genes were significantly altered (> 2-fold change and FDR p-value < 0.05) in pIAA26::IAA26-P108H-GFP plants compared to non-transformed control plants (Dataset S1). 236 of these genes were altered more than ten-fold, and 28 genes were reduced more than 100-fold. Overall we observed that the majority of the transcripts (78.5%) were reduced in IAA26 stabilized plants, while only 21.5% were up regulated. Additionally, 70% of the identified transcriptionally altered genes contain at least one ARF binding - auxin responsive element (AuxRE) in their promoter region within 1500 bp upstream of the start codon and 35% of identified genes contain an AuxRE within 500 bp upstream of

the start codon, indicating that a significant portion of these genes could be directly impacted by the excess accumulation of IAA26-P108H-GFP.

Gene ontology (GO) annotations were incorporated into our gene list and hypergeometric distributions used to identify GO categories that occur more frequently in our subset of differentially expressed genes as compared to that expected by chance (384, 385). We found that genes annotated as involved in 'response to stress' were over represented and accounted for 21% of the 1,228 genes displaying altered expression levels in Aux resistant pIAA26::IAA26-P108H-GFP plants (Dataset S1). More specific categories of over represented genes included 54 genes involved in 'response to wounding', 46 genes involved in 'systemic acquired resistance' 43 genes involved in 'response to salicylic acid' and 65 genes involved in 'response to jasmonic acid' (Table 2.1 and Dataset S1). In addition, genes that respond to Aux were also found to be overrepresented in the transcriptome analysis, which is consistent with IAA26-P108H-GFP functioning in Aux regulation (Dataset S1). Additional differentially expressed groups of genes that were not found to be overrepresented but of known impact on virus biology were also identified including those involved in callose deposition (14 genes) and virus movement (three genes) (Table 2.1).

Table 2.1. Subset of genes differentially expressed in IAA26 stabilized plants with known links to virus movement or defense responses.

AGI Identifier[1]	Gene Name	Fold Change[2]	AuxRE[3] 500bp	AuxRE[3] 1500bp	Description[4]
Callose					
AT2G02310	PP2-B6	15.86	0	2	defense response by callose deposition
AT1G72520	LOX4	9.21	0	1	defense response by callose deposition
AT4G17615	CBL1	3.75	0	0	defense response by callose deposition
AT3G04010	O-Glycosyl hydrolases family 17	2.75	0	0	β-1,3-glucanase
AT4G39950	CYP79B2	2.61	1	1	defense response by callose deposition
AT4G18010	AT5PTASE2	2.50	1	3	defense response by callose deposition
AT4G31500	CYP38B1	2.48	0	3	defense response by callose deposition
AT5G62570	CBP60A	2.36	1	1	defense response by callose deposition
AT1G74360	LRR protein kinase family	2.25	0	1	defense response by callose deposition
AT1G18650	PCBP3	-2.20	1	2	callose binding
AT1G06490	CalS7, GSL7	-2.14	0	0	callose synthase
AT4G29360	O-Glycosyl hydrolases family 17	-2.68	0	1	β-1,3-glucanase
AT5G67460	O-Glycosyl hydrolases family 17	-3.57	0	2	β-1,3-glucanase
AT5G08000	PCBP2	-6.45	0	0	callose binding
Virus Movement					
At2G33330	PDLP3	-2.22	1	2	PD-mediated intercellular transport
AT3G47690	EB1A	-2.49	0	1	viral process
AT5G47500	PME5	-12.07	1	1	cell wall modification
SA Mediated Defense					
At2G35980	NHL10	30.42	1	1	SA mediated signaling pathway
AT1G71390	RLP11	22.18	0	0	SA mediated signaling pathway
At2g14610	PR1	10.57	0	1	response to SA, marker for SAR
AT3G57260	PR2	8.42	0	1	response to SA, marker for SAR

AT1G28480	GRX480, ROXY19	6.63	1	1	SA inducible, SA/JA cross-talk
AT4G27410	ANAC072	5.76	0	0	inhibition of SA synthesis
AT4G04490	CRK36	5.18	0	2	SA mediated signaling pathway
AT1G52890	ANAC019	4.89	0	0	inhibition of SA synthesis
AT4G14365	XBAT34	4.24	0	0	SA mediated signaling pathway
AT2G32680	RLP23	4.19	0	1	SA mediated signaling pathway
AT1G75040	PR5	3.89	0	4	response to SA, marker for SAR
AT5G60900	RLK1	2.31	0	0	SA mediated signaling pathway
AT1G74360	LRR protein kinase family	2.25	0	1	SA mediated signaling pathway
AT2G17290	CPK6	2.16	1	2	SA mediated signaling pathway
AT3G05660	RLP33	2.15	2	2	SA mediated signaling pathway
AT5G10380	RING1	2.04	0	2	SA mediated signaling pathway
AT4G33070	PDC1	-6.21	0	1	SA mediated signaling pathway
AT3G02550	LBD41	-6.68	1	4	SA mediated signaling pathway
AT5G15120	PCO1	-9.79	0	0	SA mediated signaling pathway
AT1G43800	SAD6	-156.34	0	0	SA mediated signaling pathway
JA Signaling					
AT2G44810	DAD1	32.97	2	2	JA biosynthesis
AT2G34600	JAZ7	30.96	0	1	negative regulator of JA signaling
AT5G63450	CYP94B1	21.47	1	3	oxidative turnover of JA-Ile
AT2G27690	CYP94C1	17.95	0	0	oxidative turnover of JA-Ile
AT1G17420	LOX3	15.49	0	1	jasmonic acid biosynthetic process
At3G22275	JAZ13	13.67	1	3	negative regulator of JA signaling
AT1G30135	JAZ8	11.53	0	0	negative regulator of JA signaling
AT1G17380	JAZ5	9.96	0	3	negative regulator of JA signaling
AT1G72520	LOX4	9.21	0	1	jasmonic acid biosynthetic process
AT5G13220	JAZ10	9.05	1	1	negative regulator of JA signaling
AT1G19180	JAZ1	6.81	0	1	negative regulator of JA signaling

AT3G25780	AOC3	6.42	1	4	JA biosynthesis
AT2G06050	ORP3	5.80	0	1	JA biosynthesis
AT1G74950	JAZ2	3.04	0	1	negative regulator of JA signaling
At1G32640	MYC2	2.60	0	0	bHLH transcriptional activator
AT2G46510	JAM1	2.45	0	2	bHLH transcriptional activator
AT1G01260	JAM2	2.10	0	1	bHLH transcriptional activator
WRKY Transcription Factors					
At5g24110	WRKY30	7.46	0	0	WRKY transcription factor
At2g40740	WRKY55	5.53	1	3	WRKY transcription factor
At5g64810	WRKY51	3.38	1	1	WRKY transcription factor
At5g22570	WRKY38	3.23	0	1	WRKY transcription factor
At3g01080	WRKY58	2.93	1	3	WRKY transcription factor
At2g37260	WRKY44	-2.85	0	1	WRKY transcription factor
At2g34830	WRKY35	-14.01	0	0	WRKY transcription factor
At2g44745	WRKY12	-15.67	1	2	WRKY transcription factor
At1g30650	WRKY14	-25.84	2	2	WRKY transcription factor

[1]AGI Identifier - unique locus identifier that is part of the Arabidopsis genome sequence annotation at TAIR (367).

[2]RNAseq fold change expression values determined after empirical analysis of digital gene expression using the CLC Genomics Workbench (386). The RNAseq experiment compares three biological replicates of A. thaliana Shahdara pIAA26::IAA26-P108H-GFP plants to three biological replicates of non-transformed *A.thaliana* Shahdara control plants.

[3]Number of auxin responsive elements (AuxRE) found in the upstream promoter region of each gene. AuxRE is defined as a pattern match to TGTCTC, TGTCGG, or TGTSTSBC on either strand 500bp or 1500bp upstream of the start codon.

[4]Description of the predicted biological process each gene is involved in collected from TAIR (367).

As a means to validate our transcriptome analysis we selected a set of eight genes that displayed varying levels of regulation in response to the over accumulation of IAA26-P108H-GFP for further qRT-PCR analysis. Total RNA from two new seven-week-old biological replicates was isolated from the leaves of four to six plants from two independent pIAA26::IAA26-P108H-GFP plants lines. qRT-PCR results clearly demonstrated that the mRNA levels for each of the eight selected genes mirrored that obtained in our RNAseq studies (Fig. 2.9A). In addition, we also compared mRNA levels from the leaf tissue of both three and seven week old pIAA26::IAA26-P108H-GFP plants. We speculated that if these genes are being altered due to the over accumulation of IAA26-P108H-GFP then this regulation should occur primarily older tissues where the IAA26-P108H-GFP protein was found to accumulate and not in younger tissues where IAA26-P108H-GFP does not significantly accumulate (Fig. 2.2B and C). Results indicated that in three-week-old tissue none of the eight selected genes show a significant alteration in expression in comparison to a non-transformed control plant (Fig. 2.9B). In contrast, gene expression levels in seven-week-old plants showed all eight genes display altered expressions levels that roughly corresponded to their alterations within our transcriptome analysis (Fig. 2.9C). These findings are consistent with the accumulation of IAA26-P108H-GFP protein in only older leaf tissues, supporting a role for IAA26-P108H-GFP in the regulation of these genes.

Fig. 2.9. Validation of IAA26-P108H-GFP affected gene expression.

qRT-PCR expression analysis for eight selected genes that displayed significant transcriptional alterations within pIAA26::IAA26-P108H-GFP *A. thaliana* Shahdara plants. (A) Fold change comparisons between qRT-PCR (black bars) and RNAseq (white bars) studies. qRT-PCR fold change was averaged from two biological replicates. RNAseq fold change was determined by empirical analysis of digital gene expression for three biological replicates (386). (B and C) Fold change comparisons for the eight selected genes in three week old and seven week old pIAA26::IAA26-P108H-GFP plants (black bars) versus non-transformed control plants (white bars). In three week old tissue none of the eight selected genes show a significant alteration in expression. In contrast, in seven week old tissue all eight genes display significantly altered expression levels. Each bar represents the average ± standard error from two biological replicates composed of leaf tissue from four to six plants from two independent plant lines. The 18S RNA gene was chosen as an internal control for normalization.

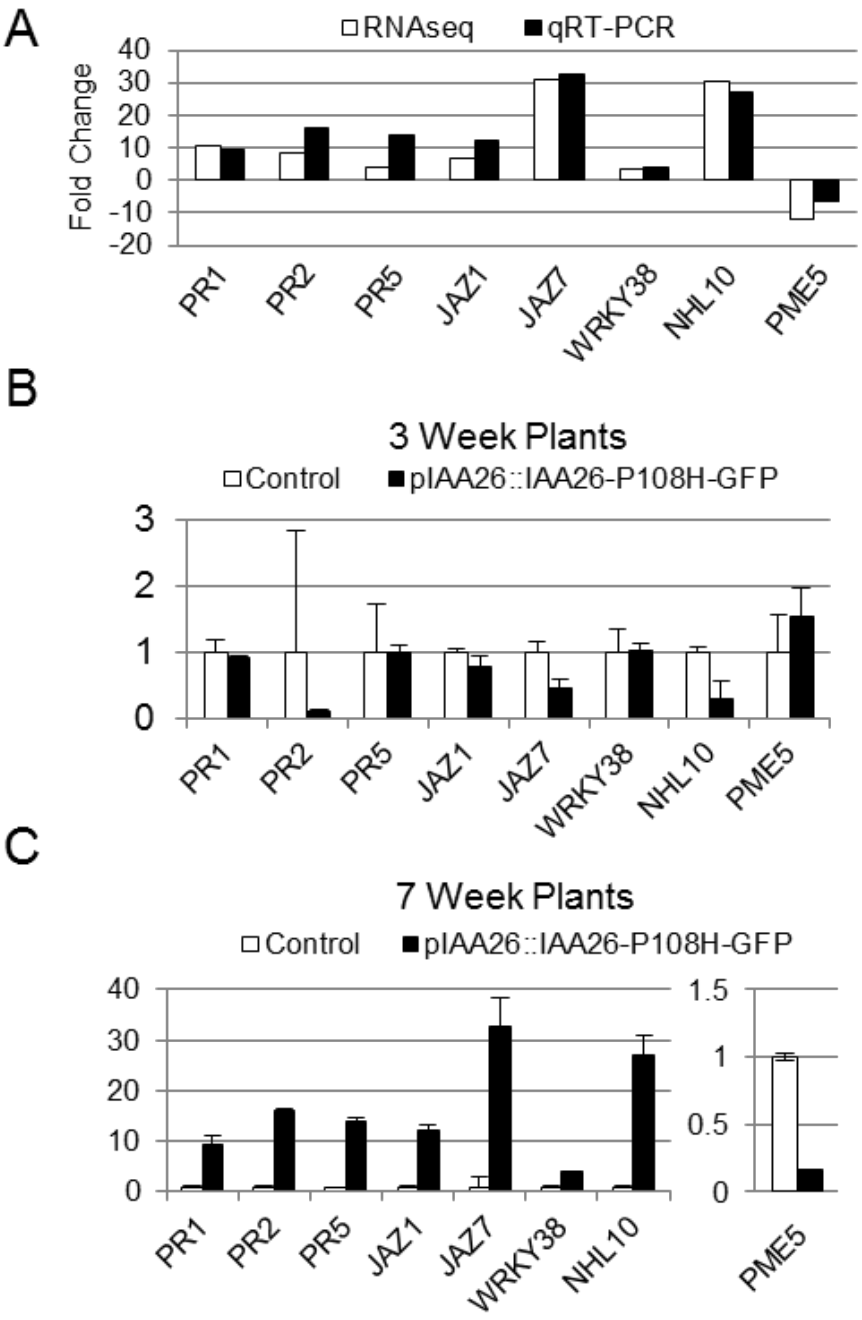
A
RNAseq
qRT-PCR
Fold Change
40
30
20
10
0
-10
-20
PR1
PR2
PR5
JAZ1
JAZ7
WRKY38
NHL10
PME5
B
3 Week Plants
Control
pIAA26::IAA26-P108H-GFP
3
2
1
0
PR1
PR2
PR5
JAZ1
JAZ7
WRKY38
NHL10
PME5
C
7 Week Plants
Control
pIAA26::IAA26-P108H-GFP
40
30
20
10
0
1.5
1
0.5
0
PR1
PR2
PR5
JAZ1
JAZ7
WRKY38
NHL10
PME5

2.3 Discussion

For many plant viruses achieving access to the vascular phloem is an essential step in a successful infection. However, in order to maintain physiological functions plants must tightly regulate the movement of molecules into and out of the vascular network. The gatekeeper function of the vascular phloem thus represents a significant obstacle through which viruses must navigate to achieve a systemic infection. For TMV our studies indicate that access to the vascular gateway is significantly enhanced by the disruption of select phloem expressed Aux/IAA transcriptional regulators. Aux, an essential plant hormone is involved in many processes including the development and regulation of the vascular network (387). Aux/IAA proteins are a key component in this regulatory system, playing a central role in converting Aux concentrations into gene expression levels (332, 376). The targeted disruption of specific phloem localized Aux/IAA proteins results in the transcriptional reprograming of the vascular tissue. This reprogramming corresponds with enhanced phloem loading and virus systemic movement and confers a significant advantage to TMV over viruses that are unable to disrupt these Aux/IAAs. Controlling the transcriptional output of the vascular tissue is thus an important contributor in the TMV infection cycle.

Aux/IAA proteins are transcriptional regulators that interact with and control ARF transcription factors (375, 376). ARFs target the AuxRE that include TGTCTC, TGTCGG and TGTSTSBC located in the promoters of Aux responsive genes (388). Within Arabidopsis 71% of mapped genes contain at least one AuxRE within 1500 bp upstream of the start codon and 31% contain at least one AuxRE within 500 bp

upstream of the start codon. Thus, Aux/IAA proteins have the potential to impact the regulation of a significant portion of the plant's genome. In previous studies we found that only three of ten tested Arabidopsis Aux/IAA proteins were capable of interacting with the TMV replication protein (212). In this study we have shown that all three interacting Aux/IAA family members are predominately expressed in the phloem and in the case of the strongest interactor, IAA26, in the phloem CCs. Consistent with our results, *IAA26*, *IAA27* and *IAA18* have been reported to be three of the six Aux/IAA family members enriched in vascular tissue isolated from mature *A. thaliana* leaves (389). Furthermore, in translatome profiling studies *IAA26* was found to be enriched in root and shoot CCs (390). It is also interesting to note that in micro-grafting experiments the mRNA of IAA18 has been shown to be phloem mobile and transported to the roots where it negatively regulates lateral root development (389). Together these findings confirm that TMV targeted Aux/IAA proteins are predominantly phloem expressed.

Within the CC-SE complex SEs provide the transport conduit between distal tissues and lacking a nucleus are dependent upon CCs for RNA and protein synthesis. For viruses such as TMV that require an assembly functional CP to move systemically, it seems likely that viral genomic RNA and CP are transported separately through the specialized PD pore units that connect CCs and SEs with virion assembly then occurring within the SEs (96, 166). Once loaded into SEs the virus moves from source (photoassimilate production) to sink (photoassimilate use/storage) (185). Thus, TMV loading from CCs to the SEs is likely to function differently than the cell-to-cell movement that occurs between other cell types and

does not require CP. Enhancing a virus's ability to move through this unique gateway would thus confer a significant advantage. This is clearly the case for TMV where phloem loading is very efficient for TMV, but delayed for the non-Aux/IAA interacting virus (Fig. 2.6B) or when IAA26 over accumulates in the phloem (Fig. 2.7). Additionally, the advantage conferred through the disruption of Aux/IAA functions in the phloem is of particular importance for a mechanically inoculated virus like TMV that does not have a vector and therefore no control over the types or age of the tissue it infects.

The targeting of these specific Aux/IAA proteins indicates they function in the transcriptional regulation of genes that directly impact TMV phloem loading. This possibility is strengthened by the inability of IAA26-P108H-GFP to effect CF dye movement, suggesting that observed effects on phloem loading are specific to TMV (Appendix D). Transcriptome analysis of plants expressing a stabilized Aux resistant version of IAA26 from its native promoter identified a number of host genes known to impact the transport of molecules across PD or modulate host defense signals as affected by IAA26 (Table 2.1 and Dataset S1). Additionally, as expected, several Aux responsive genes were altered when IAA26 is stabilized (Dataset S1). The known function of these IAA26 altered genes defines several potential mechanisms through which disruption of phloem specific Aux/IAA proteins could enhance the ability of TMV to move systemically.

At the local level, genes affected by IAA26 may be directly involved in regulating the cell-to-cell movement of TMV. Three genes with established connections to virus movement that displayed altered expression in IAA26 stabilized

plants included pectin methylesterase 5 (*PME5*), microtubule end-binding 1a (*EB1a*) and PD-located protein 3 (*PDLP3*) (Table 2.1). PME5 is of particular interest as it displays a 12-fold reduction in pIAA26::IAA26-P108H-GFP plants. Pectin methylesterases (PMEs) catalyze the de-methylesterification of pectin, releasing both protons and methanol. PME-dependent methanol emission has been shown to trigger PD dilation (391). In addition, PMEs have also been shown to be involved with Tobamovirus local cell-to-cell movement through PD via an interaction with the TMV MP (195). When TMV MP is mutated so it no longer binds PME, the local spread of virus is reduced. Additionally, knock outs of PMEs also reduce local viral movement (392, 393). PMEs may also play a role in systemic viral movement since TMV systemic movement is delayed in PME knock down plants (195). Overexpression of PME inhibitors in tobacco and Arabidopsis also limited Tobamovirus systemic movement (394). Furthermore, *PME5* contains an AuxRE in its promoter region, suggesting it could be directly regulated by IAA26. Reduction of *PME5* expression in IAA26 stabilized plants could explain the reduced phloem loading of TMV in these plants.

Both *EB1a* and *PDLP3* displayed > two fold reductions in expression when IAA26 is stabilized. EB1 proteins are evolutionarily conserved and localize to growing microtubule plus ends where they regulate microtubule dynamics. TMV MP has been shown to co-localize and interact with GFP tagged EB1a in Arabidopsis (73). It has been suggested that this EB1a/TMV-MP association could assist in the movement of TMV replication complexes to the PD. Consistent with the role of microtubule polymerization in cell-to-cell viral movement, tobacco mutants that have

reduced microtubule dynamics also have reduced TMV cell-to-cell movement (140). Thus, altering the expression of EB1a may be advantageous for virus movement. PDLPs are another group of proteins involved in the movement of viruses through PD. PDLPs interact with tubule-forming MPs and disruption of this interaction leads to delayed infection and attenuated symptoms (165). While TMV does not form tubules, down regulation of PDLPs suggests IAA26 may regulate host pathways involved in the general movement of macromolecules within the vascular phloem.

Additional genes linked to virus movement include members of the β-1,3-Glucanase family, two of which show two to three fold reductions in pIAA26::IAA26-P108H-GFP plants (Table 2.1). β-1,3-Glucanases are enzymes that degrade callose. Several studies have shown that callose deposition at PD leads to decreased cell-to-cell movement, while treatments inhibiting callose deposition lead to increased SEL of PD (164, 262, 263). Reduction of β-1,3-Glucanases could lead to the accumulation of callose at PD and decreased cell-to-cell movement when IAA26 accumulates. Additionally, two PD callose binding proteins (PDCB2 and PDCB3) were also significantly down regulated in pIAA26::IAA26-P108H-GFP plants, 6.4 and 2.2 fold respectively (Table 2.1). PDCBs specifically bind to callose *in vitro* and have been proposed to be involved in callose-mediated regulation within the PD (160). Combined, the observed down regulation of genes that positively impact virus movement suggests that IAA26 functions to negatively regulate these genes.

Host defense pathways including SA and JA have been shown to be key factors in the development of systemic resistance against TMV (395-397). Transcriptome analysis of pIAA26::IAA26-P108H-GFP plants showed marked

changes in genes associated with these defense pathways. Of particular interest were genes related to SA defense responses, including SA defense markers *PR1*, *PR2*, and *PR5,* which are all up regulated 10.5, 8.4 and 3.8 fold respectively upon IAA26 stabilization in the phloem (Table 2.1) (225). The up regulation of SA-mediated defense genes is consistent with previously published results that show when another Aux/IAA family member, AXR2/IAA7, is stabilized AvrRpt2 a *Pseudomonas syringae* Type III effector is no longer able to suppress the induction of SA-mediated defense genes (398). Additional genes involved in SA biosynthesis including *ANAC019* and *ANAC072* and genes involved in SA mediated signaling were also up regulated in pIAA26::IAA26-P108H-GFP plants (Table 2.1, Dataset S1). Thus, targeting IAA26 provides a mechanism through which TMV can directly modulate this important pathogen defense response.

We also observed transcriptional alterations in several key genes associated with cross communication between SA and JA defense pathways. In particular, we identified nine WRKY transcription factors that were altered in IAA26 stabilized plants (Table 2.1). WRKY transcription factors function as regulators between SA and JA defense pathways (399). Five WRKY family members were up regulated (*WRKY30, 38, 51, 55* and *58*), while four were down regulated (*WRKY12, 14, 35,* and *44*). Interestingly, the five up regulated WRKYs have all been previously shown to be induced in response to SA treatment, while the four that were down regulated were all undetectable (*WRKY12, 14* and *35*) or repressed (*WRKY44*) by SA treatment (400). *WRKY38* expression has been linked to the degradation of NPR1 and in combination with WRKY62 is required for systemic acquired resistance (401). While WRKY51

has been shown to mediate SA dependent repression of JA signaling (402). Another important regulator affecting the antagonism between SA and JA-mediated signaling is GRX480, which showed a six-fold increase in IAA26-P108H-GFP plants (403). Additionally, seven JAZ repressor proteins were also up regulated (Table 2.1). JAZ proteins negatively regulate the JA-signaling pathway by repressing transcription factors that control JA-regulated genes (404). It has been proposed that stabilization of JAZ proteins may be one way SA exerts an antagonistic effect on JA signaling (405). Additional JA repressors *JAM1* and *JAM2* were also up regulated (Table 2.1). The up regulation of both SA defense and JA signaling genes in response to the over accumulation of IAA26-P108H-GFP indicates that IAA26 positively impacts the regulation of these pathways. Combined, IAA26 likely functions as an important regulator of these host defense pathways within the phloem of mature tissues.

There is growing evidence for Aux involvement in disease resistance through cross talk with the SA and JA signaling pathways. Treatment of *A. thaliana* with the SA analog, BTH resulted in an overall reduction of Aux responses (360). One mechanism by which SA might inhibit Aux signaling is through transcriptional repression of the Aux receptor genes, leading to reduced degradation of Aux/IAA proteins and thus repression of Aux responses. Support for this mechanism comes from observations that Aux receptor genes are down regulated in response to BTH treatment, and detection of Aux/IAA proteins by western blot is increased after SA treatment (360). Conversely, activation of Aux signaling leads to the suppression of SA biosynthesis and signaling (361). It has also been reported that Aux triggers induction of genes involved in JA biosynthesis (362). Consistent with these findings

are studies that have linked the stabilization of Aux/IAA proteins to bacterial resistance. For example, when *axr2-1* plants, which produce a nondegradable form of AXR2/IAA7, were infected with the bacterial pathogen *P. syringae* pv. *maculicola* there was a 10-fold reduction in bacterial growth (360). Correspondingly, activation of Aux signaling and increased degradation of Aux/IAA proteins by over-expressing the Aux receptor *AFB1* resulted in increased growth of *P. syringae* pv *tomato* and enhanced disease symptoms (364). Consistent with these findings our results also demonstrate a role for Aux as a negative regulator of the SA pathway, perhaps via activation of JA signaling.

Interestingly, the biological advantage of the TMV-Aux/IAA interaction was observed only in older plant tissues (Figs. 2.5 and 2.6). In particular, inhibition of TMV phloem loading occurred in nine and not seven-week-old pIAA26::IAA26-P108H-GFP plants even though both developmental stages expressed and accumulated similar levels of IAA26-P108H-GFP mRNA and protein (Fig. 2.2B and C). We speculate that developmental backgrounds differentially impact the ability of IAA26-P108H-GFP to regulate gene transcription, resulting in threshold levels of key molecular traits that affect virus phloem loading and resistance. To investigate this possibility we performed additional qRT-PCR analysis of SA associated genes *PR1*, *PR2* and *PR5* that were found to be significantly altered in response to the accumulation of IAA26-P108H-GFP in seven-week-old plants (Appendix F). Comparisons between seven and nine-week-old pIAA26::IAA26-P108H-GFP plants showed dramatic variations with significantly higher levels of *PR1* and *PR2* present in nine week-old-plants and higher *PR5* levels present in seven-week-old plants.

These findings indicate that the developmental age of the tissue significantly influences the effect of IAA26-P108H-GFP accumulation on cell transcription. This suggests that IAA26 is a factor in the regulation of age related resistance. The targeting of IAA26 thus represents a mechanism whereby TMV can overcome this resistance response.

Based on our findings IAA26 plays an important role in regulating the phloem environment within mature plant tissues. The diverse array of genes impacted through the stabilization of IAA26 indicates that this Aux regulated protein has a significant role in modulating both the local environment of the CC – SE complex as well as surrounding and distal tissues. The regulation of genes that impact PD function and the inability of TMV to move into the phloem in IAA26 stabilized plants suggests that this Aux/IAA protein regulates the transport of macromolecules within the phloem. For TMV, targeting the disruption of this and related Aux/IAA proteins likely enhances access to the SE, increasing its ability to achieve a systemic infection. Impacts on JA and SA defense pathways provide a mechanism through which IAA26 could produce a wider cellular response both in tissues surrounding the vascular phloem as well as those distal from its site of expression. Disrupting the activation of these defense responses within the initially infected vascular tissues could provide a means for TMV to moderate systemic acquired resistance responses, leaving distal uninfected tissues more receptive to virus invasion. In summary, from these studies we conclude that TMV - Aux/IAA interactions that occur within the phloem result in the reprogramming of local and systemic cellular environments the combined effect of which enhances TMV's ability to establish a systemic infection.

2.4 Methods

2.4.1 Promoter Constructs and GUS Assays

Promoter fragments of 2 kb for IAA26 and IAA18 and 1.5 kb for IAA27 were amplified from genomic DNA extracted from *A. thaliana* ecotype Shahdara using promoter specific primers (Appendix E). Cloned promoter fragments were moved into pBI101.1 (Clontech, Palo Alto, CA, USA) upstream of the GUS reporter ORF via primer generated restriction sites. Promoter pIAA::GUS constructs were introduced into the *Agrobacterium tumerfaciens* strain GV3101 (406) and a floral dip method used for plant transformation (407). All plants were maintained in growth chambers for a 12-h photoperiod at 24°C. Histochemical staining for GUS activity was performed as previously described (408). In summary, plant tissues were vacuum infiltrated in a solution containing 1 mg/ml X-Gluc (5-bromo-4-chloro-3-indolyl p-D-glucuronide) (Gold Biotechnology, St. Louis, MO), 10mM EDTA, 100mM NaH_2P0_4 pH 7.0, 5mM potassium ferricyanide , 5mM potassium ferrocyanide and 0.1% v/v Triton and incubated at 37C for 12 hours. After clearing in 70% ethanol overnight, whole leaves or hand sectioned petioles or stems were imaged using an Olympus Stereo MVX10 microscope with 1X (numerical aperture of 0.25, dry) lens or Olympus BX60 Microscope with 10X (numerical aperture of 0.30, dry) lens. Representative images were acquired using cellSens Standard software (Olympus, Center Valley, PA) and were processed for printing with Adobe Photoshop (Grand Prairie, TX).

2.4.2 pIAA26::IAA26-P108H-GFP Construction and Characterization

To create pIAA26::IAA26-P108H-GFP the ORF of our previously described 35S::IAA26-P108H-GFP (212) construct was removed by *BamHI* and *Sac*I digestion and ligated into a similarly cut pIAA26::GUS (described above), replacing the GUS ORF with that of IAA26-P108H-GFP. *A. thaliana* ecotype Shahdara plants were transformed with pIAA26::IAA26-P108H-GFP as described above (409). Three to nine week old T2 generation plants from two independent transgenic lines were analyzed for IAA26-P108H-GFP mRNA and protein expression. For mRNA expression total RNA was isolated using the RNeasy Plant Mini Kit (Qiagen). One microgram of isolated RNA was pretreated with RQ1 DNase (Promega), followed by reverse transcription using SuperScript III First-Strand cDNA Synthesis System and random hexamer primers (Invitrogen). SYBR green real-time qRT-PCR was performed in 96-well reaction plates in an ABI Prism 7100 (Applied Biosystems). Experiments were done in three biological replicates, with each containing three technical replicates. The 18S RNA gene was chosen as an internal control for normalization and amplified using 5' CGTCCCTGCCCTTTGTACAC and 3' CGAACACTTCACCGGATCATT primers. Primers 5' TCAAGAAGGAAACAGAAGACAAATC and 3' TGTGAGATGTGAGGAACAGAAG were used to detect endogenous *IAA26* transcripts in control plants. Primers 5' GATGCAGTAAGCAAGAGAAGATG and 3' CTGAACTTGTGGCGTTTAC that span the IAA26-P108H to GFP fusion were used to detect the IAA26-P108H-GFP transgene mRNA. For protein expression, leaf tissue from three to nine week old plants were collected and ground in Laemmli

sample buffer (410). Samples were loaded onto denaturing polyacrylamide gels and blotted onto nitrocellulose membranes. Blotted proteins were probed with anti-GFP antibodies (Santa Cruz Biotechnology Inc.) or anti-actin antibodies (Sigma) as a loading control. GFP fluorescence localization for IAA26-P108H-GFP was done by hand sectioning petioles. Sectioned tissues were stained with 1 μg/ml DAPI and imaged using a Zeiss LSM700 laser scanning confocal microscope (Carl Zeiss, Inc).

2.4.3 *Nb*IAA26 Cloning and Characterization

Whole leaf RNA from *N. benthamiana* isolated via RNeasy minipreps (Qiagen) was used to generate cDNA via the SuperScript first-strand synthesis system (Invitrogen by Life Technologies). *Nb*IAA26-specific 5' CGGATCCAATGGAGGGTTATTCAAG and 3' GCTCGAGTCAGGTCAGCTTATTTCC primers containing *BamH*I and *Xho*I restriction sites were used to amplify the 828 bp *Nb*IAA26 ORF. The amplified ORF was cloned into pCRII-TOPO (Invitrogen) and sequenced. Protein sequence alignments for *Nb*IAA26, *Nt*IAA26, and *At*IAA26 were performed using CLC Genomics Workbench v 7.5.1 (CLCbio).

In situ analysis of *NbIAA26* mRNA localization was done using plant stem tissues fixed in methanol-glacial acetic acid (3:1) for 45 min, followed by chlorophyll removal in methanol and in absolute ethanol. Fixed tissue samples were rehydrated (95%, 75%, 50%, 25% ethanol), re-fixed, and washed in PBS (phosphate buffered saline, 137 mM NaCl, 2.7 mM KCl, 10 mM Na_2HPO_4, 2 mM KH_2PO_4) with 0.1% Tween-20 at room temperature. Pre-hybridization occurred at 55°C for 1 hr in buffer (0.1% Tween-20, 50% formamide, 2x saline sodium citrate buffer, pH 7.0) and a

digoxigenin labeled probe specific for *Nb*IAA26 was hybridized for 16 hrs. Probed tissues were washed and incubated with Anti-DIG-AP Fab-fragments. Incubated tissues were subsequently stained for hybridization via alkaline phosphatase. Stained leaves were imaged using an Olympus Stereo MVX10 microscope.

2.4.4 Virus Accumulation

Seven and nine week-old Shahdara control and transgenic pIAA26::IAA26-P108H-GFP plants were used for virus accumulation studies. Rosette leaves were dusted with carborundum and mechanically inoculated with ten µg of purified TMV or TMV-V1087I. Leaf punches were collected from 18 independently inoculated rosette leaves at three, six and nine dpi. For studies in *N. benthamiana*, plants were inoculated with five µg of TMV or TMV-V1087I with leaf punches collected from six inoculated leaves at two, four and six dpi. All samples were ground in Laemmli sample buffer (410) and analyzed by western immunoblot analysis using TMV specific antibodies as previously reported (365, 374).

2.4.5 Virus CP *In situ* Localizations

Whole leaf *in situ* localizations for the detection of the TMV CP were done as previously described (411). Leaves were fixed in PBS containing 4% paraformaldehyde overnight at 4C. Plant leaf tissue was dehydrated through a graded ethanol series (30, 50, 70% ethanol) with a final overnight incubation in 100% ethanol. After rehydration (75, 50 and 30% ethanol), the cell walls were digested with 0.2% macerozyme (Fisher Scientific, Fair Lawn, NJ) and 0.1% cellulase (Sigma, St. Louis, MO). After washes in PBS leaves were incubated for 20 min in PBS

containing 0.1% Triton X (Fisher Scientific, Fair Lawn, NJ). Additional washes with PBS removed the detergent, and were followed by a proteinase K (10 μg ml−1) digestion for 20 min at RT. Digestion was stopped by washing with PBS, and then tissue was blocked for 2 hours at RT in blocking solution (BS: PBS, 0.1% Triton X, 2% BSA, fraction V, Sigma). Incubation with a polyclonal rabbit antiserum raised against TMV coat protein at a dilution of 1:500 in BS occurred overnight at 4C. Washes in blocking solution and PBS were used to remove the unbound primary antibodies, and then samples were incubated overnight at 4C with a goat anti-rabbit secondary IgG antibody coupled to horseradish peroxidase (Sigma, St. Louis, MO) at a dilution of 1:1000 in BS. The color reaction was carried out by incubating the tissue in a diaminobenziding H_20_2 solution prepared from DAB ready tabs (Sigma, St. Louis, MO) according to the manufacturer's instructions. Stained leaves were imaged using an Olympus Stereo MVX10 microscope with 1X (numerical aperture of 0.25, dry) lens. Representative images were acquired using cellSens Standard software (Olympus, Center Valley, PA USA) and were processed for printing with Adobe Photoshop (Grand Prairie, TX, USA).

2.4.6 Systemic Movement Assays

For systemic movement assays lower leaves of *N. tabaccum* cv. Xanthi plants were inoculated with ten ng of virus. Three plants were used for each inoculation treatment. Plants were randomly assigned to one of five inoculation treatments: single inoculation with either TMV or TMV-V1087I and simultaneous inoculations of either 1:1, 1:5 or 1:10 ratios of TMV to TMV-V1087I. The infectivity of TMV and TMV-V1087I inoculum was determined by local lesion assays on *N. tabaccum*

cv. Xanthi-NC and standardized to insure an equal infection potential. RNA was isolated from systemic leaves at ten dpi when mosaic disease symptoms were first observed and cDNA was prepared as described above for pIAA26::IAA26-P108H-GFP plants. A 500 bp region of the 126 kDa gene that contains the point mutation, G to A, for TMV-V1087I, was amplified using PCR primers 5' CTTTGTCATGAGCACTTCTTCG and 3' TTGTGTTCCTGCATCGACC. The PCR products were purified using GeneJet PCR purification kit (Fermentas, Thermo Fisher Scientific,) and sequenced using the 5' amplification primer. The relative quantification of TMV and TMV-V1087I was determined using sequencing chromatograms as previously published (383). Briefly, the peak height ratio at the polymorphic site (height of A peak) / (height of A peak + height of G peak) was determined for each sample and compared to a standard curve developed by sequencing nine known ratios (1:0, 1:1, 1:2, 1:5, 1:10, 2:1, 5:1, 10:1, 0:1) of TMV and TMV-V1087I.

2.4.7 Transcriptome Analysis

Total RNA was isolated from seven week old pIAA26::IAA26-P108H-GFP transgenic plants and non-transformed control Shahdara plants using the RNeasy kit (Qiagen). Four fully expanded leaves were collected from each test plant and total RNA from four to six individual test plants was pooled for each of the three biological replicates. Pooled RNA was run on a 2100 Bioanalyzer Eukaryotic Total RNA Nanochip (Agilent Technologies) to check RNA quality. RNA integrity number (RIN) for all samples were between 7.2 and 8.0. Library preparation with Illumina TruSeq RNA sample preparation kit and sequencing with Illumina

HiSeq1500 rapid run was done by the UM-IBBR Sequencing Core at University of Maryland College Park (http://ibbr.umd.edu/facilities/sequencing). Each cDNA library generated between 21 and 64 million 50 bp single-end sequence reads. Raw sequencing data files are available upon request (e-mail jculver@umd.edu). Reads were mapped to the *Arabidopsis thaliana* Col-0 genome reference TAIR10 using the CLC Genomics Workbench v 7.5.1 RNA-seq analysis tool and default parameters. (Mismatch cost 2, Insertion cost 3, Deletion Cost 3, Length fraction 0.8, Similarity fraction 0.8, Max hits for a read 10) (CLC Bio) (367, 412). Approximately 93.9 to 98.5% of total reads mapped for each cDNA library, and 96.6 to 98.0% of mapped reads aligned to exons (Dataset S1). Reads aligned to exons were used in all subsequent analyses. Statistical analysis to identify differentially expressed genes was performed using the CLC Genomics Workbench Empirical Analysis of DGE tool with default dispersion estimation parameters (Total count filter cutoff 5.0) (386). Results were filtered with a cut of value of fold change > 2.0 and the FDR corrected p-value being smaller than 0.05. Gene symbols, gene model descriptions, and gene ontology (GO) annotations were retrieved from TAIR on August 4, 2015 (367). The generic GO term finder tool developed at the Lewis-Sigler Institute at Princeton (385) was used to identify GO annotation terms that occurred more frequently than expected by chance in the list of differentially regulated genes. A Bonferroni corrected p-value of < 0.01 was used as a cut off for significantly enriched GO terms. Analysis of gene promoter regions for AuxREs was done using the PatMatch tool (413). AuxRE was defined as a pattern match to TGTCTC, TGTCGG, or TGTSTSBC on either strand 1500bp or 500bp upstream of the start codon.

2.4.8 Transcriptome Validation

To validate RNAseq findings total RNA from three or seven week old pIAA26::IAA26-P108H-GFP plants or non-transformed control plants was isolated and used to generate cDNA. qRT-PCR was performed as described above for characterization of pIAA26::IAA26-P108H-GFP plant lines for two new biological replicates, with each containing three technical replicates. Primer sequences used for the amplification of selected genes are provided in Appendix E. The 18S RNA gene was chosen as an internal control for normalization.

2.4.9 Dye Loading Assays

To detect alterations to the SEL of plasmodesmata, we used 6(5)-CF diacetate (CFDA) as previously described with slight modifications (228). Briefly, 5 μL of 1 mM CFDA was applied to the adaxial surface of a mature source leaf of intact nine week old non-transformed control or pIAA26::IAA26-P108H-GFP plants. After 1 hour any remaining dye was removed and leaves were washed with sterile water. The abaxial surface of the leaf was then imaged using an Olympus Stereo MVX10. The area of CF spread was measured using ImageJ (414). For SA treatments, plants were sprayed with 100 μM of SA 24 hours prior to CFDA application.

To examine phloem loading, the adaxial surface of a mature source leaf of intact nine week old non-transformed control or pIAA26::IAA26-P108H-GFP plants was gently abraded with fine sandpaper. 20 μL of CFDA (60 μg/mL) was applied to the adaxial leaf surface as previously described (170). The abaxial side of the leaf was imaged after translocation in the light for 2 hours.

Chapter 3: *Tobacco mosaic virus* induced alterations to the phloem translatome of *Arabidopsis thaliana*

3.1 Introduction

As plants evolved to live on land, they developed long distance transport systems consisting of xylem and phloem to carry water, nutrients, sugars and other molecules to decentralized organs (415). The phloem is the main sugar conductive tissue in plants but is also involved in the transport of RNA, proteins, phytohormones, and other small regulatory molecules (8, 416, 417). The long distance transport of these host molecules play a key role in plant development and defense. For example, in Arabidopsis the FT protein and possibility the *FT* mRNA are phloem-mobile signals that are involved in the induction of flowering (418). Phloem-mobile molecules are also involved in defense signaling leading to SAR (225). The transport of several host mRNAs in the phloem has been demonstrated using heterograft experiments. For example, in tomato the transcript of a KNOTTED1-like homobox gene can cross graft junctions and induce a phenotypic change in sions (419). Two recent studies have attempted to identify phloem mobile mRNAs in Arabidopsis using high-throughput approaches combining grafting experiments and RNAseq (420, 421). Plant viruses have evolved to use this host long distance transport system to establish a systemic infection (169).

Phloem tissue is comprised of SEs and CCs. CCs and SEs originate from the same precursor cell and are often considered as a CC-SE complex (422, 423). As SEs mature they undergo a controlled incomplete autolysis process that is in some ways

similar to programmed cell death (422, 424). At maturation SEs are dependent on corresponding CCs to provide all genetic and metabolic capabilities and are connected via specialized PD known as PPUs (425). PPUs are branched on the CC side and fuse to form a single pore on the SE side (422). Presumably due to their unique structure PPUs have a higher SEL and have been shown to allow for movement of molecules larger than 60 kDa from CCs to SEs (146). This suggests that some molecules like proteins or RNA may diffuse from CC to SEs without special regulation (146, 422). However, this cannot be true for viral particles or even vRNP complexes which are still too large to freely move though PPUs (169).

To gain access to the phloem, many viruses must first cross multiple cell types moving cell-to-cell through PD. Viruses cross into CCs from neighboring phloem parenchyma then once in CCs must travel through the PPUs to the SEs (169). These cell borders present possible barriers to virus movement. In certain host/virus combinations viral transport can be specifically blocked at one of these cell boundaries, suggesting plants are able to precisely regulate PD permeability (426). Once in the SEs viruses are able to travel much more rapidly at a rate of mm/hr compared to μm/hr for cell-to-cell movement (169, 423, 427).

Viruses travel through the phloem as either an assembled virion or a vRNP complex. The requirement of a functional viral CP for systemic movement as either part of the assembled virion or vRNP complex is a common theme, but not universal (169). Other viral components besides the CP may also be important for long distance transport. For example, MPs increase PD permeability and some viruses

require MPs for long distance movement (169, 426). Additionally, viral encoded RSS are often multifunctional and can be required for long distance movement (169).

In this study we use TMV as a model to study virus-induced changes to the phloem in *A. thaliana*. The wealth of literature describing TMV along with the mapped and annotated Arabidopsis genome make this an system ideal for characterizing transcriptional changes in response to virus infection (20, 366, 367, 428). TMV requires its MP and replication protein for cell-to-cell movement through PD as a vRNP complex (20). TMV's long distance transport form is thought to be a virion with assembly occurring within the SE (429). TMV additional requires its replication protein for long distance movement in the phloem (187, 188).

Less is known about host factors involved in viral phloem loading and long distance transport. However, there is some evidence for host proteins involved in the regulation of callose contributing to tobamovirus systemic movement. For example, cdiGRP is a vascular protein localized in the cell wall of SE and CC. Reduction of cdiGRP mRNA allowed for systemic movement of TVCV, while over-expression of cdiGRP reduced TVCV systemic movement. Increased callose deposition in the cell wall of phloem cells was observed after constitutive expression of cdiGRP suggesting callose is involved in the blocking capacity of cdiGRP (197). Additionally, callose deposition at PD is known to be involved in regulating PD SEL (157). Thus, regulation of callose may be important for viral movement from CCs to SEs and systemic movement.

Host components involved in phloem loading have been challenging to identify in part due to the technical difficulty of isolating phloem tissues. CCs and

SEs form a pressurized system, and disruption of this system, as is done in many phloem sampling techniques can lead to the introduction of contaminates from neighboring cells (8). In this study, we use a sampling technique where His-FLAG (HF)-tagged ribosomal proteins are expressed from tissue specific promoters. These tagged ribosomes are used to immuno-purify mRNA-ribosome complexes. This population of mRNAs is referred to as the translatome (390). An advantage of this method is that it does not require invasive techniques prior to mRNA harvesting. Additionally, mRNAs associated with ribosomes are generally being translated and thus better represent the cellular condition than profiling total cellular RNA.

To investigate the effects of virus infection on the phloem translatome we expressed tagged ribosomes from two phloem promoters (pSUC2 and pSULTR2;2) and the CaMV 35S promoter as a control in the systemic TMV host *A. thaliana* ecotype Shahdara. We compared the translatome RNA populations in mock infected and TMV infected plants. We found the phloem is uniquely altered during TMV infection with to 88 to 90% of genes down regulated in the phloem translatomes compared to only 31% in the whole plant translatome. Many of the genes down regulated only in phloem tissues are involved in defense responses, callose deposition, and RNA silencing. Alteration of genes in these pathways may be advantageous for TMV phloem loading and systemic movement. To our knowledge this study is the first profiling of the phloem translatome in response to virus infection.

3.2 Results

3.2.1 Generation and Characterization of Transgenic Plants

In order to investigate how the phloem environment is altered during virus infection, we acquired plasmids containing ribosomal protein L18 (RPL18) tagged with a His6-FLAG (HF) dual-epitope driven by the Arabidopsis phloem specific promoters pSUC2 and pSULTR2;2 as well as the CaMV 35S promoter as a control from professor Bailey-Serres at UC Riverside (Fig 3.1A). pSUC2 is expressed in shoot companion cells, pSULTR2;2 is expressed in shoot companion cells and bundle sheath cells, and p35S has near constitutive expression (390, 430-432). It has been previously demonstrated that expressing HF-RPL18 from tissue specific promoters allows for the immunopurificatin of polysome-mRNA complexes from different tissue types (390). This population of mRNAs attached to ribosomes has been termed the translatome.

All three acquired constructs were transformed into the systemic TMV host *A. thaliana* ecotype Shahdara (365). Fully expanded leaves from five T2 generation plants were combined and qRT-PCR analysis confirmed the expression of the transgene *HF-RPL18* mRNA for two independent lines for each promoter construct (Fig 3.1B). No amplification of *HF-RPL18* mRNA was observed in non-transformed controls. All of the transgenic plant lines grew and developed similarly to non-transformed controls (Fig 3.1C).

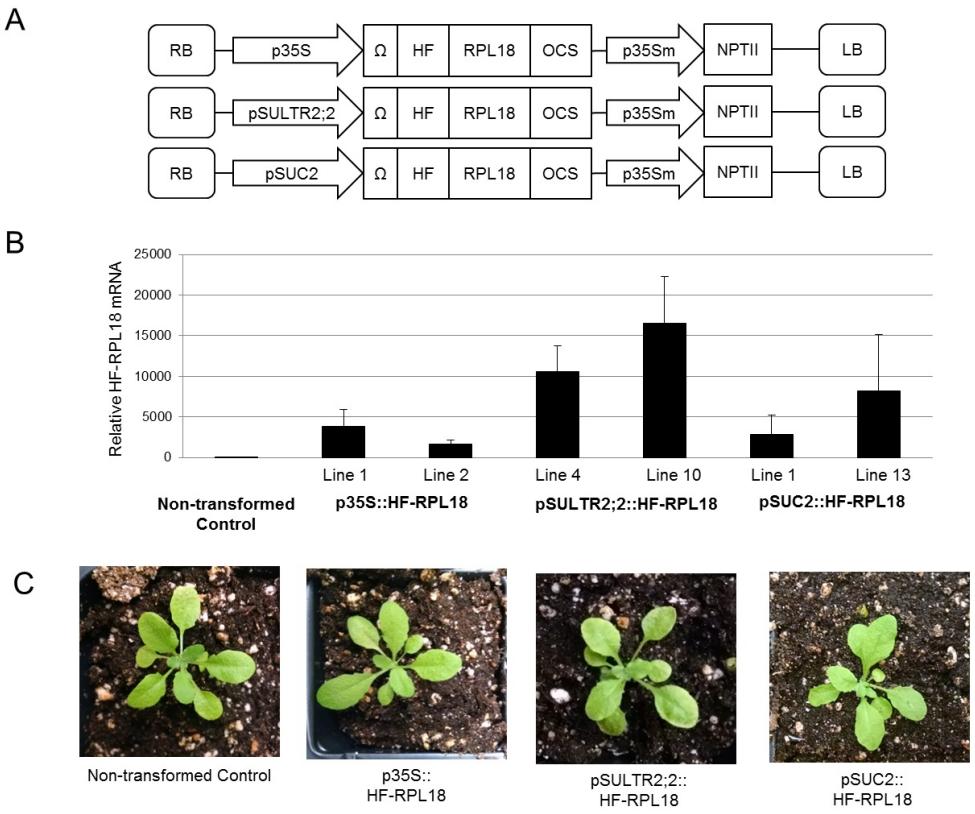

Figure 3.1. Generation and Characterization of Arabidopsis Accession Shahdara Promoter:HF-RPL18 Transgenic Plants. (A) Diagram of control p35S and phloem specific pSULTR2;2 and pSUC2 driving His_6-FLAG (HF) epitope-tagged 60S ribosomal subunit protein L18B, *HF-RPL18*, and a kanamycin resistance gene, *NPTII*, from the minimal 35S promoter (p35Sm). Omega translation enhancer from TMV (Ω); *Octopine Synthatse* (OCS) terminator; LB, left border of T-DNA; RB, right border of T-DNA. (B) Relative *HF-RPL18* transgene expression in T2 transgenic plants. 18SRNA was used as the internal control. Bars represent the average of two biological replicates ± standard error. (C) Representative photographs of four week old control and transgenic Arabidopsis accession Shahdara plants. All promoter::HF-RPL18 transgenic plant lines display no developmental phenotypes.

Four week old T2 plants from two independent lines for each promoter construct were infected with TMV or mock infected with sterile water and all shoot tissue was harvested six dpi. At this time point TMV has begun to accumulate in the vascular phloem but we do not observe disease symptoms (Appendix G) (365). Shoot tissue from 20 plants was pooled for each biological replicate, for a total of two replicates per biological condition. Biological replicates were collected four months apart. To control for environmental and circadian effects, plants were maintained under identical growth chamber conditions with both inoculations and tissue collection done at the same time of day.

Frozen plant tissue was ground in a polysome-stabilizing extraction buffer and the FLAG epitope was used to purify polysome-mRNA complexes using FLAG antibody associated magnetic beads as previously described (390, 433). mRNAs were isolated from captured polysomes and used for cDNA library preparation with the Illumina TruSeq RNA sample preparation kit. Library preparation and sequencing with Illumina HiSeq1500 rapid run was done by the UM-IBBR Sequencing Core at University of Maryland, College Park.

3.2.2 Analysis of Translatome RNAseq Data

After filtering reads that mapped to the Illumina adapters, approximately 29 to 60 million 50 bp single-end sequence reads were generated for each biological condition (Table 3.1). Reads were mapped to the *A. thaliana* Col-0 genome reference TAIR10 and the TMV genome (NCBI Reference Sequence NC_001367) using the CLC Genomics Workbench v 7.5.1 (367, 412). 97 to 98% of reads for mock infected samples and 80 to 94% of reads for TMV infected samples mapped to the

Arabidopsis genome (Table 3.1). 0.07 to 1.73% of reads from TMV infected samples mapped to the TMV genome. All mock infected samples have less than 0.0001% of reads mapping to the TMV genome and these reads predominately map to the 5' UTR Ω sequence (Fig. 3.2). Reads aligned to the Ω sequence in mock samples are expected as the Ω sequence is used as a translational enhancer upstream of transgene *HF-RPL18* (Fig. 3.1A). Notably, there was a wide range of coverage of the Ω sequence in mock samples with only 4X coverage in the pSUC2 mock 2 sample to 500X coverage in the p35S mock 2 sample. Lower coverage of the Ω sequence in pSUC2 mock samples may indicate that the SUC2 promoter is not expressing *HF-RPL18* to as high levels compared to the other two promoters in these transgenic plant lines. Pairwise comparisons between biological replicates showed that all biological replicates had a Pearson correlation between 0.93 and 0.97 (Figure 3.3) indicating high reproducibility between biological replicates.

Average RPKM values for each biological condition were used to determine the number of genes represented in each translatome. Only genes with an average RPKM of > 0.3 were included in the analysis. 18,225 (pSUC2 TMV) to 19,525 (p35S TMV) genes out of 28,496 predicted *A. thaliana* genes were expressed in each translatome, with 82 to 85% between 1 to 100 RPKM (Fig. 3.4).

Table 3.1. Summary of reads mapped.

Library Name	Bio Rep	Reads	Reads/ Biological Condition	Reads Mapped	%	Mapped Exons	%	Mapped TMV	%
p35S Mock	1	34970086		34037392	97.33%	32093368	94.29%	90	0.00%
	2	25924405	60894491	25376729	97.89%	24236158	95.51%	909	0.00%
pSULTR2;2 Mock	1	22258836		21888431	98.33%	21207007	96.89%	402	0.00%
	2	29639394	51898230	28934367	97.62%	24383902	84.27%	169	0.00%
pSUC2 Mock	1	20525694		20125348	98.05%	18822090	93.52%	162	0.00%
	2	35259093	55784787	34249590	97.14%	30924158	90.29%	40	0.00%
p35S TMV	1	32473401		28727649	88.47%	25665123	89.34%	30308	0.09%
	2	13215654	45689055	11506666	87.07%	8552010	74.32%	44028	0.33%
pSULTR2;2 TMV	1	16858610		14468905	85.83%	10987774	75.94%	74690	0.44%
	2	12507773	29366383	11798596	94.33%	7944550	67.33%	8804	0.07%
pSUC2 TMV	1	30967352		27209291	87.86%	12930807	47.52%	535096	1.73%
	2	9037503	40004855	7240847	80.12%	4015230	55.45%	8183	0.09%

Library Name	Bio Rep	Mapped Mt	%	Mapped Chloroplast	%	Mapped 18S rRNA	%	Mapped 25S rRNA	%
p35S Mock	1	20299	0.06%	368475	1.08%	238461	0.70%	373004	1.07%
	2	16130	0.06%	100279	0.40%	78194	0.31%	155692	0.60%
pSULTR2;2 Mock	1	5261	0.02%	24605	0.11%	38171	0.17%	1453730	6.53%
	2	56362	0.19%	1105710	3.82%	1145529	3.96%	71625	0.24%
pSUC2 Mock	1	24517	0.12%	113200	0.56%	144512	0.72%	258331	1.26%
	2	43754	0.13%	864144	2.52%	647778	1.89%	966118	2.74%
p35S TMV	1	67753	0.24%	811224	2.82%	679396	2.36%	834857	2.57%
	2	88230	0.77%	680743	5.92%	669415	5.82%	1228280	9.29%
pSULTR2;2 TMV	1	62177	0.43%	1294792	8.95%	685725	4.74%	1320171	7.83%
	2	57048	0.48%	329756	2.79%	1455409	12.34%	1784392	14.27%
pSUC2 TMV	1	312941	1.15%	7235704	26.59%	2087918	7.67%	4516319	14.58%
	2	96921	1.34%	821843	11.35%	721096	9.96%	1453345	16.08%

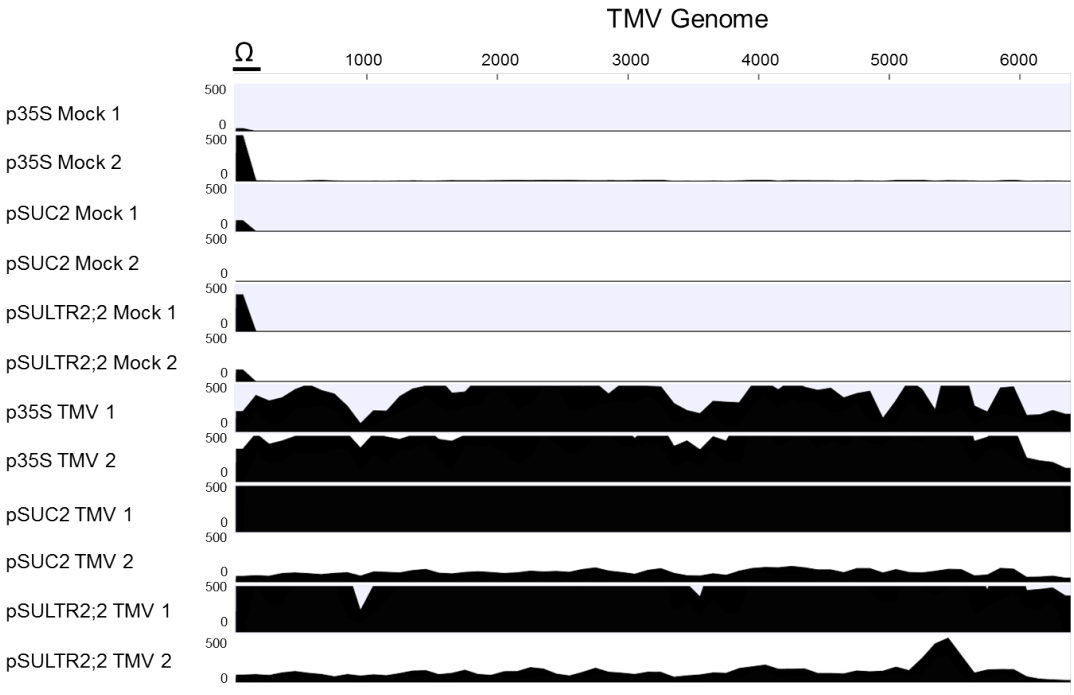

Figure 3.2. Reads mapped to the TMV genome.

Dark shading indicates number of reads mapped to the TMV genome for each library. The omega (Ω) sequence is labeled with a black bar.

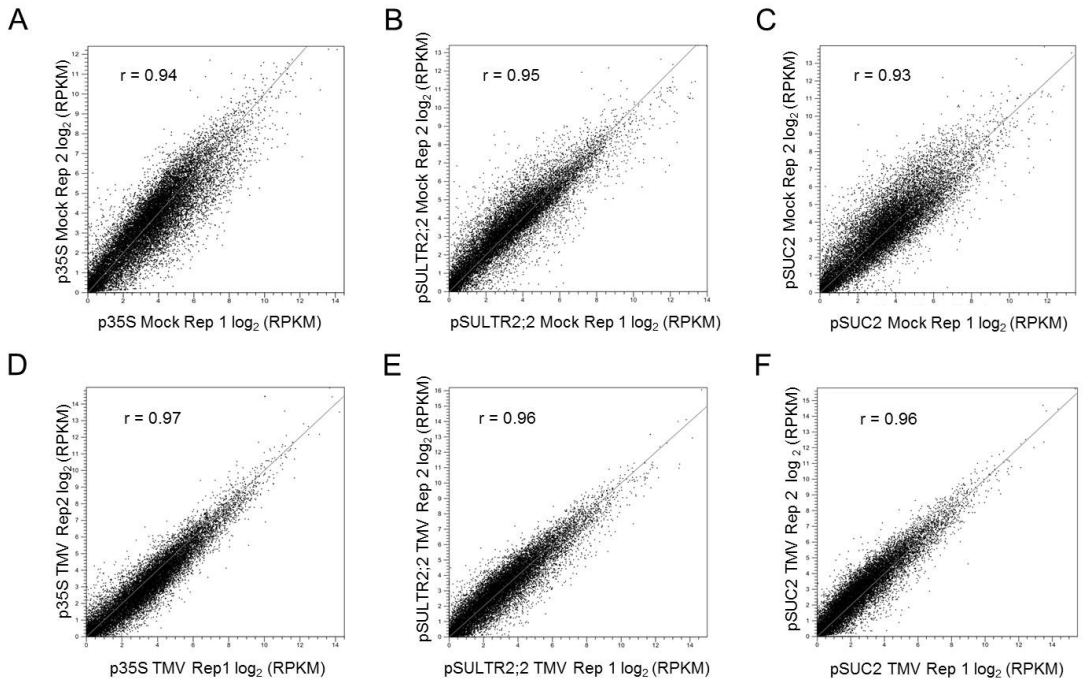

Figure 3.3. Pairwise Comparison of Biological Replicates.

Scatter plots and Pearson product-moment correlation coefficients comparing two biological replicates for each of the six experimental groups. RPKM, Reads Per Kilobase of transcript per Million mapped reads. (A) p35S mock infected. (B) pSULTR2;2 mock infected. (C) pSUC2 mock infected. (D) p35S TMV infected. (E) pSULTR2;2 TMV infected. (F) pSUC2 TMV infected.

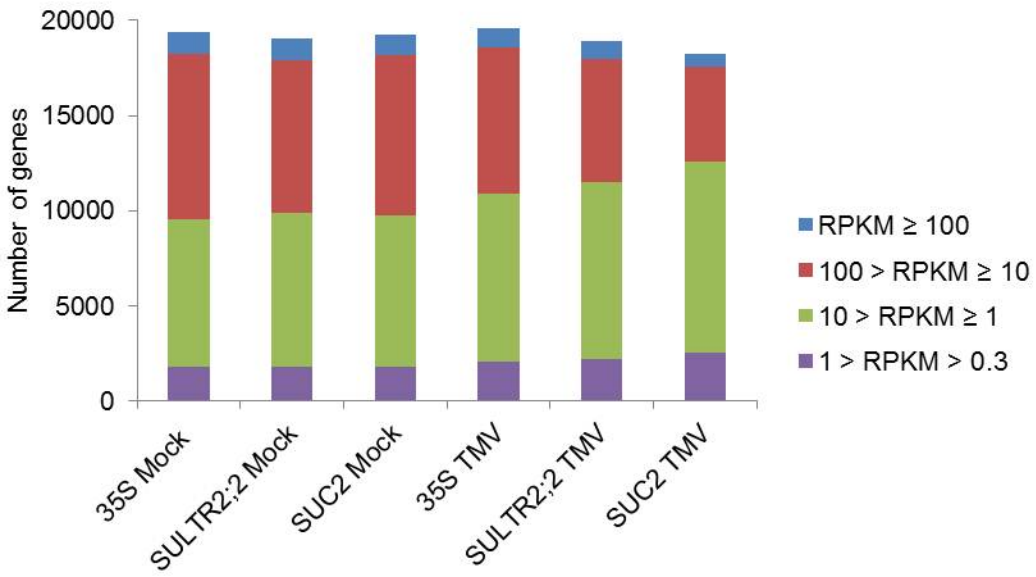

Figure 3.4. Analysis of Global Gene Expression.

Number of genes expressed in each translatome with an average RPKM greater than 0.3. RPKM, Reads per Kilobase of transcript per Million mapped reads.

3.2.3 Identification and Classification of Phloem Enriched Genes

We defined phloem enriched genes as those genes that are significantly up regulated (Fold Change > 1.5, FDR P-Value < 0.05) in pSUC2 mock or pSULTR2;2 mock samples compared to p35S mock samples using the CLC genomics workbench test on proportions (434). We found a total of 69 genes significantly up regulated in the pSUC2 translatome and 128 genes significantly up regulated in the pSULTR2;2 translatome. Four genes were significantly enriched in both pSUC2 and pSULTRR2;2 phloem translatomes (Fig. 3.5A, Dataset S2). An additional 36 genes were identified as being significantly enriched in the p35S translatome compared to both the pSUC2 and pSULTR2;2 translatome (Dataset S2).

As expected *SULTR2;2* was significantly enriched in the pSULTR2;2 translatome, suggesting mRNAs were effectively isolated form the targeted tissue. Conversely, *SUC2* was not significantly enriched in the pSUC2 translatome unlike previous reports (390). However, another known CC marker gene *APL3* is significantly enriched in the pSUC2 translatome (Dataset S2) (435). Furthermore, when the list of pSUC2 and pSULTR2;2 translatome phloem enriched genes was compared to previously published phloem translatome data we found that 7/69 (10.1%) and 31/128 (24.2%) of identified genes overlapped with previously reported shoot phloem enriched genes. Conversely, none of the 36 p35S translatome enriched genes overlapped with published shoot phloem translatome data (Dataset S2) (390). There are many reasons why there may be incomplete overlap between our study and previously published results, but one key factor may be plant age.

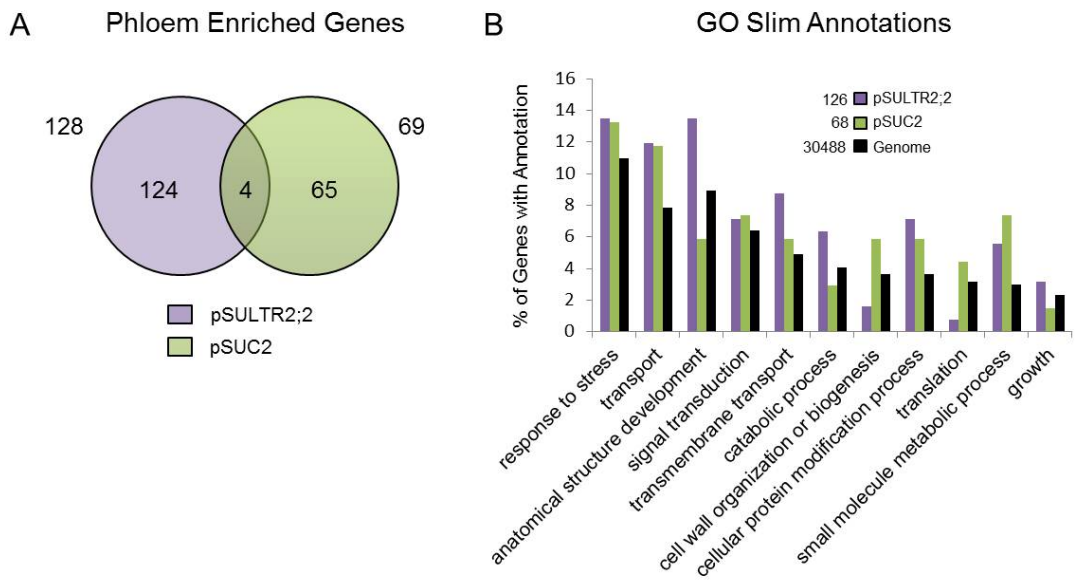

Fig. 3.5. Characterization of Phloem Enriched Genes.

Phloem enriched genes were defined as genes in the pSULTR2;2 mock or pSUC2 mock translatome with a fold-change > 1.5 and FDR P-Value < 0.05 when compared to the p35S mock translatome. (A) Venn diagram of total number of genes characterized as phloem enriched in the pSULTR2;2 and pSUC2 translatomes. (B) Percentages of identified phloem enriched genes in the pSULTR2;2 tranlstome (purple) or pSUC2 translatome (green) belonging to Go Slim categories compared to the Arabidopsis genome (shown in black). The total number identified genes with an available GO Slim category is indicated next to the color key for each translatome.

Published phloem translatome experiments were done in one week old Arabidopsis ecotype Columbia plants, while our samples were collected from 6 week Arabidopsis ecotype Shahdara plants. It is also possible the difference in Arabidopsis ecotype may have some effect. Thus, the fact that 10% and 24% of our identified phloem enriched genes have been previously reported combined with the enrichment of known CC marker gene *APL3* leads us to conclude we have successfully isolated target phloem tissues.

GO Slim terms were assigned as a first step to identify categories of genes represented in the phloem enriched dataset. Percentages of genes placed in each GO Slim category were compared to the percentages of genes assigned to that category in the entire Arabidopsis genome (Fig. 3.5B). While many phloem enriched genes are annotated as being involved in "response to stress" and "transport", none of the GO Slim categories were over represented in the phloem enriched gene lists compared to what is expected by chance. In fact, only one GO ontology term was over represented in either the pSUC2 or pSULTR2;2 phloem enriched genes lists which was "sulfate transmembrane transport" in the pSULTR2;2 gene list.

3.2.4 Identification and Classification of TMV Responsive Genes

To identify changes to the translatomes in response to viral infection, TMV infected samples were compared to mock infected samples for each tissue type and differentially expressed genes (fold change >2, FDR P-Value < 0.05) were identified using CLC genomics workbench test on proportions (434). During TMV infection a total of 650 genes are altered in the p35S translatome, 587 genes altered in pSULTR2;2 translatome and 4708 genes altered in pSUC2 translatome. In the p35S

translatome only 31% of genes are down regulated compared to 90% and 88% of genes that are down regulated in the two phloem translatomes (Figure 3.6A). A set of 11 and 21 genes were up or down regulated, respectively, in all samples in response to TMV infection (Fig. 3.6B and C).

As expected, the pSUC2 and pSULTR2;2 translatomes had some but not complete overlap with nine genes up regulated and 279 genes down regulated in both of the phloem translatomes but not in the p35S translatome (Fig. 3.6B and C). This incomplete overlap is consistent with pSUC2 expression in CCs and pSULTR2;2 expression in shoot CCs and bundle sheath cells (390, 431). Gene symbols, gene model descriptions, and gene ontology (GO) annotations were retrieved from TAIR (367). GO Slim terms were used to identify categories of genes that were up regulated or down regulated during TMV infection. Percentages of genes placed in each GO Slim category were compared to expected percentages based on the number of genes assigned to that category in the entire Arabidopsis genome (Fig. 3.7A and B). Genes involved in response to stress were significantly enriched (Corrected P-Value = 0.00153) in the pSULTR2;2 up regulated gene group and conversely in the pSUC2 down regulated gene group (Corrected P-Value = 0.009).

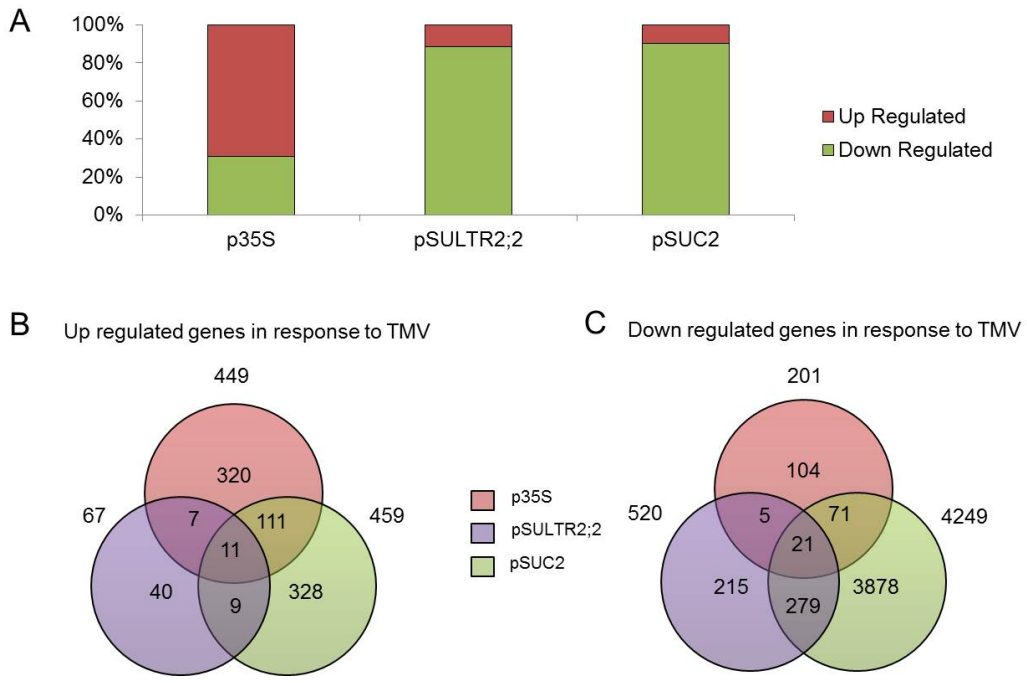

Figure 3.6. Differentially Expressed Genes during TMV Infection.

(A) Percentages of up regulated (red) and down regulated (green) differentially expressed genes during TMV infection for each translatome compared to mock infected controls. (B) and (C) Total number of differentially expressed genes in TMV infected tissues. Overlapping sets of up regulated (B) and down regulated (C) genes during TMV infection are shown in the Venn diagrams.

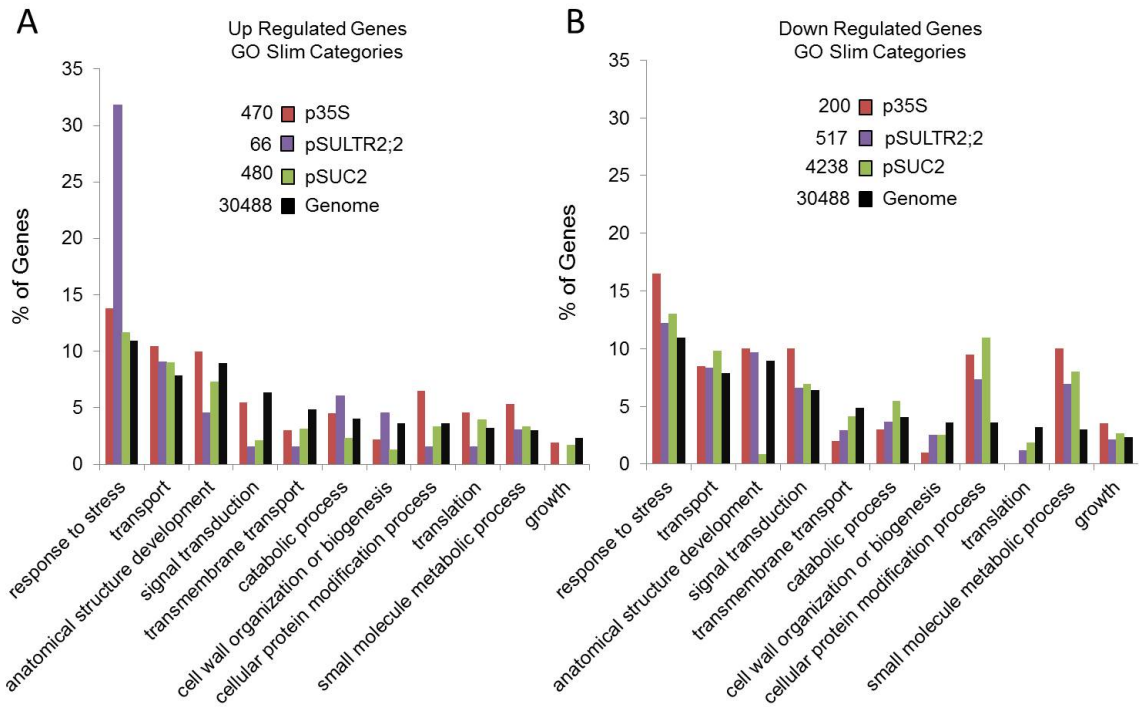

Figure 3.7. GO Slim Characterization of Genes Altered during TMV Infection. Percentage of up regulated (A) or down regulated (B) genes belonging to specific GO Slim categories. The total number of up or down regulated genes in each translatome with an available GO Slim category is indicated next to the color key. Percentage of total annotated genes in the genome belonging to each GO Slim category serves as a control and is colored in black.

3.2.5 Transcription Factors altered during TMV Infection

We hypothesized that the unique changes observed in the phloem tissues in response to virus infection may be due to the alteration of phloem transcription factors. Thus, we identified all the transcription factors altered during TMV infection. In the p35S translatome 46 transcription factors are up regulated while 22 are down regulated. In contrast in the pSULTR2;2 and pSUC2 translatomes transcription factors are predominately down regulated 41/45 and 231/253 respectively (Fig. 38A). Altered transcription factors belong to many families associated with response to stress including basic-domain leucine-zipper (bZIP), WRKY, AP2-EREBP and MYB proteins (Figure3.8B and C) (436-438). Additionally, many ARF genes are altered during TMV infection. ARF proteins are of particular interest because TMV has been shown to interact with select Aux transcriptional regulators in the phloem vascular tissue and this interaction is important for TMV phloem loading (Chapter 2). Nine ARF family members and significantly down regulated in the pSUC2 translatome during TMV infection, two ARF proteins are down regulated in the pSULTR2;2 translatome and only ARF11 is down regulated in the p35S translatome (Fig. 3.9).

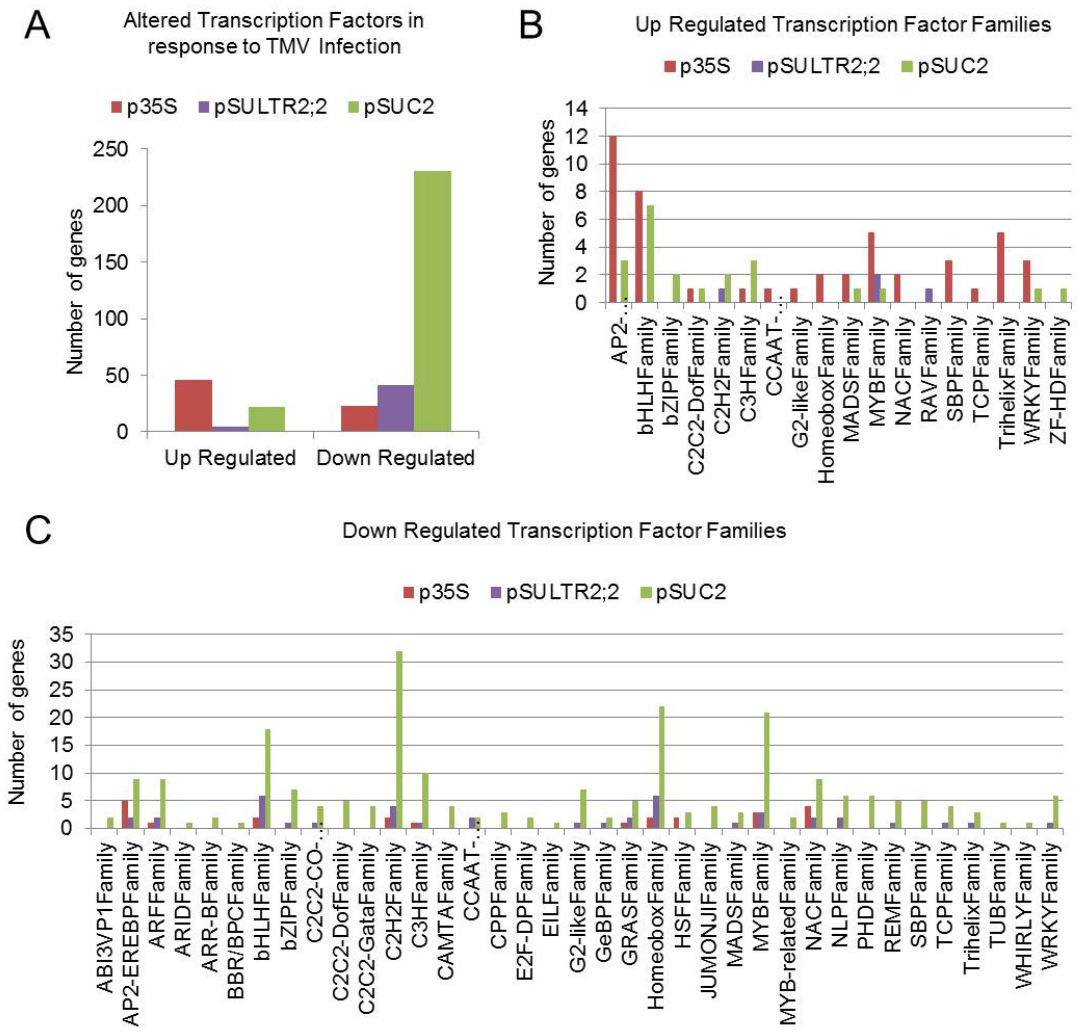

Figure 3.8. Transcription Factors Altered During TMV Infection.

(A) Total number of transcription factors up and down regulated in each translatome in response to TMV infection. (B) Characterization of transcription factor families up regulated in response to TMV infection. (C) Characterization of transcription factor families down regulated in response to TMV infection.

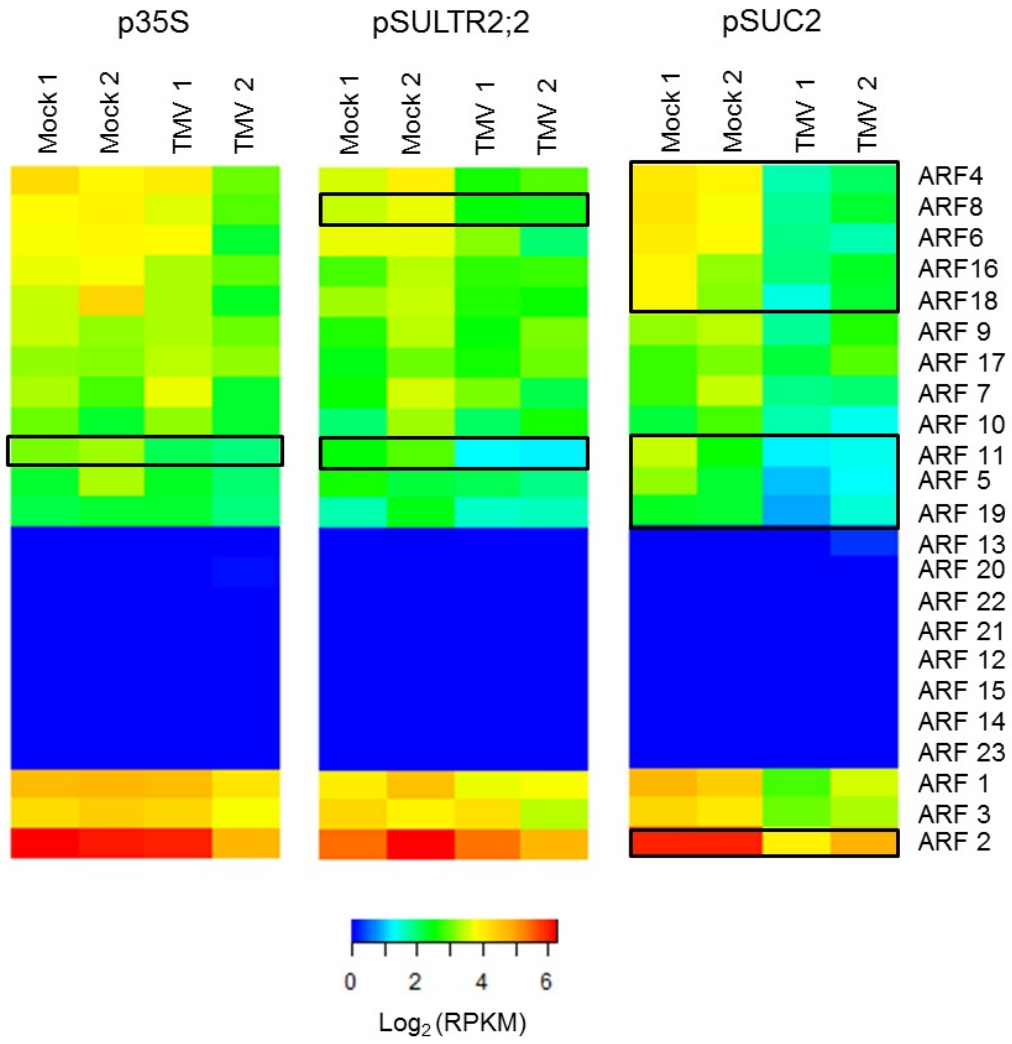

Figure 3.9. ARF Gene Expression in Response to TMV Infection.

Heat map depicting $\log_2$ (RPKM) value for all ARF genes in mock and TMV infected tissues. Genes boxed in black are significantly altered > 2 fold.

3.2.6 Viral Movement and Defense Related Genes altered during TMV Infection

Gene families besides transcription factors were also uniquely altered in phloem tissues. Many of these genes are involved in callose deposition at the plasmodesmata which can limit virus cell-to-cell movement (263). One example is the glucan synthase-like/callose synthase genes. Seven family members are down regulated > 2-fold in the pSUC2 translatome but not in p35S or pSULTR2;2 translatome samples (Fig. 3.10A). While it did not make our filter cut off, GSL12 is also down regulated 1.85 fold in the pSULTR2;2 translatome. PDLP proteins are another family of proteins that localize to the plasmodesmata and are known to be involved in viral cell-to-cell movement (165). Two family members PDLP2 and PDLP3 are significantly down regulated only in the pSUC2 translatome (Fig. 3.10B). Additional genes annotated as involved in "defense response to virus" or "response to virus" are also uniquely altered in the pSUC2 translatome (Fig. 3.10C). These include genes involved in RNA silencing DLC2, DCL4 and RDR6 (439) which were all down regulated only in the pSUC2 traslatome. Additionally, NHL10 which has been shown to be up regulated in HR to CMV infection was significantly up regulated in the p35S and pSULTR2;2 translatomes but not in the pSUC2 translatome (440).

Fig. 3.10. Expression of Genes Involved in Defense Responses to Viruses.

Heat map depicting log2 (RPKM) value mock and TMV infected tissues. Genes boxed in black are significantly altered > 2 fold. (A) Glucan synthase-like/callose synthase gene family. (B) Plasmodesmata localized protein (PDLP) gene family. (C) Altered genes annotated as "response to virus" or "defense response to virus".

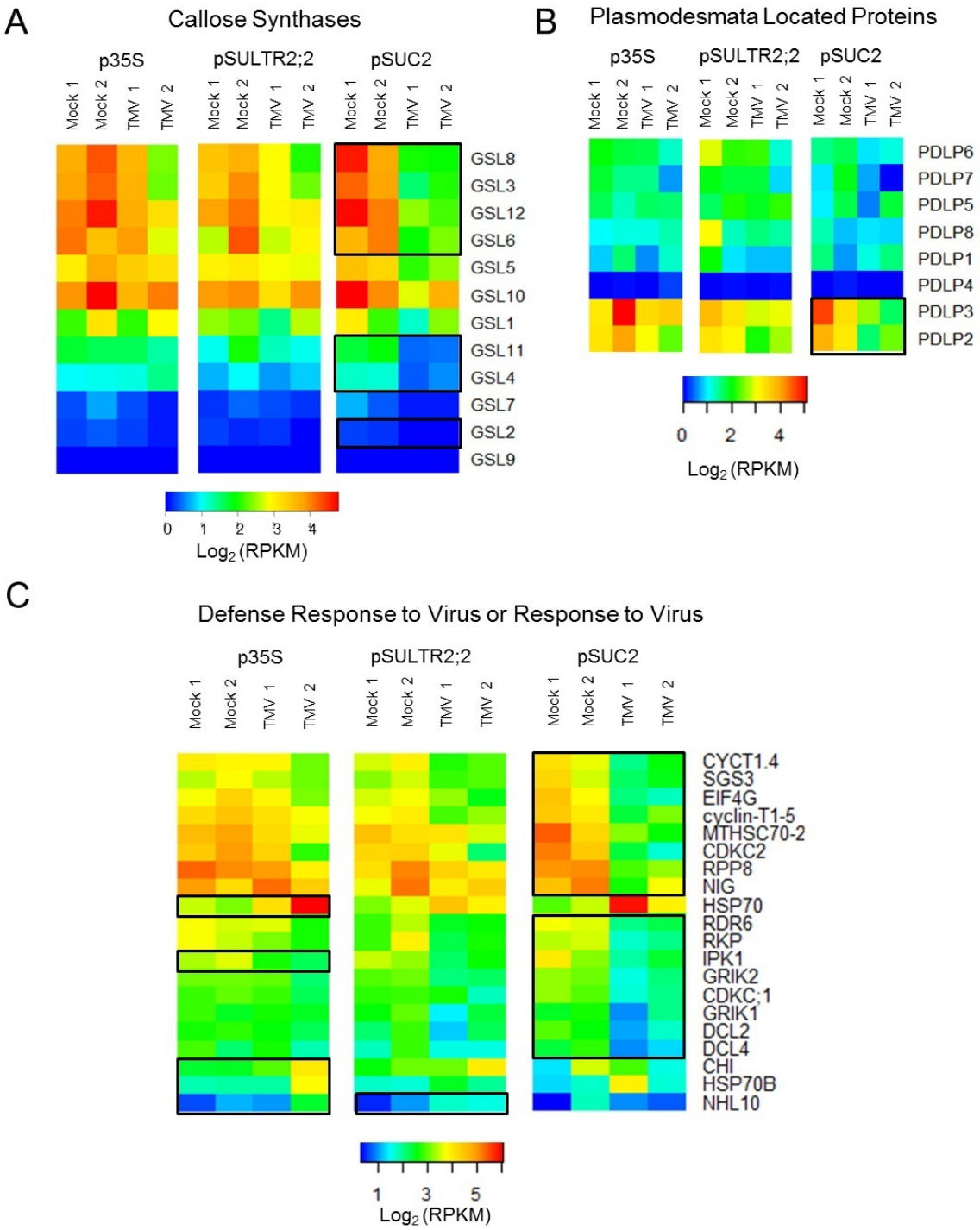
A
Callose Synthases
p35S
pSULTR2;2
pSUC2
Mock 1
Mock 2
TMV 1
TMV 2
GSL8
GSL3
GSL12
GSL6
GSL5
GSL10
GSL1
GSL11
GSL4
GSL7
GSL2
GSL9
0 1 2 3 4
Log2 (RPKM)
B
Plasmodesmata Located Proteins
PDLP6
PDLP7
PDLP5
PDLP8
PDLP1
PDLP4
PDLP3
PDLP2
0 2 4
Log2 (RPKM)
C
Defense Response to Virus or Response to Virus
CYCT1.4
SGS3
EIF4G
cyclin-T1-5
MTHSC70-2
CDKC2
RPP8
NIG
HSP70
RDR6
RKP
IPK1
GRIK2
CDKC;1
GRIK1
DCL2
DCL4
CHI
HSP70B
NHL10
1 3 5
Log2 (RPKM)

3.2.7 Phloem Enriched Genes altered during TMV Infection

The genes we identified as being uniquely altered in phloem tissues in response to TMV infection may belong to one of two possible groups. The first group is those genes that are similarly expressed the in phloem and the rest of the plant in mock infected plants but are down regulated or up regulated during TMV infection only in the phloem tissue. The second group of genes is those that are only expressed in phloem tissues and altered during TMV infection. To try to distinguish these two groups we compared the list of phloem enriched genes (Dataset S2) to the list of genes altered in the pSUC2 and pSULTR2;2 translatomes during TMV infection (Dataset S3). We identified 38 genes enriched in pSUC2 phloem tissue and also altered during viral infection in the pSUC2 translatome and 18 genes enriched in pSULTR2;2 phloem tissue and also altered during viral infection in the pSULTR2;2 translatome (Table 3.1). These genes are expressed predominately in phloem tissues and also altered during viral infection. Included on this list are six transcription factors which are all down regulated in response to TMV infection. These represent candidates that may be responsible for the unique regulation of the phloem translatome. Additionally, three genes are associated with plasmodesmata (highlighted genes on Table 3.1). Other GO biological processes represented in this gene list that may be important for viral infection and movement include response to stress, SA and JA mediated signaling pathways, response to ER stress, and response to Aux.

Table 3.2. Phloem enriched genes altered during TMV infection.

Locus Identifier	Fold-Change[1]	Translatome	Gene Symbol	GO Biological Process
Oxidation-Reduction Process				
AT1G09400	-2.25	pSUC2		oxidation-reduction process
AT1G11780	-3.85	pSUC2		oxidation-reduction process
Response to Abiotic or Biotic Stimulus				
AT3G44450	-3.53	pSUC2		response to karrikin
Response to Stress				
AT5G62210	-2.07	pSUC2		JA biosynthetic process
AT1G07890	-2.17	pSULTR2;2	APX1	response to oxidative stress
AT1G61740	-2.66	pSULTR2;2		regulation of plant-type HR
AT5G64000	-2.94	pSUC2	SAL2	response to ER stress
AT1G43800	-4.78	pSUC2	FTM1	SAR, SA mediated signaling pathway
Signal Transduction				
AT1G22690	2.36	pSUC2		GA mediated signaling pathway
AT2G37670	-9.4	pSUC2		signal transduction
Transcription factors				
AT5G28040	-2.06	pSULTR2;2		regulation of transcription
AT1G08810	-2.21	pSUC2	MYB60	regulation of transcription
AT1G52880	-2.34	pSULTR2;2	NAM	regulation of transcription
AT3G05690	-2.4	pSULTR2;2	NF-YA2	regulation of transcription
AT3G15790	-2.68	pSULTR2;2	MBD11	regulation of transcription
AT2G21650	-13.28	pSUC2	MEE3	regulation of transcription
Translation				
AT2G01010	18.5	pSUC2		translation
AT1G61580	-4.42	pSUC2	RPL3B	translation
Transport				
AT2G07687	4.59	pSUC2		hydrogen ion transmembrane transport
AT2G07671	2.2	pSUC2		proton transport
AT5G62730	-2.63	pSUC2		oligopeptide transport
AT1G70230	-2.7	pSULTR2;2	TBL27	nitrate transport
AT4G17970	-3.62	pSUC2	ALMT12	anion transmembrane transport
Other Biological Process				
AT4G17220	-4.5	pSUC2	MAP70-5	xylem and phloem pattern formation
AT1G69700	-2.82	pSULTR2;2	HVA22C	response to abscisic acid
AT1G75580	-2.71	pSUC2		response to auxin

Other Cellular Process				
AT2G43840	-2.69	pSULTR2;2	UGT74F1	SA metabolic process
AT1G62180	-6.93	pSUC2	APR2	cell redox homeostasis
AT1G22260	-16.58	pSUC2	ZYP1a	cell division
Other Metabolic Process				
AT2G07698	5.59	pSUC2		ATP synthesis coupled proton transport
AT1G58370	-2	pSUC2	RXF12	xylan biosynthetic process
AT5G16230	-2.08	pSULTR2;2		oxidation-reduction process
AT1G03920	-3.08	pSUC2		protein phosphorylation
AT1G78500	-3.23	pSUC2		sterol biosynthetic process
AT1G19640	-3.93	pSUC2	JMT	JA mediated signaling pathway
AT3G23630	-4.43	pSULTR2;2	IPT7	cytokinin biosynthetic process
AT5G45400	-6.72	pSUC2	RPA70C	DNA replication
AT1G30640	-7.17	pSUC2		protein phosphorylation
AT4G39210	-7.58	pSUC2	APL3	starch biosynthetic process
Unknown Biological Process				
AT2G07708	3.49	pSUC2		
AT3G52070	3.27	pSULTR2;2		
AT3G51632	-2.18	pSUC2	CPuORF44	
AT3G24460	-2.36	pSUC2		
AT2G39690	-2.41	pSUC2		
AT3G60160	-2.47	pSULTR2;2	ABCC9	
AT3G25572	-2.66	pSUC2	CPuORF11	
AT5G10770	-2.7	pSULTR2;2		
AT1G53542	-2.76	pSUC2		
AT5G08360	-3.69	pSUC2		
AT1G34060	-3.97	pSULTR2;2		
AT2G18969	-4.55	pSUC2		
AT2G24545	-6.37	pSULTR2;2		
AT3G11405	-7.17	pSULTR2;2		
AT1G24430	-8.42	pSUC2		
AT5G28370	-11.62	pSUC2		

Highlighted genes are plasmodesmata associated.
[1]Fold-change in TMV infected cells compared to mock infected controls.

3.3 Discussion

The vascular phloem is important for the transport of host molecules including sugars, phytohormones, proteins, RNAs and other small regulatory molecules to regulate plant development and defense (8). Viruses usurp this host transport conduit to spread from initially infected leaves to distil tissues (169). In this study we show this important tissue is uniquely altered during TMV infection with 88% to 90% of phloem translatome transcripts down regulated compared to 31% of transcripts in the whole plant translatome. The down regulation of host genes predominantly in phloem tissue during virus infection could be advantageous for viral phloem loading and systemic movement.

In order to spread systemically, plant viruses must gain access to the phloem vascular tissue. This involves the crossing of multiple cell borders moving from the initially infected cell to the vascular tissue and traveling through the PPU that connect CCs and SEs (169). For TMV this first involves cell-to-cell movement as a vRNP complex through PD. Once the virus reaches the CCs it must travel through the PPU and assemble in the SEs. TMV requires a functional CP for systemic movement and likely travels in the phloem as an assembled virion (96, 166). Once in the SEs TMV moves from source (photoassimilate production) to sink (photoassimilate use/storage) (185). Phloem loading and systemic transport is essential for a successful virus infection. However, the molecular mechanisms and virus-host interactions required for phloem loading and long distance transport remain poorly characterized.

Recent studies have a suggested a role for viral alterations to host transcription as an important factor for viral systemic movement. For example, the TVCV MP has

been found to localize in the nucleus and disruption of the NLS blocked MP nuclear localization and delayed TVCV systemic movement in *N. benthamiana* and Arabidopsis (198). Additionally, the study presented in Chapter 2 describes an interaction between the TMV replication protein and IAA26, an Aux/IAA transcriptional regulator in phloem CCs. In mature tissues, viruses that cannot interact with IAA26 showed reduced phloem loading and are outcompeted in systemic movement assays. Together these studies suggest viral components can alter host gene regulation to promote viral phloem loading and long distance movement.

In this study, we identified TMV induced alterations to the phloem translatome using FLAG-tagged ribosomes expressed from two phloem promoters pSULTR2;2 and pSUC2. We found that the majority of transcriptional changes occurred in pSUC2 samples with 4708 altered genes compared to 587 altered genes in pSULTR2;2 samples and 650 altered genes in p35S samples. This suggests phloem companion cells, where pSUC2 is specifically expressed, may be an important cell type for TMV directed reprogramming of gene expression. We also observed a lower percentage of reads mapping to exons in pSUC2 TMV infected samples. It is possible that reads mapping to rRNAs in these samples are responsible for the decreased percentage of reads mapping to exons. Increased rRNA reads could have an impact on the high number of altered genes in pSUC2 samples. To account for this possibility, we mapped all the translatome samples to the 18S rRNA and 25S rRNA sequences. We found no significant difference between 18S or 25S rRNA in pSUC2 and pSULTR2;2 TMV infected samples (Table 3.1). This suggests a

difference in 18S or 25S rRNA abundance is not responsible for the large number of uniquely altered genes we observe in pSUC2 samples and not in pSULTR2;2 samples.

However, we did find a higher percentage of reads mapping to the chloroplast in pSUC2 TMV samples compared to pSULTR2;2 TMV samples. We hypothesize reads mapping to the chloroplast account for the majority of reads that do not map to exons. To test if differences in chloroplast reads are responsible for the large number of genes altered in pSUC2 samples during TMV infection, all filtered reads for each translatome sample were mapped only to annotated gene regions. This method of mapping eliminated all reads mapped to the chloroplast. After statistical analysis to identify differentially expressed genes, we found that during TMV infection pSUC2 samples still have the most changes in gene expression with 3,858 genes altered compared to 469 genes altered in pSULTR2;2 samples and 718 genes altered in p35S samples. Additionally, in both pSUC2 and pSULTR2;2 samples genes altered during TMV infection are still predominately down regulated (82% and 72% respectively) and in p35S samples genes altered during TMV infection are still predominately up regulated (77%). This additional analysis supports our conclusion that gene expression in companion cells is dramatically and uniquely reprogrammed during TMV infection compared to other cell types.

We found several categories of genes associated with viral movement and defense responses uniquely altered in the pSUC2 phloem translatome. One of these gene families is the glucan synthase-like/callose synthase genes. Seven family members were down regulated during TMV infection. Callose is deposited at the PD

neck region where it acts as a physical barrier decreasing the SEL of the PD (159). Increased callose deposition at PD has been shown to inhibit viral cell-to-cell movement (263). Alternatively, expression of β-1,3-glucanase, which degrades callose, from the TMV genome increased viral spread (158). Down regulation of callose synthase genes in phloem tissues could help to reduce the accumulation of callose at the PPU to promote viral movement from CCs to SEs.

Another set of genes known to impact viral cell-to-cell movement are the PD located proteins (PDLP). PDLPs may be involved in regulation of callose at PD and have been shown to bind to the MPs of some tubule forming viruses to mediate viral cell-to-cell movement (165). PDLP2 and PDLP3 were both down regulated only in the pSUC2 phloem translatome. Altering the expression of these PD associated proteins may lead to changes in callose deposition at the PD and enhanced viral movement.

Another category of altered genes are components of the RNA silencing pathway. RNA silencing is a sequence specific RNA-guided gene regulatory mechanism conserved in a wide range of eukaryotic organisms (441). In plants this includes mRNA degradation or translation inhibition at the post-transcriptional gene level (named PTGS) or epigenetic modification at the transcriptional level, dependent on RNA-directed DNA methylation (RdDM) (442). Virus infection can trigger RNA silencing and RNA silencing is thought to be a natural antiviral response in plants (441). In the pSUC2 translatome DLC2, DLC4, and RDR6 were all down regulated in response to TMV infection. DLC2 and DCL4 have both been implicated in generating viral siRNAs (443, 444). RDR6 along with RDR1 are also required in the

cytoplasmic RNA silencing pathway involved in silencing viruses (444). Furthermore, siRNAs are known to move systemically in the phloem (445). Down regulation of RNA silencing components the phloem tissue may help prevent the accumulation of viral siRNAs and promote viral infection.

We also found several transcription factors including bZIP, ARF and WRKY family members that were uniquely altered in the phloem translatome. Several members of these transcription factors have been linked to host defense responses. For example, TGA proteins are a class of bZIP proteins involved in SA mediated defense responses (436). Both TGA1 and TGA2 are down regulated in only the pSUC2 translatome. Down regulation of TGA transcription factors in phloem tissue may be a possible mechanism to dampen SA mediated defense responses.

Another transcription family differentially altered in phloem tissue is ARFs, which are key regulators of Aux signaling (354). While Aux is generally associated with plant growth and development, it can also contribute to host defense responses though an antagonistic relationship with the SA signaling pathway (360, 361). ARFs can act as either transcriptional activators or repressors and dimerization or oligomerization of different combinations of ARFs allow for the fine tuning of Aux responses (340). During TMV infection, we found nine ARF family members were down regulated in the pSUC2 translatome. Four of these family members, ARF5, ARF6, ARF8, and ARF19 are characterized as activators. While the remaining five, ARF2, AFF4, AFR11, ARF16, and ARF18 are considered repressors (333). ARF8 and ARF11 were also altered in the pSULTR2;2 translatome while only ARF11 was altered in the p35S translatome. Down regulation of ARF transcriptional repressors

in the phloem may help to suppress SA mediated defense responses and be advantageous for viral infection. Conversely, down regulation of ARF transcriptional activators may be advantageous for the host plant.

WRKY proteins have also been linked to defense with specific family members showing enhanced expression and/or DNA-binding activity in response to pathogens or defense signals (400). In response to TMV infection three WRKY family members are up regulated in the p35S translatome while six WRKY family members are down regulated in the pSUC2 translatome. Interestingly, WRKY8 is one of the family members that is up regulated in the p35S translatome, but is not altered in the pSUC2 or pSULTR2;2 phloem translatomes. WRKY8 has been linked to viral systemic movement where suppression of WRKY8 during infection with TMV-cg correlated with viral systemic accumulation (200). Another family member, WRKY57 is down regulated in both the pSUC2 and pSULTR2;2 translatomes but not in the p35S translatome. WRKY57 has been reported to function as a node for JA and Aux mediated signaling (446). It is possible that down regulation of this key node could also impact SA mediated defense responses as Aux and JA both have an antagonistic relationship with SA signaling (204).

It is clear that many genes with possible connections to virus movement and host defense responses are altered in the phloem during virus infection. Genes altered during TMV infection in the phloem translatomes represent two possible groups. One group of genes are expressed in the phloem and other tissues but only altered by TMV in phloem tissues. The second group of genes is those that are expressed predominately in phloem tissues and altered by TMV in the phloem. We identified

this second group of genes by comparing all genes uniquely altered in the phloem translatomes to phloem enriched genes. Phloem enriched genes were defined as genes up regulated in pSUC2 and pSULTR2;2 mock samples compared to p35S mock samples. This group of identified phloem enriched and TMV altered genes included six transcription factors. It is possible that alteration of transcription factors specifically in the phloem is responsible for large differences in gene regulation observed in the phloem translatomes. One of these transcription factors NAM, belongs to the NAC family of plant-specific transcription factors. The NAC family of transcription factors has been reported to be involved in plant development, senescence, and defense (447). Interestingly, several NAC family members have been shown to associate with virus encoded proteins including the TMV replication protein and ATAF2 (241, 448, 449).

Another gene of particular interest that is enriched in phloem tissues and also altered during TMV infection is MAP70-5. MAP70-5 binds to microtubules *in vitro* and associates with microtubules in a punctate manner *in vivo* (450). It remains controversial whether microtubules are involved in the transport of TMV replication complexes to the plasmodesmata or alternatively provide a route to a MP degradation site (71, 368). Another microtubule-associated protein, MPB2C, has been shown to bind to MP and interfere with cell-to-cell transport of TMV MP (70). MAP70-5 is downregulated 4.5 fold in response to TMV infection in the pSUC2 phloem translatome. Down regulation of MAP70-5 may alter microtubule dynamics and be advantageous for viral movement from CCs to SEs.

Based on our findings, the phloem translatome is uniquely altered during virus infection with the majority of genes being down regulated. Genes altered in the phloem include transcription factors, callose synthases, components of the RNA silencing pathway, and genes involved in host defense responses. At the CC-SE boundary viral directed alterations to the phloem could lead to decreased callose deposition at the PPU and increased phloem loading. Alterations to the silencing pathway and other host defense pathways may provide a mechanism to dampen systemic defense signals. Combined virus directed alterations to the phloem translatome may be essential for the long distance movement of viruses.

3.4 Methods

3.4.1 Generation of promoter::HF-RPL18 Transgenic Lines and Plant Growth

p35S::HF-RPL18 , *pSUC2::HF-RPL18* and *pSULTR2;2::HF-RPL18* constructs were provided by J. Bailey-Serres, University of California, Riverside, CA, USA. These constructs are a modification of the T-DNA binary vector pPZP111 (451). They include the TMV omega 5' leader (66-bp) fused to an open reading frame that consists of $M(H)_6(G)_3$DYKDDDDK(the FLAG epitope)$(G)_7$ fused to the 187 amino acid coding sequence of *RPL18B*, followed by the OCS3' terminator. Constructs were introduced into the *Agrobacterium tumerfaciens* strain GV3101 (409) and *Arabidopsis thaliana* ecotype Shahdara plants were transformed by the floral dip method (407). Transformants were selected on 1X Marushige and Skoog agar containing 50 mg/liter of kanamycin then moved to soil. All plants were maintained in growth chambers for a 12-h photoperiod at 24°C.

3.4.2 Characterization of promoter::HF-RPL18 Transgenic Plant Lines

Transformed plant lines were confirmed by PCR analysis of leaf-extracted genomic DNA. No abnormalities in seedling growth or plant development were observed in any of the promoter::HF-RPL18 transgenic lines. T2 plants from two confirmed transgenic lines for each promoter::HF-RPL18 construct were used for qRT-PCR analysis of transgene *HF-RPL18* mRNA expression. Total RNA was isolated from five week old promoter::HF-RPL18 plants or non-transformed control plants using the RNeasy Plant Mini Kit (Qiagen, Valencia, CA USA) according to the manufacturer's instructions. One microgram of isolated RNA was pretreated with RQ1 DNase (Promega, Madison, WI USA), followed by reverse transcription using SuperScript III First-Strand Synthesis System and random hexamer primers (Invitrogen by Life Technologies, Carlsbad, CA USA). SYBR green real-time qRT-PCR was performed in 96-well reaction plates in an ABI Prism 7100 (Applied Biosystems, Foster City, CA USA). Experiments were done in three biological replicates, with each containing three technical replicates. The 18S RNA gene was chosen as an internal control for normalization and amplified using primers 5' CGTCCCTGCCCTTTGTACAC and 3' CGAACACTTCACCGGATCATT. Primers 5' ATTTACAATTACCATGGGACATCAC and 3'CACCACCTCCCTTATCATCATC were used to amplify the *HF-RPL18* transgene.

3.4.3 Virus Infections

Four week plants were used for virus inoculation. All rosette leaves were dusted with carborundum (Fisher Scientific Company, Pittsburgh, PA) and

mechanically inoculated with 1 mg/ml of TMV or mock infected with sterile water. Shoot tissue was collected six days post inoculation and immediately frozen in liquid nitrogen and stored at -80 C. The shoot tissue from 20 plants was combined for each biological replicate. Two biological replicates were generated for each promoter construct. Biological replicates were grown in different months under the same growth chamber conditions.

3.4.4 Tissue Print Immunoblots

Inoculated leaves were cut from plants and placed onto nitrocellulose sheets and sandwiched between two sheets of filter paper. Leaves were pressed to the nitrocellulose using a rolling pin. Leaves were then carefully removed from the nitrocellulose, leaving an imprint of the leaf. Tissue prints were washed in 1X TBS and blocked in 5% nonfat dry milk for 20 min at room temperature. Prints were then probed with rabbit anti-CP antiserum for two hours, followed by a two hour incubation with alkaline phosphatase conjugated goat anti-rabbit antibodies (Sigma). CP accumulation was visualized by the addition of 5-bromo-4-chloro-3-indolyl phosphate and nitroblue tetrazolium, as previously described (452).

3.4.5 Immunopurification of Ribosomes and RNA Extraction

The immunopurification of ribosomes from *promoter::HF-RPL18* lines was done as previously described (390) with slight modification. Frozen tissue was homogenized in Polysome Extraction Buffer (PEB; 200 mM Tris-HCl, pH 9.0, 200 mM KCl, 25 mM ethylene glycol tetraacetic acid (EGTA), 36 mM MgCl2, 1% (v/v) octylphenyl-polyethylene glycol (Igepal CA-630), 1% (v/v) polyoxyethylene 10

tridecyl ether, 1% (v/v) sodium deoxycholate, 1 mM dithiothereitol (DTT), 50 ug/mL cycloheximide, 50 ug/mL chloramphenicol, 0.5 mg/mL heparin) using 10 mL PEB per 5 g of tissue. Homogenates were clarified by centrifugation at 16,000 *g* for 15 min and filtrated with cheesecloth. An aliquot of 100 µL of the supernatant was reserved for isolation of total RNA. To the remaining supernatant 50 µL of anti-FLAG magnetic beads (Sigma) were added and incubated at 4 C for 2 hours with gentle rocking. The beads were recovered using a magnet and washed four times for 5 min with 5 mL of wash buffer (200 mM Tris-HCl, pH 9.0, 200 mM KCl, 25 mM EGTA, 36 mM $MgCl_2$, 1 mM DTT, 50 µg/mL cycloheximide, 50 µg/mL chloramphenicol). 1 mL of TRIzol reagent was then added directly to the FLAG magnetic beads to isolate mRNA bound to polysomes. Samples were left at room temperature for 10 min. 200 µL of chloroform was added and tubes were shaken vigorously by hand for 15 seconds and incubated at room temperature for 3 min. Samples were then centrifuged at room temperature for 15 min at 12,000 *g*. The upper aqueous phase was transferred to a new tube. 0.5x volume of 100% ethanol was added to the aqueous phase then transferred to a Qiagen RNeasy column. Washes and RNA elution was performed according to the manufacturer's instructions. Isolated RNA was measured on a NanoDrop 1000 and then run on a 2100 Bioanalyzer Eukaryotic Total RNA Nanochip (Agilent Technologies Palo Alto, CA, USA) to check RNA quality. Library preparation with Illumina TruSeq RNA sample preparation kit and sequencing with Illumina HiSeq1500 rapid run was done by the UM-IBBR Sequencing Core at University of Maryland College Park (http://ibbr.umd.edu/facilities/sequencing). Approximately 15.6 to 59.4 million 50bp

single-end raw reads were generated for each library. Raw sequencing data files are available upon request (e-mail jculver@umd.edu).

3.4.6 Mapping of Reads

Raw reads were filtered to eliminate sequences matching the illuminia adapters then mapped to the Arabidopsis thaliana Col-0 genome reference TAIR10 using the CLC Genomics Workbench v 7.5.1 RNA-seq analysis tool and default parameters (Mismatch cost 2, Insertion cost 3, Deletion Cost 3, Length fraction 0.8, Similarity fraction 0.8, Max hits for a read 10) (CLC Bio, Aarhus, Denmark). Total reads aligned to genes were used in all subsequent analyses. Filtered reads were similarly mapped to the TMV genome (NC_001367) retrieved from NCBI.

3.4.7 Gene Expression Analysis

Statistical analysis to identify differentially expressed genes was performed using the CLC Genomics Workbench Baggerly's test on proportions (434). Results were filtered with a cut of value of Fold change > 1.5, FDR corrected p-value < 0.05 for phloem enriched genes and Fold change > 2, FDR corrected p-value < 0.05 for TMV altered genes.

3.4.8 Assignment of GO Terms, GO Enrichment Analysis, and Identification of Transcription Factors

Gene symbols, gene model descriptions, and gene ontology (GO) annotations were retrieved from TAIR (37). The generic GO term mapper and GO term finder tools developed at the Lewis-Sigler Institute at Princeton (385) were used to assign GO Slim terms and identify GO annotation terms that occurred more frequently than

expected by chance. A Bonferroni corrected p-value of < 0.01 was used as a cut off for significantly enriched GO terms. Transcription factors were identified using the Arabidopsis gene regulatory information server (AGRIS), AtTFDB (453).

3.4.9 Heatmap Generation

All heatmaps were generated in R using the heatmap.2 function in the gplots CRAN library (http://cran.r-project.org/web/packages/gplots/index.html). Log_2 (RPKM) values exported from the CLC genomics workbench were used to generate all heatmaps.

Chapter 4: Conclusions and Perspectives

A successful plant viral infection involves the spread of the virus from the initially infected cell to neighboring cells through plasmodesmata, then loading into the vascular tissue and systemic movement throughout the plant (169). Movement of molecules into the phloem vascular tissue is a highly regulated aspect of plant biology important for plant development and defense (454). It is still unclear what precisely is required for viruses to load into the phloem tissue. Some viral components, such as a functional CP, have been identified as required for the systemic movement of many diverse plant viruses (166, 169, 429). However, exceptions do exist, and some viruses do not need a CP for systemic movement (169). Other viral proteins besides the CP may also be required for systemic movement. For example, TMV also requires its replication protein (187, 188).

Much less is known about host components or pathways involved in viral phloem loading and long distance movement. One of the best studied examples are the restricted TEV movement (RTM) genes. At least three RTM genes restrict the long distance movement but not local cell-to-cell movement of several potyviruses in Arabidopsis Col-0 and WS plants (455, 456). RTM1 encodes a jacalin-like lectin protein belonging to a family associated with pathogen defense (457). RTM2 is related to the multigene family of small heat-shock proteins (458). RTM1 and RTM2 are expressed in the phloem and localize to the SE (459). RTM3 has been shown to interact with RTM1 in yeast and plants (460). These studies suggest that RTM proteins form a complex that disrupts potyvirus movement within the vascular tissue,

however the molecular mechanisms remain unknown. Mutations in the CP can overcome this resistance and restore long distance movement, but a direct interaction between CP and RTM proteins has yet to be demonstrated (461). These studies indicate that host components in the phloem can impact virus long distance movement.

There is also an emerging theme of viral directed reprograming of transcriptional responses to promote viral systemic movement. For example, the TVCV MP has been found to localize in the nucleus and disruption of the NLS not only blocked MP nuclear localization but also delayed TVCV systemic movement in *N. benthamiana* and Arabidopsis (198). Additionally, the MP of ToMV has been shown to interact with KELP, a transcriptional coactivator (199). Furthermore, TMV-cg infection has been shown to suppress transcriptional factor WRKY8 binding to the ABI4 promoter and this WRKY8 mediated alteration in gene expression impacts virus systemic movement (200).

In this thesis, I determined that the TMV replication protein interacts with a host Aux/IAA transcriptional regulator, IAA26, in phloem CCs. This interaction is important for TMV phloem loading and long distance movement through the phloem vascular tissue. Furthermore, Aux/IAA proteins act as negative regulators of Aux signaling. Thus, the TMV replication protein Aux/IAA interaction results in changes to downstream target genes including changes in SA and JA mediated defense signaling. Translatome profiling experiments further demonstrate phloem tissue is uniquely altered during TMV infection with genes involved in virus defense being down regulated only in phloem tissues. Together, this work describes a novel

mechanism where the TMV replication protein reprograms the phloem environment to promote viral systemic movement.

4.1 Proposed Model

Based on the research detailed in this manuscript and previous work on the IAA26 - TMV replication protein interaction (212, 213) I propose the following updated model (Fig 4.1). In uninfected mature tissues, Aux/IAA proteins accumulate and act as negative regulators of ARFs preventing them from activating target Aux responsive genes. During TMV infection, the TMV replication protein interacts with a subset of Aux/IAA proteins (IAA26, IAA27, IAA18, *Nb*IAA26) in the phloem vascular tissue and either targets the proteins for degradation by some yet identified mechanism or prevents Aux/IAA entry into the nucleus. Due to the rapid turnover of Aux/IAA proteins, this interaction quickly depletes the concentration of Aux/IAA proteins in the nucleus. Depletion of Aux/IAA proteins leaves ARFs free to dimerize or oligomerize to regulate Aux responsive genes (294, 340). The result is Aux-independent regulation of target genes, and a reprogramming of the phloem cells to mimic the environment of younger tissues where Aux levels are higher and Aux/IAA proteins are degraded. Regulation of target defense related genes and cross-talk between the Aux signaling pathway and SA and JA pathways results in changes in SA and JA mediated defense responses and possible changes in callose deposition at the PD. The combined effect is to reprogram the vascular phloem to be more amenable to TMV systemic movement.

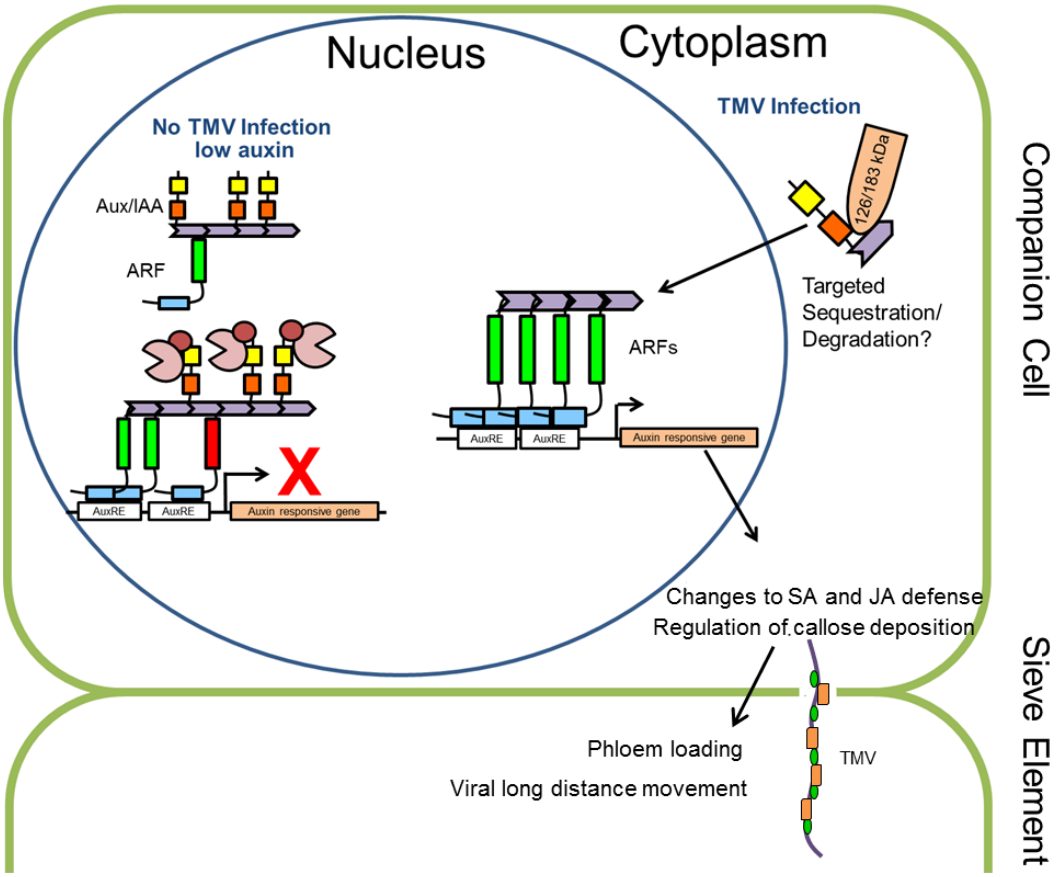

Figure 4.1. Model for TMV and Aux/IAA Interaction.

During TMV infection Aux/IAA proteins are prevented from localizing to the nucleus, leaving ARF proteins free to form dimers or oligomers to regulate Aux responsive genes. Some of these target genes are involved in SA and JA defense responses and regulation of callose deposition at the plasmodesmata. The combined effect is to promote TMV movement from companion cells to sieve elements allowing the virus to load into the phloem and move long distances.

Reprogramming the cellular environment may be of particular importance for TMV and related viruses that are mechanically transmitted, and thus have no mechanism to direct them to the host tissues that are optimal for their replication and spread.

This model is supported by several findings. First, the TMV helicase – Aux/IAA protein interactions occur in a wide range of TMV hosts including Arabidopsis, Tomato and Tobacco (Chapter 2) (374). The fact that this interaction is conserved in diverse hosts suggests that it is of fundamental importance for TMV infection. In Arabidopsis, all three interacting Aux/IAA proteins are expressed in the phloem vascular tissue (Chapter 2, Fig. 2.1) and in *N. benthamiana Nb*IAA26 is similarly expressed in the phloem (Appendix C). Additionally, I have shown the *At*IAA26 protein localizes to the nucleus of phloem CCs and its nuclear localization pattern is disrupted during TMV infection (Chapter 2, Figs. 2.3 and 2.4) supporting that TMV is interacting with Aux/IAA proteins specifically in the phloem. The ability of TMV to disrupt the CC nuclear localization of IAA26 correlates with enhanced phloem loading and systemic movement compared to a non-interacting virus TMV-V1087I (Chapter 2, Fig. 2.6B and 2.8). Furthermore, stabilization of IAA26 in companion cells leads to reduced accumulation and phloem loading of TMV in 9 week old plants (Chapter 2, Figs. 2.5 and 2.7). Transcriptional changes in IAA26 stabilized plants suggest IAA26 target genes include those involved in SA and JA mediated defense responses and genes involved in callose deposition at PD (Chapter 2, Table 2.1). Translatome profiling of the phloem during TMV infection further identified defense related genes including callose synthases being uniquely altered in the phloem compared to all tissue types (Chapter 3, Fig. 3.10).

4.2 TMV Replication Protein is multifunctional

Virus proteins often function in multiple processes. The TMV replication protein is required for replication, cell-to-cell movement through PD, activation of HR, and acts as a RSS (20, 38, 44, 46). In addition, the TMV replication protein has been shown to interact with many host factors including P58 an inhibitor of protein kinase that inhibits host defense, the *N* gene product which activates HR, and TOM1 a membrane protein involved in viral replication complexes (133, 138, 462, 463). This study has identified an additional role for the TMV replication protein in viral systemic movement through its interaction with Aux/IAA proteins. A common theme in these interactions is the involvement of the helicase domain. Conventionally, helicases are responsible for unwinding dsRNA (36). However, it is apparent that the TMV helicase domain is not just a RNA-binding protein, but is also a key player in virus-host interactions. The mechanistic details that allow this protein to function in diverse processes remain to be elucidated.

4.3 Developmental Age and Defense Responses

Interestingly, the interaction between the TMV replication protein and Aux/IAA proteins described in this manuscript occurs primarily in mature tissues where Aux/IAA proteins accumulate. It is in these mature tissues that there is a biological advantage of increased phloem loading and systemic movement for Aux/IAA interacting viruses compared to viruses that cannot interact. In Arabidopsis, the majority of what we know about host defense signaling and resistance comes from experiments using young plants. However, there are examples

of developmentally regulated disease resistance (464-466). Young Arabidopsis plants are susceptible to virulent strains of *P. syringae* pv. *tomato*, while mature plants show a robust defense response called age-related resistance (ARR) (466, 467). It is hypothesized that mature ARR-competent plants are able to alleviate bacterial mediated suppression of SA accumulation (466). The ability to accumulate SA is required for ARR in Arabidopsis and plants defective in SA biosynthesis or accumulation are ARR-defective and mature plants are then susceptible to *P. syringae* (467-469). Unlike SA mediated defense responses in young plants, NPR1 is not required for ARR (467, 470). ARR additionally occurs independently of defense regulator WHY1 (466). These studies make it clear that developmental age is an important factor in virus-host interactions.

4.4 Future Goals

The finding that alteration of Aux/IAA signaling by stabilizing IAA26 in CCs leads to changes in the expression of genes involved in general viral cell-to-cell movement as well as SA and JA mediated defense responses raises the question if this is a conserved mechanism that will affect other plant viruses or even other pathogens. There is some evidence that stabilization of Aux/IAA proteins is detrimental to other pathogens. Plants that produce a nondegradable form of AXR2/IAA7 have a 10-fold reduction in *P. syringae* pv. *maculicola* growth (360). Correspondingly, increased degradation of Aux/IAA proteins by over-expressing the Aux receptor *AFB1* resulted in increased growth of *P. syringae* pv. *tomato* and enhanced disease symptoms (364).

In this study we found that in nine-week-old IAA26 stabilized plants, TMV accumulation was reduced. We also observed reduced phloem loading compared to

control plants (Chapter 2 Fig. 2.5). We plan to use these transgenic plants lines at the nine-week time point to repeat these experiments with additional plant viruses. If we observe that diverse plant viruses also show reduced accumulation and phloem loading in IAA26 stabilized plants, this would suggest genes or pathways regulated by IAA26 represent a conserved mechanism for reducing or promoting viral phloem loading. Conversely, if we see no difference in accumulation and phloem loading for other plant viruses, this would suggest the mechanism is specific to TMV or Tobamoviruses.

Additionally, an alternative approach we could take to stabilize Aux/IAA proteins in the phloem is to express mir393 which targets TIR1 and two AFB genes from a phloem specific promoter (364, 471). Reduction of TIR1 and AFB proteins in the phloem would result in reduced degradation of all phloem expressed Aux/IAA proteins. If we observe reduced accumulation and phloem loading of TMV in these plant lines this would provide further support for my model.

4.4.1 Candidate IAA26 Regulated Genes

To narrow the list of candidate genes that may be regulated by IAA26 we compared the 1228 genes that are altered in IAA26 stabilized plants (Dataset S1) to those identified as being altered during TMV infection in the translatome datasets (Dataset S3). Of those genes that are altered when IAA26 is stabilized 307/1228 (25.0%) were also altered during TMV infection in at least one of the translatomes. The majority of these genes, 279/307 (90.9%), were altered in at least one of the phloem translatomes (pSUC2 and pSULTR2;2) (Fig 4.2A, Table 4.1). Looking at this set of 307 genes that were altered in both IAA26 stabilized plants and TMV

infected plants we found 227 were down regulated and 16 were up regulated under both conditions compared to controls. 31 genes were up regulated in IAA26 stabilized plants but down regulated in TMV infected plants, and 33 genes were conversely down regulated in IAA26 stabilized plants and up regulated during TMV infection (Figure 4.2B). In IAA26 stabilized plants, IAA26 is abundant in the nucleus, while in TMV infected plants IAA26 is relocalized from the nucleus. Thus, we hypothesize that genes regulated directly by IAA26 should behave oppositely under these two conditions. The set of 64 genes that are differentially altered in IAA26 stabilized plants and TMV infected plants is therefore of particular interest and represent possible targets of IAA26 regulation (Table 4.1). qRT-PCR can be used to compare the expression of these candidate genes during TMV and TMV-V1087I (non-Aux/IAA interacting) infection. If any of these genes are altered during TMV infection but not TMV-V1087I infection this would further suggest they are regulated by IAA26. Acquisition of SALK T-DNA knockout lines or overexpression using the CaMV 35S promoter for this narrowed candidate gene list will allow us to test for an effect on TMV systemic movement and phloem loading using CP immuno-detection as done in Chapter 2.

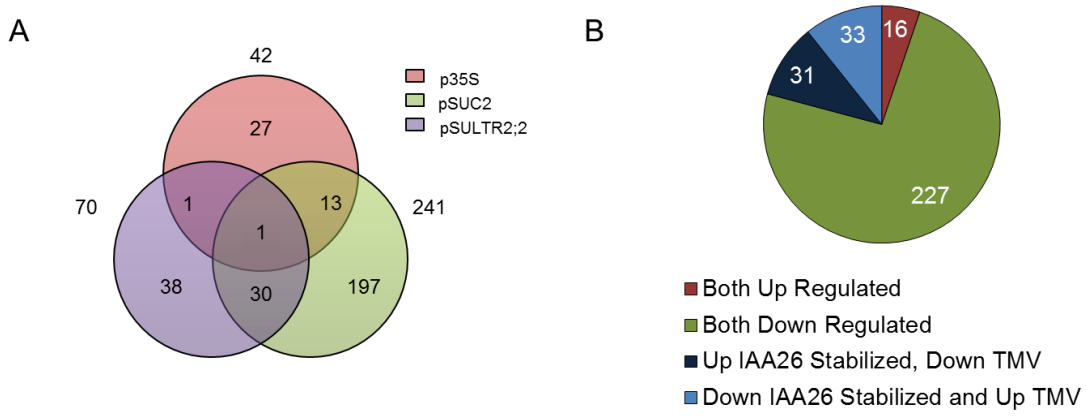

Figure 4.2. Comparison of IAA26 Stabilized Dataset and TMV Altered Translatome Dataset.

(A) Venn diagram displaying genes that are altered in IAA26 stabilized plant lines and at least one of the TMV translatome data sets. (B) Pie graph depicting the regulation of overlapping genes.

Table 4.1. Genes oppositely regulated in IAA26 stabilized plants and TMV infected plants.

Locus Identifier	IAA26 Stabilized Fold-Change	TMV Fold-Change		Translatome Sample	Gene Symbol
AT1G16370	7.24	-3.25		pSUC2	OCT6
AT2G18660	6.99	-2.17		pSULTR2;2	PNP-A
AT1G74430	5.81	-6.69		pSUC2	MYB95
AT4G27410	5.76	-2.65		p35S	RD26
AT4G04490	5.18	-8.12		pSUC2	CRK36
AT3G59710	4.67	-2.45		p35S	
AT1G32960	4.19	-2.95		pSUC2	SBT3.3
AT1G11670	4.01	-2.37		pSUC2	
AT4G22780	3.64	-2.72		pSUC2	ACR7
AT5G60890	3.61	-2.79		pSUC2	MYB34
AT1G01140	3.28	-2.57		pSUC2	CIPK9
AT1G09932	3.21	-2.09		pSUC2	
AT4G08170	2.92	-2.03		pSUC2	
AT5G23020	2.85	-3.33		pSUC2	IMS2
AT5G53050	2.85	-2.66		pSUC2	
AT4G39950	2.61	-4.62		pSUC2	CYP79B2
AT4G23240	2.52	-2.07		pSUC2	CRK16
AT5G61350	2.51	-2.24	-3.44	p35S, pSUC2	
AT4G31500	2.48	-2.74		pSUC2	CYP83B1
AT5G66640	2.46	-7.55	-4.74	pSUC2, pSULTR2;2	DAR3
AT4G01540	2.27	-7.63		pSUC2	NTM1
AT1G69610	2.26	-3.02	-3.47	pSUC2, pSULTR2;2	
AT3G19830	2.17	-3.58		pSUC2	NTMC2T5.2
AT2G17290	2.16	-2.25		pSUC2	CPK6
AT1G01260	2.1	-2.95		pSUC2	
AT2G39980	2.08	-2.27		p35S	
AT5G40390	2.07	-2.09		pSULTR2;2	SIP1
AT5G04020	2.03	-5.36		pSUC2	
AT1G76360	2.02	-2.02		pSUC2	
AT4G19960	2.02	-2.61		pSUC2	KUP9
AT5G07700	2.02	-2.38		pSUC2	MYB76
AT5G04470	-2.05	2.39		p35S	SIM
AT5G66170	-2.14	2.09		p35S	STR18
AT5G40730	-2.62	2.63		pSULTR2;2	AGP24
AT2G47930	-2.63	2.31	2.92	p35S, pSUC2	AGP26

AT5G15530	-3.04	2.36		pSUC2	BCCP2
AT2G14890	-3.06	2.92	3.85	p35S, pSUC2	AGP9
AT1G09460	-3.12	2.47		p35S	
AT1G64220	-3.21	8.64		pSUC2	TOM7-2
AT5G28490	-3.24	2.37	2.42	p35S, pSUC2	LSH1
AT3G17680	-4.12	2.09		p35S	
AT5G65390	-4.32	4.98	4.09	p35S, pSUC2	AGP7
AT5G10430	-4.36	4.39	3.08	p35S, pSUC2	AGP4
AT3G14190	-4.39	2.08		pSUC2	
AT4G37409	-4.54	4.46		p35S	
AT2G42110	-4.68	2.8		p35S	
AT3G05980	-4.68	2.07		pSUC2	
AT5G56320	-5.09	2.29		p35S	EXPA14
AT1G23410	-5.74	2.6		p35S	
AT1G78260	-5.89	2.65		p35S	
AT5G45630	-5.89	6.38		pSULTR2;2	
AT3G02120	-5.97	3.94		pSUC2	
AT3G57920	-6.68	2.43		p35S	SPL15
AT5G09980	-7.36	2.13		pSUC2	PROPEP4
AT3G05890	-7.57	2.75	6.08	p35S, pSUC2	RCI2B
AT3G12870	-8.21	2.52		pSUC2	
AT1G02065	-11.71	2.68		p35S	SPL8
AT3G04510	-15.65	2.4		p35S	LSH2
AT2G01520	-16.35	2.33	2.61	p35S, pSUC2	MLP328
AT1G76420	-27	2.21		p35S	CUC3
AT4G22485	-33.95	4.83	2.07	p35S, pSUC2	
AT4G28680	-126.6	2.13		pSUC2	TYRDC
AT4G22505	-149.78	2.32		pSUC2	
AT5G06640	-302.18	6.98		p35S	EXT10

4.4.2 Translatome Profiling of Phloem Tissues

Host components involved in viral systemic movement have been difficult to identify in part due to the difficulty of sampling phloem tissue. The translatome profiling technique used in Chapter 3 provides a new way to sample phloem tissue and together with advancements in next generation sequencing is a powerful tool to identify changes to the host phloem environment during viral infection. Expansion of this work into other virus-host combinations would provide greater information about how diverse viruses alter this unique tissue. Additionally, monitoring transcriptional changes within the phloem will give insights into the pathways that contribute to movement of host molecules affecting both plant development and defense.

One host system of particular agriculture importance is fruit trees. Virus infection in fruit trees can result in reduced growth, yields, and/or fruit quality and in severe cases, such as infection with PPV, has largely wiped out fruit production in affected parts of the world. PPV causes a severe disease known as Sharka which is associated with reduced tree vigor, premature fruit drop, deformation of fruits, and tree death (4).

In northern climates fruit trees undergo a period of dormancy during the winter followed by proliferation and growth in the spring. Thus, viruses that infect fruit trees spend much of their time in a dormant state, after which they must move long distances through the newly developing phloem vascular tissue in the spring. Currently, very little is known about the molecular mechanisms involved in virus movement in fruit trees, especially during the breaking of dormancy.

To begin to investigate virus activity within phloem tissues, we plan to focus on three positive sense RNA viruses of fruit trees PPV, *Tomato ringspot virus* (ToRSV) and *Prunus necrotic ringspot virus* (PNRSV). These viruses were chosen to represent different viral taxa and are all of economic importance. These viruses additionally represent two different viral movement strategies. PPV and PNRSV require their CP and MP for cell-to-cell movement, but do not require an assembled virion. Alternatively, ToRSV moves cell-to-cell in particle form via MP derived tubules (169, 429).

Transgenic plum tree lines expressing HF-RPL18 from phloem specific and control promoters have been created by our collaborators using the constructs described in Chapter 3. I have done preliminary immunopurifications of polysome complexes (as described in Chapter 3) from plum lines expressing pSUC2::HF-RPL18 and pSULTR2;2::HF-RPL18. qRT-PCR analysis of the ribosomal isolated mRNA from these pull-downs show significant enrichment of the endogenous *SUC2* mRNA in comparison to RNA obtained from total leaf tissue (Fig. 4.3). The enrichment of *SUC2*, a known phloem gene, suggests that these plants lines can be used to successfully isolate the phloem translatome.

Additionally, I have created *N. benthamiana* transgenic plants expressing HF-RPL18 from pSUC2, pSULTR2;2 and p35S. qRT-PCR analysis was used to confirm expression of HF-RPL18 in these plant lines (Fig. 4.4). We plan to utilize these transgenic plant lines to isolate phloem associated mRNAs from virus infected and non-infected plants.

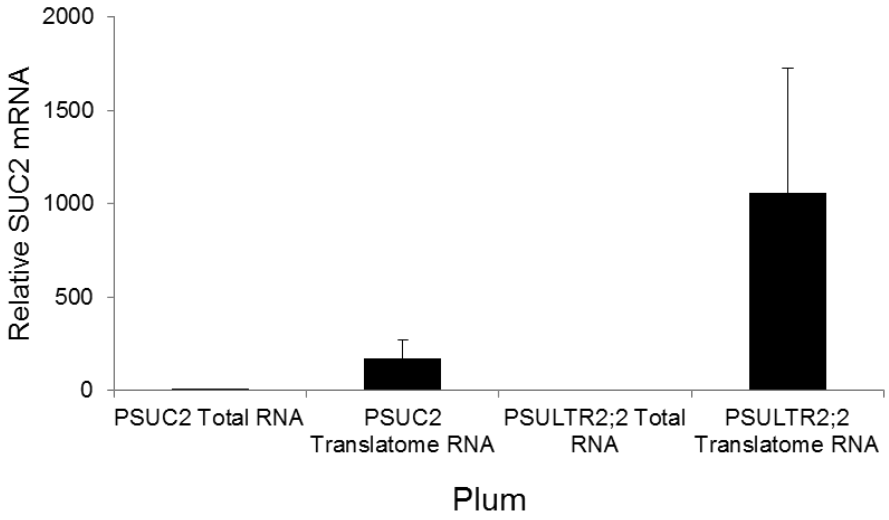

Figure 4.3. Plum Translatome Plant Lines.

(A) qRT-PCR amplification of the endogenous plum sucrose transporter 2 (SUC2) mRNA as a marker for the pull-down of vascular phloem specific mRNA from plum. Total RNA from whole leaf tissue and RPL18 pull-down translatome RNA were amplified for the SUC2 mRNA. 18sRNA was used as an internal control. Data is averaged from two biological replicates and error bars represent the standard error.

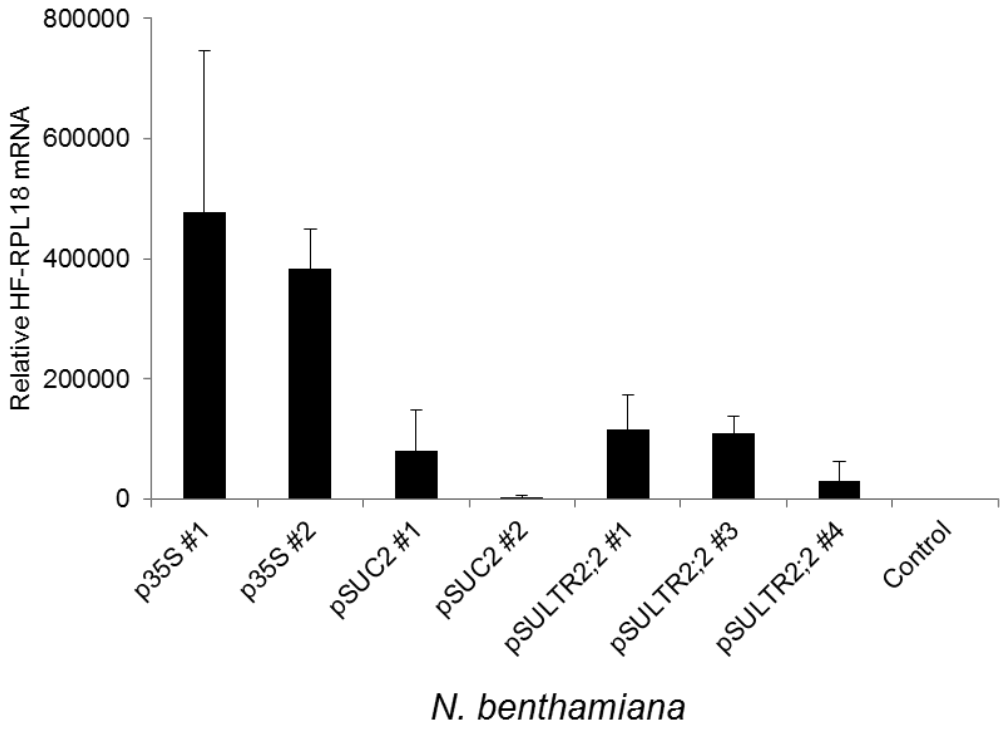

Figure 4.4. ***N. benthamiana*** **Translatome Plant Lines.**

qRT-PCR amplification of HF-RPL18 transgene in N. benthamiana. 18sRNA was used as an internal control. Data is averaged from three biological replicates and error bars represent the standard error.

N. benthamiana is highly susceptible to many plant viruses and additionally there is a 63X draft genome available which can be used to identify relevant orthologs of genes of interest identified in the plum and Arabidopsis studies (472, 473). Working with the *N. benthamiana* system also allows us to take advantage of existing tools for the overexpression, silencing and localization of target genes for further investigation of genes of interest (472).

Our knowledge about how fruit tree viruses travel long distances or persist during periods of dormancy is very limited. The ability to prevent or limit viruses at this stage represents a possible broad spectrum control of virus diseases of fruit and nut crops. Translatome profiling during viral infection is an innovative tool that makes it possible to begin to identify phloem specific alterations that correspond with viral movement and disease development.

Appendix A

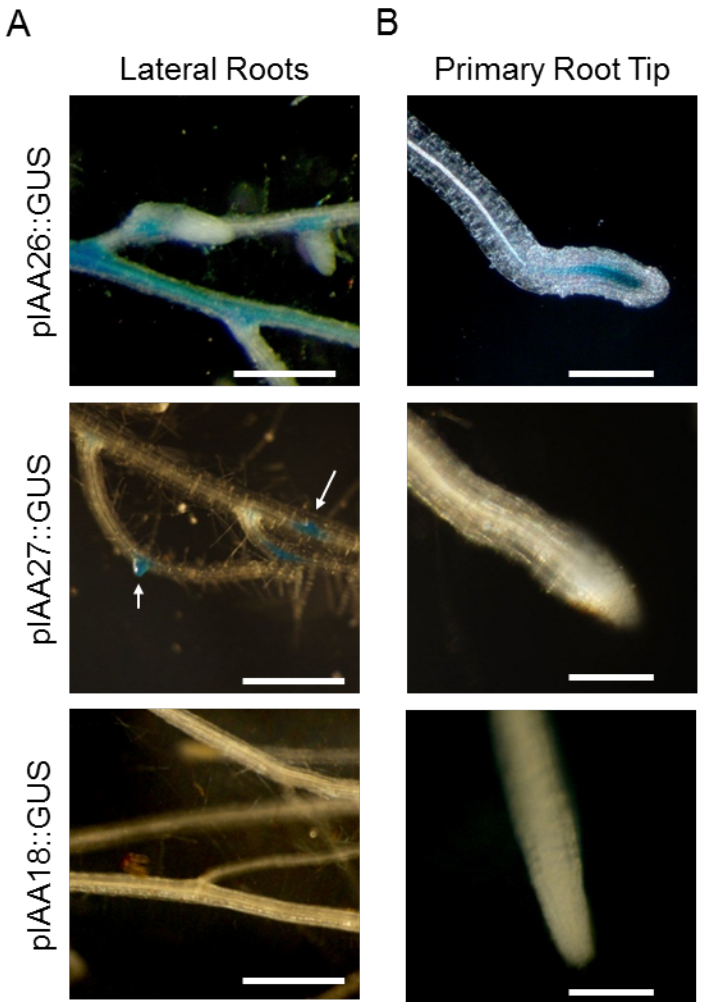

Histochemical analysis of pIAA26::GUS, pIAA27::GUS and pIAA18::GUS expression in *A. thaliana* roots. (A) GUS expression in lateral roots after staining overnight. Bars are 500 µm. (B) Primary root tip. Bars are 200 µm.

Appendix B

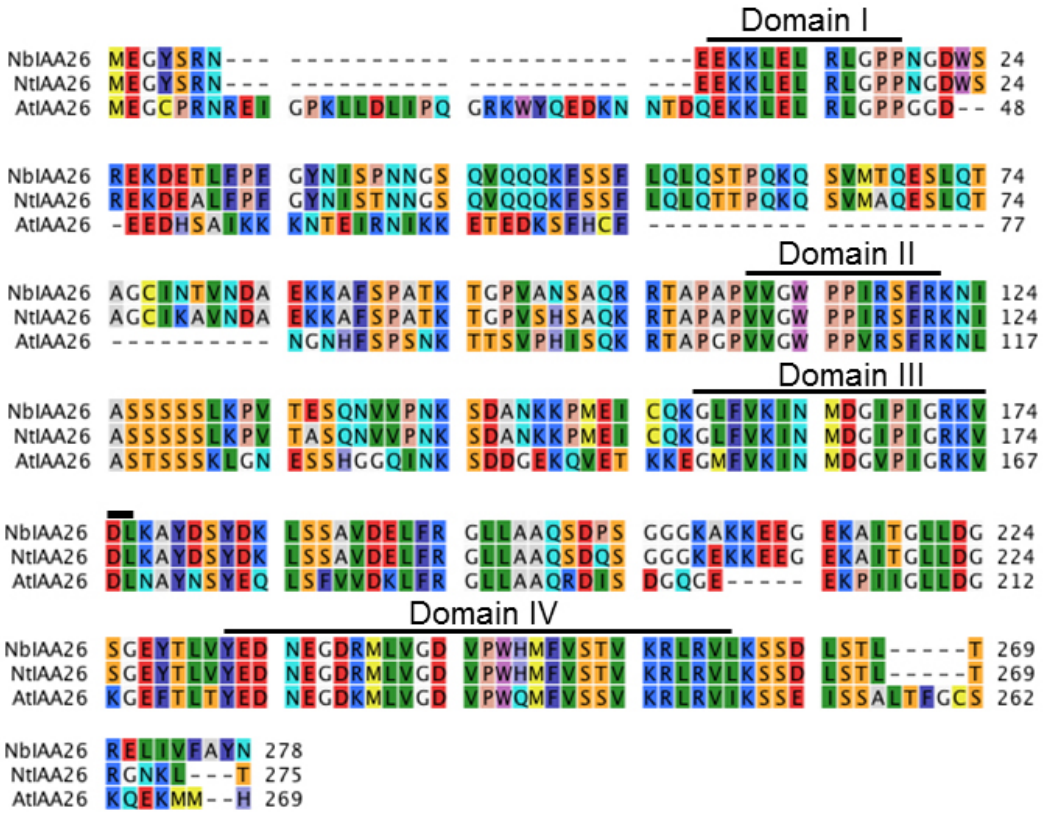

Sequence alignment of *Nb*IAA26, *Nt*IAA26 and *At*IAA26. Similar residues are displayed in the same color. The four conserved Aux/IAA domains are underlined.

Appendix C

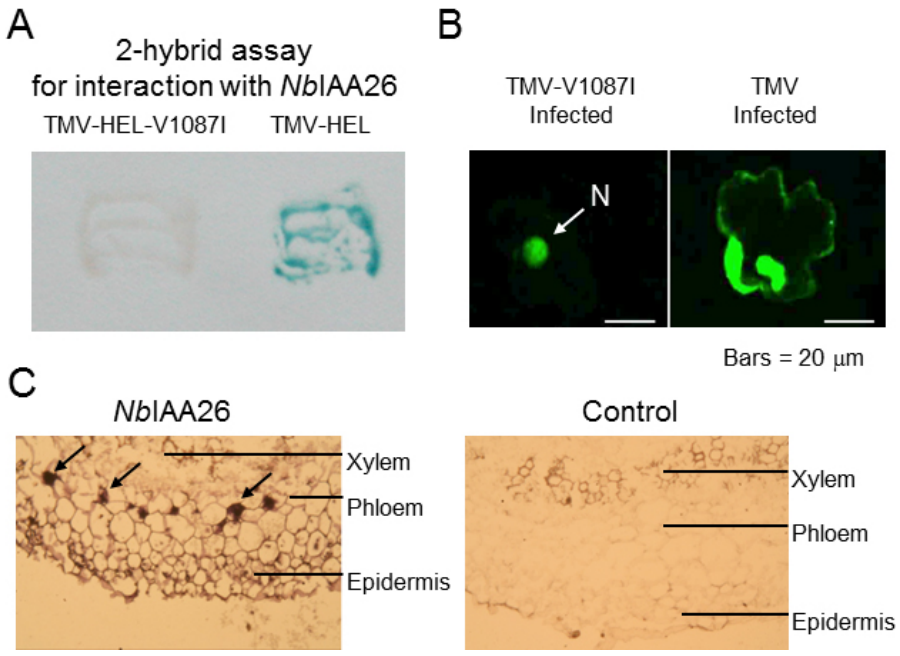

Characterization of *Nb*IAA26. (A) Yeast two-hybrid assay showing the interaction of the TMV-Helicase-Bait protein and *Nb*IAA26-Prey protein and no interaction between TMV-V1087I-Helicase-Bait protein and *Nb*IAA26-Prey protein. (B) TMV infection interferes in the nuclear localization of *Nb*IAA26-GFP. Fluorescent images of *N. bethamiana* leaf tissue transiently expressing *Nb*IAA26-GFP fusion protein in TMV-V1087I infected or TMV infected cells. Yeast two hybrid and transient localization assays were done as previously described (213). Bars are 20 µm. (C) *In situ* immunolocalization of *NbIAA26* in *N. benthamiana* stem cross sections. Dark brown color indicates *NbIAA26* mRNA accumulation. Arrows denote phloem location.

Appendix D

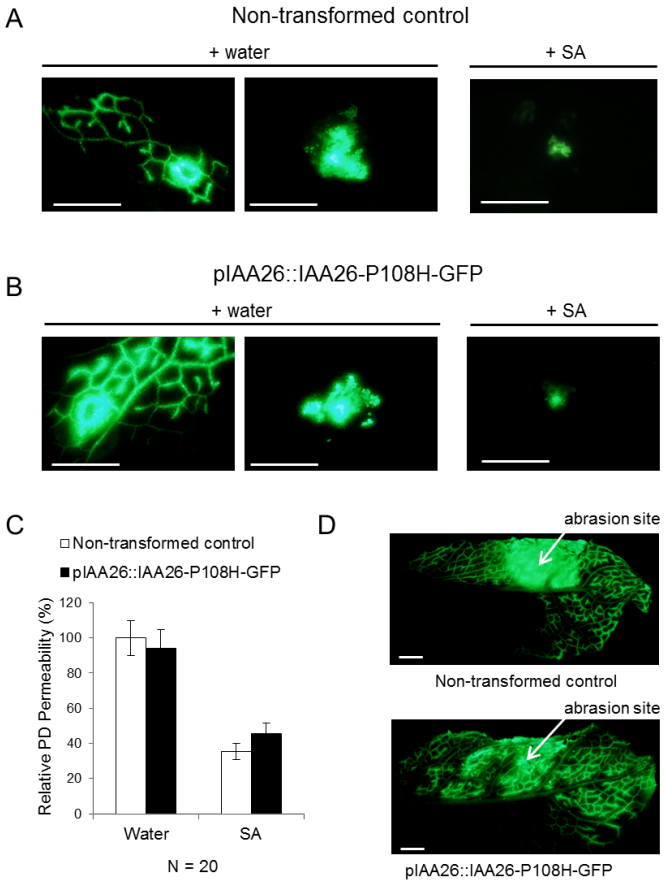

PD permeability in control and IAA26 stabilized plants. PD permeability and phloem loading was examined by CFDA-based dye loading assays. (A) Nine week old control plants treated with water (2 panels) or SA (1 panel). (B) Nine week old pIAA26::IAA26-P108H-GFP plants treated with water (2 panels) or SA (1 panel). (C) Quantification of CF movement. One leaf with two CFDA spot treatments was used from at least ten plants for each assay. The extent of dye diffusion was quantified by measuring the area and normalized to non-transformed control plants. Bars represent average ± standard error. (D) Phloem loading of CF after abrasions with fine sandpaper. Scale bars equal 5 mm.

Appendix E

Name	Forward Primer	Reverse Primer
pIAA26	ATCGATCTCCTTTTTTAGTTCACTAA	GGATCCTGATCAACCCAAGATTCC
pIAA27	TCTAGATTTTGTATGTCTTCTTGCTATGTAT	CCCGGGTTTTTTCAAATATAATTGTGGAC
pIAA18	GTCGACTATCGATCTAAAGTATAAGATGAC	GGATCCTAGGATTTTTTTTAGAGGAACTACA
PR1	CCCACAAGATTATCTAAGGGTTCAC	TCCCACTGCATGGGACCTA
PR2	TCAACCAACAGCTGGACAAA	CCGATGGACTTGGCAAGGTA
PR5	AACGGCGGCGGCGTTC	GCCGCCATCGCCTACTAGA
JAZ1	GCCTGATGTCASATGGAACTTTAG	CAGATTCGTCGGTTTAACATCTTG
JAZ7	GCGACAAGCCTTACTCAATTT	TGATTCGTCCAACGAGCTATG
WRKY38	TCTAGGGATTCTTCTCCTCCTC	GTGAATCGTCCCTCCAATTCT
NHL10	CAAGTTCAGGCTTAGGGTTAGG	AGGTAGTTGTAGTTCCGTTTGAG
PME5	AGTCATCACCGTCTCACTTAAC	TAGCTGGAACCACCACTTTC

Appendix F

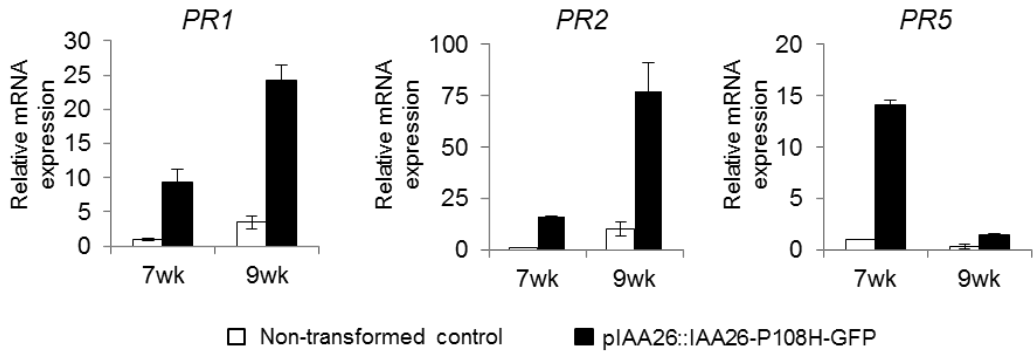

PR1, PR2 and PR5 gene expression in seven and nine week old plants. Fold change comparisons from qRT-PCR expression analysis between non-transformed control (white bars) and pIAA26::IAA26-P108H-GFP (black bars) plants. Each bar represents the average ± standard error from three biological replicates composed of leaf tissue from four to six plants from two independent plant lines. The 18S RNA gene was chosen as an internal control for normalization.

Appendix G

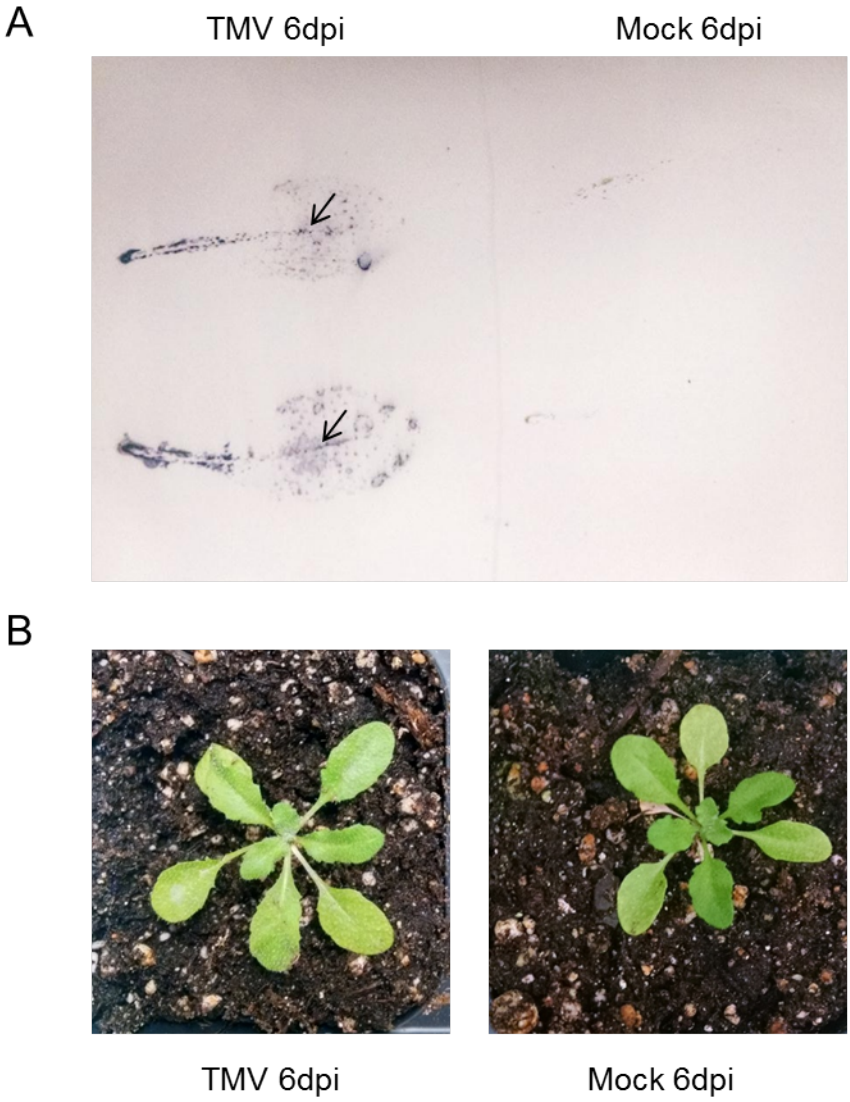

(A) Tissue print immunoblot of TMV infected or mock infected A. thaliana ecotype Shahdara leaves at 6dpi. Purple staining indicates TMV CP accumulation. Arrows denote accumulation in the mid vein. (B) Representative images of TMV or mock infected A. thaliana ecotype Shahdara plants 6dpi.

Bibliography

1. Rybicki EP (2015) A Top Ten list for economically important plant viruses. *Archives of virology* 160(1):17-20.

2. Scholthof KBG*, et al.* (2011) Top 10 plant viruses in molecular plant pathology. *Molecular Plant Pathology* 12(9):938-954.

3. García JA, Glasa M, Cambra M, & Candresse T (2014) Plum pox virus and sharka: a model potyvirus and a major disease. *Molecular plant pathology* 15(3):226-241.

4. Cambra M, Capote N, Myrta A, & Llácer G (2006) Plum pox virus and the estimated costs associated with sharka disease. *EPPO Bulletin* 36(2):202-204.

5. Fulton J, Gergerich R, & Scott H (1987) Beetle transmission of plant viruses. *Annual review of phytopathology* 25(1):111-123.

6. Verchot J, Driskel B, Zhu Y, Hunger R, & Littlefield L (2001) Evidence that soilborne wheat mosaic virus moves long distance through the xylem in wheat. *Protoplasma* 218(1-2):57-66.

7. Harries P & Ding B (2011) Cellular factors in plant virus movement: at the leading edge of macromolecular trafficking in plants. *Virology* 411(2):237-243.

8. Turgeon R & Wolf S (2009) Phloem transport: cellular pathways and molecular trafficking. *Annu Rev Plant Biol* 60:207-221.

9. Koonin EV, Dolja VV, & Morris TJ (1993) Evolution and taxonomy of positive-strand RNA viruses: implications of comparative analysis of amino acid sequences. *Critical Reviews in Biochemistry and Molecular Biology* 28(5):375-430.

10. Beijerinck M (1898) Concerning a contagium viwm fluidum as cause of the spot disease of tobacco leaves.

11. Dawson WO & Hilf ME (1992) Host-range determinants of plant viruses. *Annual review of plant biology* 43(1):527-555.

12. Culver J, Lindbeck A, & Dawson W (1991) Virus-host interactions: Induction of chlorotic and necrotic responses in plants by tobamoviruses. *Annual review of phytopathology* 29(1):193-217.

13. Goelet P*, et al.* (1982) Nucleotide sequence of tobacco mosaic virus RNA. *Proceedings of the National Academy of Sciences* 79(19):5818-5822.

14. Dawson WO, Beck DL, Knorr DA, & Grantham GL (1986) cDNA cloning of the complete genome of tobacco mosaic virus and production of infectious transcripts. *Proceedings of the National Academy of Sciences* 83(6):1832-1836.

15. Sachse C*, et al.* (2007) High-resolution electron microscopy of helical specimens: a fresh look at tobacco mosaic virus. *Journal of molecular biology* 371(3):812-835.

16. Esau K & Cronshaw J (1967) Relation of tobacco mosaic virus to the host cells. *The Journal of cell biology* 33(3):665-678.

17. Young ND & Zaitlin M (1986) An analysis of tobacco mosaic virus replicative structures synthesized in vitro. *Plant molecular biology* 6(6):455-465.

18. Osman T & Buck K (1996) Complete replication in vitro of tobacco mosaic virus RNA by a template-dependent, membrane-bound RNA polymerase. *Journal of virology* 70(9):6227-6234.

19. Buck KW (1999) Replication of tobacco mosaic virus RNA. *Philosophical Transactions of the Royal Society B: Biological Sciences* 354(1383):613-627.

20. Liu C & Nelson RS (2013) The cell biology of Tobacco mosaic virus replication and movement. *Frontiers in plant science* 4:12.

21. Zimmern D (1975) The 5′ end group of tobacco mosaic virus RNA is m7G5′ ppp5′ Gp. *Nucleic acids research* 2(7):1189-1202.

22. PleiJ CW, Abrahams JP, Belkum Av, Rietveld K, & Bosch L (1986) The spatial folding of the 3'noncoding region of aminoacylatable plant viral RNAs. *UCLA symposia on molecular and cellular biology (USA)*.

23. Rietveld K, Linschooten K, Pleij CW, & Bosch L (1984) The three-dimensional folding of the tRNA-like structure of tobacco mosaic virus RNA. A new building principle applied twice. *The EMBO journal* 3(11):2613.

24. Takamatsu N*, et al.* (1991) Deletion analysis of the 5'untranslated leader sequence of tobacco mosaic virus RNA. *Journal of virology* 65(3):1619-1622.

25. Takamatsu N, Watanabe Y, Meshi T, & Okada Y (1990) Mutational analysis of the pseudoknot region in the 3'noncoding region of tobacco mosaic virus RNA. *Journal of virology* 64(8):3686-3693.

26. Gallie DR, Sleat DE, Watts JW, Turner PC, & Wilson TMA (1987) The 5'-leader sequence of tobacco mosaic virus RNA enhances the expression of foreign gene transcripts in vitro and in vivo. *Nucleic Acids Research* 15(8):3257-3273.

27. Tanguay RL & Gallie DR (1996) Isolation and characterization of the 102-kilodalton RNA-binding protein that binds to the 5′ and 3′ translational enhancers of tobacco mosaic virus RNA. *Journal of Biological Chemistry* 271(24):14316-14322.

28. Gallie DR (2002) The 5′-leader of tobacco mosaic virus promotes translation through enhanced recruitment of eIF4F. *Nucleic acids research* 30(15):3401-3411.

29. Felden B, Florentz C, Giegé R, & Westhof E (1996) A central pseudoknotted three-way junction imposes tRNA-like mimicry and the orientation of three 5'upstream pseudoknots in the 3'terminus of tobacco mosaic virus RNA. *RNA* 2(3):201.

30. Zeenko VV*, et al.* (2002) Eukaryotic elongation factor 1A interacts with the upstream pseudoknot domain in the 3′ untranslated region of tobacco mosaic virus RNA. *Journal of virology* 76(11):5678-5691.

31. Chandrika R, Rabindran S, Lewandowski DJ, Manjunath KL, & Dawson WO (2000) Full-length tobacco mosaic virus RNAs and defective RNAs have different 3′ replication signals. *Virology* 273(1):198-209.

32. Osman T, Hemenway C, & Buck K (2000) Role of the 3′ tRNA-like structure in tobacco mosaic virus minus-strand RNA synthesis by the viral RNA-dependent RNA polymerase in vitro. *Journal of virology* 74(24):11671-11680.

33. Pelham HR (1978) Leaky UAG termination codon in tobacco mosaic virus RNA.

34. Padgett HS & Beachy RN (1993) Analysis of a tobacco mosaic virus strain capable of overcoming N gene-mediated resistance. *The Plant Cell* 5(5):577-586.

35. Hirashima K & Watanabe Y (2003) RNA helicase domain of tobamovirus replicase executes cell-to-cell movement possibly through collaboration with its nonconserved region. *Journal of virology* 77(22):12357-12362.

36. Goregaoker SP & Culver JN (2003) Oligomerization and activity of the helicase domain of the tobacco mosaic virus 126-and 183-kilodalton replicase proteins. *Journal of virology* 77(6):3549-3556.

37. Bao Y, Carter SA, & Nelson RS (1996) The 126-and 183-kilodalton proteins of tobacco mosaic virus, and not their common nucleotide sequence, control mosaic symptom formation in tobacco. *Journal of virology* 70(9):6378-6383.

38. Lewandowski DJ & Dawson WO (2000) Functions of the 126-and 183-kDa proteins of tobacco mosaic virus. *Virology* 271(1):90-98.

39. Watanabe T*, et al.* (1999) Isolation from tobacco mosaic virus-infected tobacco of a solubilized template-specific RNA-dependent RNA polymerase containing a 126K/183K protein heterodimer. *Journal of virology* 73(4):2633-2640.

40. Ishikawa M, Meshi T, Motoyoshi F, Takamalsu N, & Okada Y (1986) In vitro mutagenesis of the putative replicase genes of tobacco mosaic virus. *Nucleic acids research* 14(21):8291-8305.

41. Osman T & Buck K (2003) Identification of a region of the tobacco mosaic virus 126-and 183-kilodalton replication proteins which binds specifically to the viral 3′-terminal tRNA-like structure. *Journal of virology* 77(16):8669-8675.

42. Hirashima K & Watanabe Y (2001) Tobamovirus replicase coding region is involved in cell-to-cell movement. *Journal of virology* 75(18):8831-8836.

43. Kawakami S, Watanabe Y, & Beachy RN (2004) Tobacco mosaic virus infection spreads cell to cell as intact replication complexes. *Proceedings of the National Academy of Sciences of the United States of America* 101(16):6291-6296.

44. Guenoune-Gelbart D, Elbaum M, Sagi G, Levy A, & Epel BL (2008) Tobacco mosaic virus (TMV) replicase and movement protein function synergistically in facilitating TMV spread by lateral diffusion in the plasmodesmal desmotubule of Nicotiana benthamiana. *Molecular plant-microbe interactions* 21(3):335-345.

45. Wu X & Shaw JG (1997) Evidence That a Viral Replicase Protein Is Involved in the Disassembly of Tobacco Mosaic Virus Particlesin Vivo. *Virology* 239(2):426-434.

46. Ding XS*, et al.* (2004) The Tobacco mosaic virus 126-kDa protein associated with virus replication and movement suppresses RNA silencing. *Molecular plant-microbe interactions* 17(6):583-592.

47. Deom CM, Oliver MJ, & Beachy RN (1987) The 30-kilodalton gene product of tobacco mosaic virus potentiates virus movement. *Science* 237(4813):389-394.

48. Atkins D*, et al.* (1991) The tobacco mosaic virus 30K movement protein in transgenic tobacco plants is localized to plasmodesmata. *The Journal of general virology* 72:209-211.

49. Ding B*, et al.* (1992) Secondary plasmodesmata are specific sites of localization of the tobacco mosaic virus movement protein in transgenic tobacco plants. *The Plant Cell* 4(8):915-928.

50. Wolf S, Lucas WJ, Deom CM, & Beachy RN (1989) Movement protein of tobacco mosaic virus modifies plasmodesmatal size exclusion limit. *Science* 246(4928):377-379.

51. Tomenius K, Clapham D, & Meshi T (1987) Localization by immunogold cytochemistry of the virus-coded 30K protein in plasmodesmata of leaves infected with tobacco mosaic virus. *Virology* 160(2):363-371.

52. Waigmann E, Lucas WJ, Citovsky V, & Zambryski P (1994) Direct functional assay for tobacco mosaic virus cell-to-cell movement protein and identification of a domain involved in increasing plasmodesmal permeability. *Proceedings of the National Academy of Sciences* 91(4):1433-1437.

53. Oparka K, Prior D, Cruz SS, Padgett H, & Beachy R (1997) Gating of epidermal plasmodesmata is restricted to the leading edge of expanding infection sites of tobacco mosaic virus (TMV). *The Plant Journal* 12(4):781-789.

54. Citovsky V, Knorr D, Schuster G, & Zambryski P (1990) The P30 movement protein of tobacco mosaic virus is a single-strand nucleic acid binding protein. *Cell* 60(4):637-647.

55. Citovsky V, Wong ML, Shaw AL, Prasad B, & Zambryski P (1992) Visualization and characterization of tobacco mosaic virus movement protein binding to single-stranded nucleic acids. *The Plant Cell* 4(4):397-411.

56. Meshi T*, et al.* (1987) Function of the 30 kd protein of tobacco mosaic virus: involvement in cell-to-cell movement and dispensability for replication. *The EMBO journal* 6(9):2557.

57. Holt CA & Beachy RN (1991) In vivo complementation of infectious transcripts from mutant tobacco mosaic virus cDNAs in transgenic plants. *Virology* 181(1):109-117.

58. Cooper B & Dodds JA (1995) Differences in the subcellular localization of tobacco mosaic virus and cucumber mosaic virus movement proteins in infected and transgenic plants. *Journal of general virology* 76(12):3217-3221.

59. Cooper B, Schmitz I, Rao A, Beachy RN, & Dodds JA (1996) Cell-to-cell transport of movement-defective cucumber mosaic and tobacco mosaic viruses in transgenic plants expressing heterologous movement protein genes. *Virology* 216(1):208-213.

60. Atabekov J*, et al.* (1999) Identification and study of tobacco mosaic virus movement function by complementation tests. *Philosophical Transactions of the Royal Society B: Biological Sciences* 354(1383):629-635.

61. Vogler H*, et al.* (2008) Tobacco mosaic virus movement protein enhances the spread of RNA silencing. *PLoS Pathog* 4(4):e1000038.

62. Asurmendi S, Berg R, Koo J, & Beachy R (2004) Coat protein regulates formation of replication complexes during tobacco mosaic virus infection. *Proceedings of the National Academy of Sciences of the United States of America* 101(5):1415-1420.

63. Heinlein M*, et al.* (1998) Changing patterns of localization of the tobacco mosaic virus movement protein and replicase to the endoplasmic reticulum and microtubules during infection. *The Plant Cell* 10(7):1107-1120.

64. McLean BG, Zupan J, & Zambryski PC (1995) Tobacco mosaic virus movement protein associates with the cytoskeleton in tobacco cells. *The Plant Cell* 7(12):2101-2114.

65. Su S*, et al.* (2010) Cucumber mosaic virus movement protein severs actin filaments to increase the plasmodesmal size exclusion limit in tobacco. *The Plant Cell* 22(4):1373-1387.

66. Hofmann C, Niehl A, Sambade A, Steinmetz A, & Heinlein M (2009) Inhibition of Tobacco mosaic virus movement by expression of an actin-binding protein. *Plant physiology* 149(4):1810-1823.

67. Heinlein M, Epel BL, Padgett HS, & Beachy RN (1995) Interaction of tobamovirus movement proteins with the plant cytoskeleton. *Science* 270(5244):1983-1985.

68. Padgett HS*, et al.* (1996) Distribution of tobamovirus movement protein in infected cells and implications for cell-to-cell spread of infection. *The Plant Journal* 10(6):1079-1088.

69. Boyko V, Ferralli J, & Heinlein M (2000) Cell-to-cell movement of TMV RNA is temperature-dependent and corresponds to the association of movement protein with microtubules. *The Plant Journal* 22(4):315-325.

70. Kragler F, Curin M, Trutnyeva K, Gansch A, & Waigmann E (2003) MPB2C, a microtubule-associated plant protein binds to and interferes with cell-to-cell transport of tobacco mosaic virus movement protein. *Plant Physiology* 132(4):1870-1883.

71. Ashby J*, et al.* (2006) Tobacco mosaic virus movement protein functions as a structural microtubule-associated protein. *Journal of virology* 80(17):8329-8344.

72. Ferralli J, Ashby J, Fasler M, Boyko V, & Heinlein M (2006) Disruption of microtubule organization and centrosome function by expression of Tobacco mosaic virus movement protein. *Journal of virology* 80(12):5807-5821.

73. Brandner K*, et al.* (2008) Tobacco mosaic virus movement protein interacts with green fluorescent protein-tagged microtubule end-binding protein 1. *Plant physiology* 147(2):611-623.

74. Sambade A*, et al.* (2008) Transport of TMV movement protein particles associated with the targeting of RNA to plasmodesmata. *Traffic* 9(12):2073-2088.

75. Citovsky V, McLean BG, Zupan JR, & Zambryski P (1993) Phosphorylation of tobacco mosaic virus cell-to-cell movement protein by a developmentally regulated plant cell wall-associated protein kinase. *Genes & development* 7(5):904-910.

76. Haley A, Hunter T, Kiberstis P, & Zimmern D (1995) Multiple serine phosphorylation sites on the 30 kDa TMV cell-to-cell movement protein synthesized in tobacco protoplasts. *The Plant Journal* 8(5):715-724.

77. Kawakami S*, et al.* (1999) Phosphorylation and/or presence of serine 37 in the movement protein of tomato mosaic tobamovirus is essential for intracellular localization and stability in vivo. *Journal of virology* 73(8):6831-6840.

78. Waigmann E, Chen MH, Bachmaier R, Ghoshroy S, & Citovsky V (2000) Regulation of plasmodesmal transport by phosphorylation of tobacco mosaic virus cell-to-cell movement protein. *The EMBO journal* 19(18):4875-4884.

79. Lee J-Y*, et al.* (2005) Plasmodesmal-associated protein kinase in tobacco and Arabidopsis recognizes a subset of non-cell-autonomous proteins. *The Plant Cell* 17(10):2817-2831.

80. Beachy RN & Heinlein M (2000) Role of P30 in replication and spread of TMV. *Traffic* 1(7):540-544.

81. Fujiki M, Kawakami S, Kim RW, & Beachy RN (2006) Domains of tobacco mosaic virus movement protein essential for its membrane association. *Journal of general virology* 87(9):2699-2707.

82. Ni P & Kao CC (2013) Non-encapsidation activities of the capsid proteins of positive-strand RNA viruses. *Virology* 446(1):123-132.

83. Callaway A, Giesman-Cookmeyer D, Gillock E, Sit T, & Lommel S (2001) The multifunctional capsid proteins of plant RNA viruses. *Annual review of phytopathology* 39(1):419-460.

84. Culver JN (2002) Tobacco mosaic virus assembly and disassembly: determinants in pathogenicity and resistance. *Annual review of phytopathology* 40(1):287-308.

85. Durham A, Finch J, & Klug A (1971) States of aggregation of tobacco mosaic virus protein. *Nature* 229(2):37-42.

86. Schuster TM*, et al.* (1980) Studies on the mechanism of assembly of tobacco mosaic virus. *Biophysical journal* 32(1):313.

87. Butler P (1999) Self–assembly of tobacco mosaic virus: the role of an intermediate aggregate in generating both specificity and speed. *Philosophical Transactions of the Royal Society B: Biological Sciences* 354(1383):537-550.

88. Raghavendra K, Kelly JA, Khairallah L, & Schuster TM (1988) Structure and function of disk aggregates of the coat protein of tobacco mosaic virus. *Biochemistry* 27(20):7583-7588.

89. Bloomer A, Champness J, Bricogne G, Staden R, & Klug A (1978) Protein disk of tobacco mosaic virus at 2.8 Å resolution showing the interactions within and between subunits.

90. Namba K, Pattanayek R, & Stubbs G (1989) Visualization of protein-nucleic acid interactions in a virus: Refined structure of intact tobacco mosaic virus at 2.9 Å resolution by X-ray fiber diffraction. *Journal of molecular biology* 208(2):307-325.

91. Wilson TMA (1984) Cotranslational disassembly of tobacco mosaic virus in vitro. *Virology* 137(2):255-265.

92. Shaw J, Plaskitt K, & Wilson T (1986) Evidence that tobacco mosaic virus particles disassemble contranslationally in vivo. *Virology* 148(2):326-336.

93. Hilf ME & Dawson WO (1993) The Tobamovirus Capsid Protein Functions as a Host-Specific Determinant of Long-Distance Movement. *Virology* 193(1):106-114.

94. Siddiqui S, Sarmiento C, Valkonen S, Truve E, & Lehto K (2007) Suppression of infectious TMV genomes expressed in young transgenic tobacco plants. *Molecular Plant-Microbe Interactions* 20(12):1489-1494.

95. Dawson WO, Bubrick P, & Grantham GL (1988) Modifications of the Tobacco Mosaic-Virus Coat Protein Gene Affecting Replication, Movement, and Symptomatology. *Phytopathology* 78(6):783-789.

96. Saito T, Yamanaka K, & Okada Y (1990) Long-distance movement and viral assembly of tobacco mosaic virus mutants. *Virology* 176(2):329-336.

97. Simón-Buela L & García-Arenal F (1999) Virus particles of cucumber green mottle mosaic tobamovirus move systemically in the phloem of infected cucumber plants. *Molecular plant-microbe interactions* 12(2):112-118.

98. Reinero A & Beachy RN (1989) Reduced photosystem II activity and accumulation of viral coat protein in chloroplasts of leaves infected with tobacco mosaic virus. *Plant Physiology* 89(1):111-116.

99. Abel PP*, et al.* (1986) Delay of disease development in transgenic plants that express the tobacco mosaic virus coat protein gene. *Science* 232(4751):738-743.

100. Nelson RS, Abel PP, & Beachy RN (1987) Lesions and virus accumulation in inoculated transgenic tobacco plants expressing the coat protein gene of tobacco mosaic virus. *Virology* 158(1):126-132.

101. Beachy RN (1999) Coat–protein–mediated resistance to tobacco mosaic virus: discovery mechanisms and exploitation. *Philosophical Transactions of the Royal Society B: Biological Sciences* 354(1383):659-664.

102. Powell P, Stark D, Sanders P, & Beachy R (1989) Protection against tobacco mosaic virus in transgenic plants that express tobacco mosaic virus antisense RNA. *Proceedings of the National Academy of Sciences* 86(18):6949-6952.

103. Bazzini A, Asurmendi S, Hopp H, & Beachy R (2006) Tobacco mosaic virus (TMV) and potato virus X (PVX) coat proteins confer heterologous interference to PVX and TMV infection, respectively. *Journal of general virology* 87(4):1005-1012.

104. Saito T*, et al.* (1989) Mutational analysis of the coat protein gene of tobacco mosaic virus in relation to hypersensitive response in tobacco plants with the N′ gene. *Virology* 173(1):11-20.

105. Culver JN & Dawson WO (1989) Tobacco Mosaic-Virus Coat Protein - an Elicitor of the Hypersensitive Reaction but Not Required for the Development of Mosaic Symptoms in Nicotiana-Sylvestris. *Virology* 173(2):755-758.

106. Rodriguez MC, Conti G, Zavallo D, Manacorda CA, & Asurmendi S (2014) TMV-Cg Coat Protein stabilizes DELLA proteins and in turn negatively modulates salicylic acid-mediated defense pathway during Arabidopsis thaliana viral infection. *BMC plant biology* 14(1):210.

107. Sulzinski MA, Gabard KA, Palukaitis P, & Zaitlin M (1985) Replication of tobacco mosaic virus VIII. Characterization of a third subgenomic TMV RNA. *Virology* 145(1):132-140.

108. Palukaitis P, García-Arenal F, Sulzinski MA, & Zaitlin M (1983) Replication of tobacco mosaic virus VII. Further characterization of single-and double-stranded virus-related RNAs from TMV-infected plants. *Virology* 131(2):533-545.

109. Zelcer A, Weaber KF, Balázs E, & Zaitlin M (1981) The detection and characterization of viral-related double-stranded RNAs in tobacco mosaic virus-infected plants. *Virology* 113(2):417-427.

110. Golemboski DB, Lomonossoff GP, & Zaitlin M (1990) Plants transformed with a tobacco mosaic virus nonstructural gene sequence are resistant to the virus. *Proceedings of the National Academy of Sciences* 87(16):6311-6315.

111. Morozov SY*, et al.* (1993) A novel open reading frame in tobacco mosaic virus genome coding for a putative small, positively charged protein. *Biochimie* 75(8):659-665.

112. Canto T, MacFarlane SA, & Palukaitis P (2004) ORF6 of Tobacco mosaic virus is a determinant of viral pathogenicity in Nicotiana benthamiana. *Journal of general virology* 85(10):3123-3133.

113. Fedorkin O*, et al.* (1995) A protein product of the tobamovirus open translation frame forms a stable complex with translation elongation factor eef-1alpha. *Doklady Akademii nauk/[Rossiĭskaia akademii nauk]* 343(5):703.

114. Gushchin VA*, et al.* (2013) Dynamic localization of two tobamovirus ORF6 proteins involves distinct organellar compartments. *Journal of General Virology* 94(Pt 1):230-240.

115. Palukaitis P & Zaitlin M (1986) Tobacco mosaic virus infectivity and replication. *The plant viruses*, (Springer), pp 105-131.

116. Shaw JG (1999) Tobacco mosaic virus and the study of early events in virus infections. *Philosophical Transactions of the Royal Society B: Biological Sciences* 354(1383):603-611.

117. Caspar D (1963) Assembly and stability of the Tobacco mosaic virus particle. *Advances in protein chemistry* 18:37.

118. Mundry KW*, et al.* (1991) Complete uncoating of the 5′ leader sequence of tobacco mosaic virus RNA occurs rapidly and is required to initiate cotranslational virus disassembly in vitro. *J. Gen. Virol* 72(Pt 4):769-777.

119. Wu X & Shaw J (1996) Bidirectional uncoating of the genomic RNA of a helical virus. *Proceedings of the National Academy of Sciences* 93(7):2981-2984.

120. Ishikawa M & Okada Y (2004) Replication of tobamovirus RNA. *Proceedings of the Japan Academy, Series B* 80(5):215-224.

121. Ishibashi K, Nishikiori M, & Ishikawa M (2010) Interactions between tobamovirus replication proteins and cellular factors: their impacts on virus multiplication. *Molecular plant-microbe interactions* 23(11):1413-1419.

122. Ishikawa M, Meshi T, Ohno T, & Okada Y (1991) Specific cessation of minus-strand RNA accumulation at an early stage of tobacco mosaic virus infection. *Journal of virology* 65(2):861-868.

123. Kielland-Brandt M (1974) Studies on the biosynthesis of tobacco mosaic virus: VII. Radioactivity of plus and minus strands in different forms of viral RNA after labelling of infected tobacco leaves. *Journal of molecular biology* 87(3):489-503.

124. Jackson A, Mitchell D, & Siegel A (1971) Replication of tobacco mosaic virus: I. Isolation and characterization of double-stranded forms of ribonucleic acid. *Virology* 45(1):182-191.

125. Nilsson-Tillgren T (1970) Studies on the biosynthesis of TMV. III. Isolation and characterization of the replicative form and the replicative intermediate RNA. *Molecular and General Genetics* 109(3):246-256.

126. Grdzelishvili VZ, Chapman SN, Dawson WO, & Lewandowski DJ (2000) Mapping of the Tobacco mosaic virus movement protein and coat protein subgenomic RNA promoters in vivo. *Virology* 275(1):177-192.

127. Lehto K, Blibrick P, & Dawson WO (1990) Time course of TMV 30K protein accumulation in intact leaves. *Virology* 174(1):290-293.

128. Hagiwara Y*, et al.* (2003) Subcellular localization of host and viral proteins associated with tobamovirus RNA replication. *The EMBO journal* 22(2):344-353.

129. Más P & Beachy RN (1999) Replication of tobacco mosaic virus on endoplasmic reticulum and role of the cytoskeleton and virus movement protein in intracellular distribution of viral RNA. *The Journal of cell biology* 147(5):945-958.

130. Reichel C & Beachy RN (1998) Tobacco mosaic virus infection induces severe morphological changes of the endoplasmic reticulum. *Proceedings of the National Academy of Sciences* 95(19):11169-11174.

131. Nishikiori M*, et al.* (2006) Membrane-bound tomato mosaic virus replication proteins participate in RNA synthesis and are associated with host proteins in a pattern distinct from those that are not membrane bound. *Journal of virology* 80(17):8459-8468.

132. Das P & Hari V (1992) Intracellular distribution of the 126K/183K and capsid proteins in cells infected by some tobamoviruses. *The Journal of general virology* 73:3039-3043.

133. Liu J-Z, Blancaflor EB, & Nelson RS (2005) The tobacco mosaic virus 126-kilodalton protein, a constituent of the virus replication complex, alone or

within the complex aligns with and traffics along microfilaments. *Plant Physiology* 138(4):1853-1865.

134. Harries PA, Palanichelvam K, Yu W, Schoelz JE, & Nelson RS (2009) The cauliflower mosaic virus protein P6 forms motile inclusions that traffic along actin microfilaments and stabilize microtubules. *Plant physiology* 149(2):1005-1016.

135. Liu J*, et al.* (2006) The structure of the Tobacco mosaic virus replication complex is modulated by the 126-kDa protein and complex and protein traffic along microfilaments. *Biology of Plant–Microbe Interactions* 5:410-415.

136. Bhat S*, et al.* (2013) Influence of host chloroplast proteins on Tobacco mosaic virus accumulation and intercellular movement. *Plant physiology* 161(1):134-147.

137. Ishikawa M, Naito S, & Ohno T (1993) Effects of the tom1 mutation of Arabidopsis thaliana on the multiplication of tobacco mosaic virus RNA in protoplasts. *Journal of virology* 67(9):5328-5338.

138. Yamanaka T*, et al.* (2000) TOM1, an Arabidopsis gene required for efficient multiplication of a tobamovirus, encodes a putative transmembrane protein. *Proceedings of the National Academy of Sciences* 97(18):10107-10112.

139. Yamanaka T*, et al.* (2002) Complete inhibition of tobamovirus multiplication by simultaneous mutations in two homologous host genes. *Journal of virology* 76(5):2491-2497.

140. Ouko MO*, et al.* (2010) Tobacco mutants with reduced microtubule dynamics are less susceptible to TMV. *The Plant Journal* 62(5):829-839.

141. Gillespie T*, et al.* (2002) Functional analysis of a DNA-shuffled movement protein reveals that microtubules are dispensable for the cell-to-cell movement of Tobacco mosaic virus. *The Plant Cell* 14(6):1207-1222.

142. Boyko V, Hu Q, Seemanpillai M, Ashby J, & Heinlein M (2007) Validation of microtubule-associated Tobacco mosaic virus RNA movement and involvement of microtubule-aligned particle trafficking. *The Plant Journal* 51(4):589-603.

143. Tilsner J*, et al.* (2013) Replication and trafficking of a plant virus are coupled at the entrances of plasmodesmata. *The Journal of cell biology* 201(7):981-995.

144. Burch-Smith TM, Stonebloom S, Xu M, & Zambryski PC (2011) Plasmodesmata during development: re-examination of the importance of primary, secondary, and branched plasmodesmata structure versus function. *Protoplasma* 248(1):61-74.

145. Sevilem I, Yadav SR, & Helariutta Y (2015) Plasmodesmata: Channels for Intercellular Signaling During Plant Growth and Development. *Plasmodesmata*, (Springer), pp 3-24.

146. Stadler R*, et al.* (2005) Expression of GFP-fusions in Arabidopsis companion cells reveals non-specific protein trafficking into sieve elements and identifies a novel post-phloem domain in roots. *Plant J* 41(2):319-331.

147. Lucas WJ (2006) Plant viral movement proteins: agents for cell-to-cell trafficking of viral genomes. *Virology* 344(1):169-184.

148. Lucas WJ*, et al.* (1995) Selective trafficking of KNOTTED1 homeodomain protein and its mRNA through plasmodesmata. *Science* 270(5244):1980-1983.

149. Kurata T, Okada K, & Wada T (2005) Intercellular movement of transcription factors. *Current opinion in plant biology* 8(6):600-605.

150. Gallagher KL & Benfey PN (2009) Both the conserved GRAS domain and nuclear localization are required for SHORT-ROOT movement. *The Plant Journal* 57(5):785-797.

151. Laporte C*, et al.* (2003) Involvement of the secretory pathway and the cytoskeleton in intracellular targeting and tubule assembly of Grapevine fanleaf virus movement protein in tobacco BY-2 cells. *The Plant Cell* 15(9):2058-2075.

152. Pouwels J*, et al.* (2003) Identification of distinct steps during tubule formation by the movement protein of Cowpea mosaic virus. *Journal of general virology* 84(12):3485-3494.

153. Pouwels J*, et al.* (2004) Studies on the origin and structure of tubules made by the movement protein of Cowpea mosaic virus. *Journal of general virology* 85(12):3787-3796.

154. Radford J, Vesk M, & Overall R (1998) Callose deposition at plasmodesmata. *Protoplasma* 201(1-2):30-37.

155. Radford J & White R (2001) Effects of tissue-preparation-induced callose synthesis on est plasmodesma size exclusion limits. *Protoplasma* 216(1):47-55.

156. Sivaguru M*, et al.* (2000) Aluminum-induced 1→ 3-β-d-glucan inhibits cell-to-cell trafficking of molecules through plasmodesmata. A new mechanism of aluminum toxicity in plants. *Plant physiology* 124(3):991-1006.

157. Zavaliev R, Ueki S, Epel BL, & Citovsky V (2011) Biology of callose (β-1, 3-glucan) turnover at plasmodesmata. *Protoplasma* 248(1):117-130.

158. Bucher GL*, et al.* (2001) Local expression of enzymatically active class I β-1, 3-glucanase enhances symptoms of TMV infection in tobacco. *The Plant Journal* 28(3):361-369.

159. Chen X-Y & Kim J-Y (2009) Callose synthesis in higher plants. *Plant signaling & behavior* 4(6):489-492.

160. Simpson C, Thomas C, Findlay K, Bayer E, & Maule AJ (2009) An Arabidopsis GPI-anchor plasmodesmal neck protein with callose binding activity and potential to regulate cell-to-cell trafficking. *Plant Cell* 21(2):581-594.

161. Sagi G, Katz A, Guenoune-Gelbart D, & Epel BL (2005) Class 1 reversibly glycosylated polypeptides are plasmodesmal-associated proteins delivered to plasmodesmata via the Golgi apparatus. *The Plant Cell* 17(6):1788-1800.

162. Zavaliev R, Sagi G, Gera A, & Epel BL (2010) The constitutive expression of Arabidopsis plasmodesmal-associated class 1 reversibly glycosylated polypeptide impairs plant development and virus spread. *Journal of experimental botany* 61(1):131-142.

163. Thomas CL, Bayer EM, Ritzenthaler C, Fernandez-Calvino L, & Maule AJ (2008) Specific targeting of a plasmodesmal protein affecting cell-to-cell communication. *PLoS Biol* 6(1):e7.

164. Lee J-Y*, et al.* (2011) A plasmodesmata-localized protein mediates crosstalk between cell-to-cell communication and innate immunity in Arabidopsis. *The Plant Cell* 23(9):3353-3373.

165. Amari K*, et al.* (2010) A family of plasmodesmal proteins with receptor-like properties for plant viral movement proteins. *PLoS Pathog* 6(9):e1001119-e1001119.

166. Ding X, Shintaku MH, Carter SA, & Nelson RS (1996) Invasion of minor veins of tobacco leaves inoculated with tobacco mosaic virus mutants defective in phloem-dependent movement. *Proc Natl Acad Sci U S A* 93(20):11155-11160.

167. Overall RL & Blackman LM (1996) A model of the macromolecular structure of plasmodesmata. *Trends in plant science* 1(9):307-311.

168. White R, Badelt K, Overall R, & Vesk M (1994) Actin associated with plasmodesmata. *Protoplasma* 180(3-4):169-184.

169. Hipper C, Brault V, Ziegler-Graff V, & Revers F (2013) Viral and cellular factors involved in phloem transport of plant viruses. *Frontiers in plant science* 4.

170. Roberts AG*, et al.* (1997) Phloem unloading in sink leaves of Nicotiana benthamiana: comparison of a fluorescent solute with a fluorescent virus. *The Plant Cell* 9(8):1381-1396.

171. Oparka K, Duckett C, Prior D, & Fisher D (1994) Real-time imaging of phloem unloading in the root tip of Arabidopsis. *The Plant Journal* 6(5):759-766.

172. Cheng NH, Su CL, Carter SA, & Nelson RS (2000) Vascular invasion routes and systemic accumulation patterns of tobacco mosaic virus in Nicotiana benthamiana. *The Plant Journal* 23(3):349-362.

173. Savenkov EI, Germundsson A, Zamyatnin AA, Sandgren M, & Valkonen JP (2003) Potato mop-top virus: the coat protein-encoding RNA and the gene for cysteine-rich protein are dispensable for systemic virus movement in Nicotiana benthamiana. *Journal of General Virology* 84(4):1001-1005.

174. Torrance L*, et al.* (2009) Unusual long-distance movement strategies of Potato mop-top virus RNAs in Nicotiana benthamiana. *Molecular plant-microbe interactions* 22(4):381-390.

175. Torrance L*, et al.* (2011) Unusual features of pomoviral RNA movement. *Frontiers in microbiology* 2.

176. Pooma W, Gillette WK, Jeffrey JL, & Petty IT (1996) Host and viral factors determine the dispensability of coat protein for bipartite geminivirus systemic movement. *Virology* 218(1):264-268.

177. Sasaki T, Chino M, Hayashi H, & Fujiwara T (1998) Detection of several mRNA species in rice phloem sap. *Plant and Cell Physiology* 39(8):895-897.

178. Doering-Saad C, Newbury HJ, Bale JS, & Pritchard J (2002) Use of aphid stylectomy and RT-PCR for the detection of transporter mRNAs in sieve elements. *Journal of Experimental Botany* 53(369):631-637.

179. Lin M-K, Lee Y-J, Lough TJ, Phinney BS, & Lucas WJ (2009) Analysis of the pumpkin phloem proteome provides insights into angiosperm sieve tube function. *Molecular & Cellular Proteomics* 8(2):343-356.

180. Batailler B*, et al.* (2012) Soluble and filamentous proteins in Arabidopsis sieve elements. *Plant, cell & environment* 35(7):1258-1273.

181. Blackman LM, Boevink P, Santa Cruz S, Palukaitis P, & Oparka KJ (1998) The movement protein of cucumber mosaic virus traffics into sieve elements in minor veins of Nicotiana clevelandii. *The Plant Cell* 10(4):525-537.

182. Díaz-Avalos R & Caspar DL (1998) Structure of the stacked disk aggregate of tobacco mosaic virus protein. *Biophysical journal* 74(1):595-603.

183. Butler PJG (1984) The current picture of the structure and assembly of tobacco mosaic virus. *Journal of general virology* 65(2):253-279.

184. Klug A (1999) The tobacco mosaic virus particle: structure and assembly. *Philosophical Transactions of the Royal Society B: Biological Sciences* 354(1383):531-535.

185. Leisner SM & Turgeon R (1993) Movement of virus and photoassimilate in the phloem: a comparative analysis. *Bioessays* 15(11):741-748.

186. Bennett C (1940) Relation of food translocation to movement of virus of Tobacco mosaic. *Journal of Agricultural Research* 60(6):361-390.

187. Deom CM, Quan S, & He XZ (1997) Replicase proteins as determinants of phloem-dependent long-distance movement of tobamoviruses in tobacco. *Protoplasma* 199(1-2):1-8.

188. Goregaoker SP, Lewandowski DJ, & Culver JN (2001) Identification and functional analysis of an interaction between domains of the 126/183-kDa replicase-associated proteins of Tobacco mosaic virus. *Virology* 282(2):320-328.

189. Wang L-Y*, et al.* (2012) Multiple domains of the Tobacco mosaic virus p126 protein can independently suppress local and systemic RNA silencing. *Molecular Plant-Microbe Interactions* 25(5):648-657.

190. Knapp E, Danyluk GM, Achor D, & Lewandowski DJ (2005) A bipartite Tobacco mosaic virus-defective RNA (dRNA) system to study the role of the N-terminal methyl transferase domain in cell-to-cell movement of dRNAs. *Virology* 341(1):47-58.

191. Knapp E, Achor D, & Lewandowski DJ (2007) Tobacco mosaic virus defective RNAs expressing C-terminal methyltransferase domain sequences are severely impaired in long-distance movement in Nicotiana benthamiana. *Virology* 367(1):82-91.

192. Lartey RT, Ghoshroy S, & Citovsky V (1998) Identification of an Arabidopsis thaliana mutation (vsm1) that restricts systemic movement of tobamoviruses. *Molecular plant-microbe interactions* 11(7):706-709.

193. Pereda S, Ehrenfeld N, Medina C, Delgado J, & Arce-Johnson P (2000) Comparative analysis of TMV-Cg and TMV-U1 detection methods in infected Arabidopsis thaliana. *Journal of virological methods* 90(2):135-142.

194. Serrano C*, et al.* (2008) Genetic and histological studies on the delayed systemic movement of Tobacco Mosaic Virus in Arabidopsis thaliana. *BMC genetics* 9(1):59.

195. Chen MH & Citovsky V (2003) Systemic movement of a tobamovirus requires host cell pectin methylesterase. *The Plant Journal* 35(3):386-392.

196. Li Y, Wu M, Song H, Hu X, & Qiu B (2005) Identification of a tobacco protein interacting with tomato mosaic virus coat protein and facilitating long-distance movement of virus. *Archives of virology* 150(10):1993-2008.

197. Ueki S & Citovsky V (2002) The systemic movement of a tobamovirus is inhibited by a cadmium-ion-induced glycine-rich protein. *Nature cell biology* 4(7):478-486.

198. Levy A, Zheng JY, & Lazarowitz SG (2013) The tobamovirus Turnip Vein Clearing Virus 30-kilodalton movement protein localizes to novel nuclear filaments to enhance virus infection. *Journal of virology* 87(11):6428-6440.

199. Sasaki N*, et al.* (2009) Over-expression of putative transcriptional coactivator KELP interferes with Tomato mosaic virus cell-to-cell movement. *Molecular plant pathology* 10(2):161-173.

200. Chen L, Zhang L, Li D, Wang F, & Yu D (2013) WRKY8 transcription factor functions in the TMV-cg defense response by mediating both abscisic acid and ethylene signaling in Arabidopsis. *Proc Natl Acad Sci U S A* 110(21):E1963-1971.

201. Solovyev AG & Savenkov EI (2014) Factors involved in the systemic transport of plant RNA viruses: the emerging role of the nucleus. *J Exp Bot* 65(7):1689-1697.

202. Santner A & Estelle M (2009) Recent advances and emerging trends in plant hormone signalling. *Nature* 459(7250):1071-1078.

203. Derksen H, Rampitsch C, & Daayf F (2013) Signaling cross-talk in plant disease resistance. *Plant science* 207:79-87.

204. Robert-Seilaniantz A, Grant M, & Jones JD (2011) Hormone crosstalk in plant disease and defense: more than just jasmonate-salicylate antagonism. *Annual review of phytopathology* 49:317-343.

205. Durbak A, Yao H, & McSteen P (2012) Hormone signaling in plant development. *Current opinion in plant biology* 15(1):92-96.

206. Depuydt S & Hardtke CS (2011) Hormone signalling crosstalk in plant growth regulation. *Current Biology* 21(9):R365-R373.

207. Song S, Qi T, Wasternack C, & Xie D (2014) Jasmonate signaling and crosstalk with gibberellin and ethylene. *Current opinion in plant biology* 21:112-119.

208. Collum TD & Culver JN (2016) The impact of phytohormones on virus infection and disease. (Current Opinion in Virology), pp 25-31.

209. Whenham R (1982) Plant growth regulators and virus infection: a critical review. *Plant Growth Regulation* 1(1):37-59.

210. Jameson PE & Clarke SF (2002) Hormone-virus interactions in plants. *Critical reviews in plant sciences* 21(3):205-228.

211. Kazan K & Manners JM (2009) Linking development to defense: auxin in plant–pathogen interactions. *Trends in plant science* 14(7):373-382.

212. Padmanabhan MS, Shiferaw H, & Culver JN (2006) The Tobacco mosaic virus replicase protein disrupts the localization and function of interacting Aux/IAA proteins. *Mol Plant Microbe In* 19(8):864-873.

213. Padmanabhan MS, Gorepoker SP, Golem S, Shiferaw H, & Culver JN (2005) Interaction of the tobacco mosaic virus replicase protein with the Aux/IAA protein PAPI/IAA26 is associated with disease development. *J Virol* 79(4):2549-2558.

214. Wang R & Estelle M (2014) Diversity and specificity: auxin perception and signaling through the TIR1/AFB pathway. *Current opinion in plant biology* 21:51-58.

215. Kasschau KD*, et al.* (2003) P1/HC-Pro, a viral suppressor of RNA silencing, interferes with Arabidopsis development and miRNA function. *Developmental cell* 4(2):205-217.

216. Zhu S*, et al.* (2005) The rice dwarf virus P2 protein interacts with ent-kaurene oxidases in vivo, leading to reduced biosynthesis of gibberellins and rice dwarf symptoms. *Plant Physiol* 139(4):1935-1945.

217. Helliwell CA, Poole A, Peacock WJ, & Dennis ES (1999) Arabidopsis ent-kaurene oxidase catalyzes three steps of gibberellin biosynthesis. *Plant Physiology* 119(2):507-510.

218. Itoh H*, et al.* (2004) A rice semi-dwarf gene, Tan-Ginbozu (D35), encodes the gibberellin biosynthesis enzyme, ent-kaurene oxidase. *Plant molecular biology* 54(4):533-547.

219. Love AJ*, et al.* (2007) Cauliflower mosaic virus protein P6 is a suppressor of RNA silencing. *Journal of General Virology* 88(12):3439-3444.

220. Cecchini E, Gong Z, Geri C, Covey SN, & Milner JJ (1997) Transgenic Arabidopsis lines expressing gene VI from cauliflower mosaic virus variants exhibit a range of symptom-like phenotypes and accumulate inclusion bodies. *Molecular plant-microbe interactions* 10(9):1094-1101.

221. Geri C, Cecchini E, Giannakou ME, Covey SN, & Milner JJ (1999) Altered patterns of gene expression in Arabidopsis elicited by cauliflower mosaic virus (CaMV) infection and by a CaMV gene VI transgene. *Molecular plant-microbe interactions* 12(5):377-384.

222. Geri C*, et al.* (2004) Arabidopsis mutants that suppress the phenotype induced by transgene-mediated expression of cauliflower mosaic virus (CaMV) gene VI are less susceptible to CaMV-infection and show reduced ethylene sensitivity. *Plant molecular biology* 56(1):111-124.

223. Jones JD & Dangl JL (2006) The plant immune system. *Nature* 444(7117):323-329.

224. Vlot AC, Dempsey DMA, & Klessig DF (2009) Salicylic acid, a multifaceted hormone to combat disease. *Annual review of phytopathology* 47:177-206.

225. Fu ZQ & Dong X (2013) Systemic acquired resistance: turning local infection into global defense. *Annual review of plant biology* 64:839-863.

226. Boatwright JL & Pajerowska-Mukhtar K (2013) Salicylic acid: an old hormone up to new tricks. *Molecular plant pathology* 14(6):623-634.

227. Torres MA, Jones JD, & Dangl JL (2006) Reactive oxygen species signaling in response to pathogens. *Plant physiology* 141(2):373-378.

228. Wang X*, et al.* (2013) Salicylic acid regulates plasmodesmata closure during innate immune responses in Arabidopsis. *The Plant Cell* 25(6):2315-2329.

229. Glazebrook J (2005) Contrasting mechanisms of defense against biotrophic and necrotrophic pathogens. *Annu. Rev. Phytopathol.* 43:205-227.

230. Howe GA & Jander G (2008) Plant immunity to insect herbivores. *Annu. Rev. Plant Biol.* 59:41-66.

231. Pieterse CM, Van der Does D, Zamioudis C, Leon-Reyes A, & Van Wees SC (2012) Hormonal modulation of plant immunity. *Annual review of cell and developmental biology* 28:489-521.

232. Mur LA, Kenton P, Atzorn R, Miersch O, & Wasternack C (2006) The outcomes of concentration-specific interactions between salicylate and jasmonate signaling include synergy, antagonism, and oxidative stress leading to cell death. *Plant Physiology* 140(1):249-262.

233. Schenk PM*, et al.* (2000) Coordinated plant defense responses in Arabidopsis revealed by microarray analysis. *Proceedings of the National Academy of Sciences* 97(21):11655-11660.

234. Van Wees SC, De Swart EA, Van Pelt JA, Van Loon LC, & Pieterse CM (2000) Enhancement of induced disease resistance by simultaneous activation of salicylate-and jasmonate-dependent defense pathways in Arabidopsis thaliana. *Proceedings of the National Academy of Sciences* 97(15):8711-8716.

235. Delaney TP, Uknes S, Vernooij B, & Friedrich L (1994) A central role of salicylic acid in plant disease resistance. *Science* 266(5188):1247.

236. Takahashi H*, et al.* (2004) Antagonistic interactions between the SA and JA signaling pathways in Arabidopsis modulate expression of defense genes and gene-for-gene resistance to cucumber mosaic virus. *Plant and cell physiology* 45(6):803-809.

237. Sánchez G*, et al.* (2010) Salicylic acid is involved in the Nb-mediated defense responses to Potato virus X in Solanum tuberosum. *Molecular plant-microbe interactions* 23(4):394-405.

238. Jovel J, Walker M, & Sanfaçon H (2011) Salicylic acid-dependent restriction of Tomato ringspot virus spread in tobacco is accompanied by a hypersensitive response, local RNA silencing, and moderate systemic resistance. *Molecular Plant-Microbe Interactions* 24(6):706-718.

239. Naylor M, Murphy AM, Berry JO, & Carr JP (1998) Salicylic acid can induce resistance to plant virus movement. *Molecular Plant-Microbe Interactions* 11(9):860-868.

240. Baebler Š*, et al.* (2014) Salicylic acid is an indispensable component of the Ny-1 resistance-gene-mediated response against Potato virus Y infection in potato. *Journal of experimental botany* 65(4):1095-1109.

241. Wang X, Goregaoker SP, & Culver JN (2009) Interaction of the Tobacco mosaic virus replicase protein with a NAC domain transcription factor is associated with the suppression of systemic host defenses. *Journal of virology* 83(19):9720-9730.

242. Laird J*, et al.* (2013) Identification of the domains of cauliflower mosaic virus protein P6 responsible for suppression of RNA silencing and salicylic acid signalling. *Journal of General Virology* 94(Pt 12):2777-2789.

243. Love AJ*, et al.* (2012) Cauliflower mosaic virus protein P6 inhibits signaling responses to salicylic acid and regulates innate immunity.

244. Navarro L*, et al.* (2008) DELLAs control plant immune responses by modulating the balance of jasmonic acid and salicylic acid signaling. *Current Biology* 18(9):650-655.

245. Oka K, Kobayashi M, Mitsuhara I, & Seo S (2013) Jasmonic acid plays a negative role in resistance to Tobacco mosaic virus in tobacco. *Plant and Cell Physiology*:pct137.

246. Dhondt S, Geoffroy P, Stelmach BA, Legrand M, & Heitz T (2000) Soluble phospholipase A2 activity is induced before oxylipin accumulation in tobacco mosaic virus-infected tobacco leaves and is contributed by patatin-like enzymes. *The Plant Journal* 23(4):431-440.

247. Kovač M*, et al.* (2009) Multiple hormone analysis indicates involvement of jasmonate signalling in the early defence of potato to potato virus YNTN. *Biologia Plantarum* 53(1):195-199.

248. Lozano-Durán R*, et al.* (2011) Geminiviruses subvert ubiquitination by altering CSN-mediated derubylation of SCF E3 ligase complexes and inhibit jasmonate signaling in Arabidopsis thaliana. *The Plant Cell* 23(3):1014-1032.

249. ZHANG JF*, et al.* (2008) The disturbance of small RNA pathways enhanced abscisic acid response and multiple stress responses in Arabidopsis. *Plant, cell & environment* 31(4):562-574.

250. Earley K, Smith M, Weber R, Gregory B, & Poethig R (2010) Research An endogenous F-box protein regulates ARGONAUTE1 in Arabidopsis thaliana.

251. Li W*, et al.* (2012) Transcriptional regulation of Arabidopsis MIR168a and argonaute1 homeostasis in abscisic acid and abiotic stress responses. *Plant physiology* 158(3):1279-1292.

252. Yu D, Fan B, MacFarlane SA, & Chen Z (2003) Analysis of the involvement of an inducible Arabidopsis RNA-dependent RNA polymerase in antiviral defense. *Molecular Plant-Microbe Interactions* 16(3):206-216.

253. Alamillo JM, Saénz P, & García JA (2006) Salicylic acid-mediated and RNA-silencing defense mechanisms cooperate in the restriction of systemic spread of plum pox virus in tobacco. *The Plant Journal* 48(2):217-227.

254. Campos L*, et al.* (2014) Salicylic acid and gentisic acid induce RNA silencing-related genes and plant resistance to RNA pathogens. *Plant Physiology and Biochemistry* 77:35-43.

255. Hunter LJ*, et al.* (2013) Regulation of RNA-dependent RNA polymerase 1 and isochorismate synthase gene expression in Arabidopsis.

256. Tian M*, et al.* (2015) Salicylic acid inhibits the replication of Tomato Bushy Stunt Virus by directly targeting a host component in the replication complex. *Molecular Plant-Microbe Interactions* 28(4):379-386.

257. Huang T-S & Nagy PD (2011) Direct inhibition of tombusvirus plus-strand RNA synthesis by a dominant negative mutant of a host metabolic enzyme, glyceraldehyde-3-phosphate dehydrogenase, in yeast and plants. *Journal of virology* 85(17):9090-9102.

258. Wang RY-L & Nagy PD (2008) Tomato bushy stunt virus co-opts the RNA-binding function of a host metabolic enzyme for viral genomic RNA synthesis. *Cell host & microbe* 3(3):178-187.

259. Alazem M, Lin K-Y, & Lin N-S (2014) The abscisic acid pathway has multifaceted effects on the accumulation of Bamboo mosaic virus. *Molecular Plant-Microbe Interactions* 27(2):177-189.

260. Rezzonico E, Flury N, Meins F, & Beffa R (1998) Transcriptional down-regulation by abscisic acid of pathogenesis-related β-1, 3-glucanase genes in tobacco cell cultures. *Plant Physiology* 117(2):585-592.

261. Flors V, Ton J, Jakab G, & Mauch-Mani B (2005) Abscisic acid and callose: team players in defence against pathogens? *Journal of Phytopathology* 153(7-8):377-383.

262. Beffa RS, Hofer R-M, Thomas M, & Meins F (1996) Decreased Susceptibility to Viral Disease of [beta]-1, 3-Glucanase-Deficient Plants Generated by Antisense Transformation. *Plant Cell* 8(6):1001-1011.

263. Iglesias VA & Meins F (2000) Movement of plant viruses is delayed in a β-1, 3-glucanase-deficient mutant showing a reduced plasmodesmatal size exclusion limit and enhanced callose deposition. *The Plant Journal* 21(2):157-166.

264. Whenham R (1989) Abscisic acid metabolism in tomato plants infected with tobacco mosaic virus: relationships with growth, symptoms and the Tm-1 gene for TMV resistance. *Physiological and molecular plant pathology* 34(3):215-226.

265. Iriti M & Faoro F (2008) Abscisic acid is involved in chitosan-induced resistance to tobacco necrosis virus (TNV). *Plant Physiology and Biochemistry* 46(12):1106-1111.

266. Abe H*, et al.* (2012) Antagonistic plant defense system regulated by phytohormones assists interactions among vector insect, thrips and a tospovirus. *Plant and Cell Physiology* 53(1):204-212.

267. Lewsey MG*, et al.* (2010) Disruption of two defensive signaling pathways by a viral RNA silencing suppressor. *Molecular plant-microbe interactions* 23(7):835-845.

268. Ziebell H*, et al.* (2011) Cucumber mosaic virus and its 2b RNA silencing suppressor modify plant-aphid interactions in tobacco. *Scientific reports* 1.

269. Casteel C*, et al.* (2015) Disruption of ethylene responses by Turnip mosaic virus mediates suppression of plant defense against the aphid vector, Myzus persicae. *Plant physiology*:pp. 00332.02015.

270. Love AJ*, et al.* (2012) Cauliflower mosaic virus protein P6 inhibits signaling responses to salicylic acid and regulates innate immunity. *PLoS One* 7(10):e47535.

271. Ziebell H*, et al.* (2011) Cucumber mosaic virus and its 2b RNA silencing suppressor modify plant-aphid interactions in tobacco. *Scientific reports* 1:187.

272. Teale WD, Paponov IA, & Palme K (2006) Auxin in action: signalling, transport and the control of plant growth and development. *Nature Reviews Molecular Cell Biology* 7(11):847-859.

273. Scarpella E, Marcos D, Friml J, & Berleth T (2006) Control of leaf vascular patterning by polar auxin transport. *Genes & development* 20(8):1015-1027.

274. Tian Q & Reed J (1999) Control of auxin-regulated root development by the Arabidopsis thaliana SHY2/IAA3 gene. *Development* 126(4):711-721.

275. De Smet I*, et al.* (2010) Bimodular auxin response controls organogenesis in Arabidopsis. *Proceedings of the National Academy of Sciences* 107(6):2705-2710.

276. Vernoux T*, et al.* (2011) The auxin signalling network translates dynamic input into robust patterning at the shoot apex. *Molecular systems biology* 7(1):508.

277. Bartel B (1997) Auxin biosynthesis. *Annual review of plant biology* 48(1):51-66.

278. Korasick DA, Enders TA, & Strader LC (2013) Auxin biosynthesis and storage forms. *Journal of experimental botany* 64(9):2541-2555.

279. Tivendale ND, Ross JJ, & Cohen JD (2014) The shifting paradigms of auxin biosynthesis. *Trends in plant science* 19(1):44-51.

280. Zhao Y (2012) Auxin biosynthesis: a simple two-step pathway converts tryptophan to indole-3-acetic acid in plants. *Molecular plant* 5(2):334-338.

281. Stepanova AN*, et al.* (2008) TAA1-mediated auxin biosynthesis is essential for hormone crosstalk and plant development. *Cell* 133(1):177-191.

282. Tao Y, *et al.* (2008) Rapid synthesis of auxin via a new tryptophan-dependent pathway is required for shade avoidance in plants. *Cell* 133(1):164-176.

283. Mashiguchi K, *et al.* (2011) The main auxin biosynthesis pathway in Arabidopsis. *Proceedings of the National Academy of Sciences* 108(45):18512-18517.

284. Dai X, *et al.* (2013) The biochemical mechanism of auxin biosynthesis by an Arabidopsis YUCCA flavin-containing monooxygenase. *Journal of Biological Chemistry* 288(3):1448-1457.

285. Strader LC & Bartel B (2011) Transport and metabolism of the endogenous auxin precursor indole-3-butyric acid. *Molecular plant* 4(3):477-486.

286. Tognetti VB, *et al.* (2010) Perturbation of indole-3-butyric acid homeostasis by the UDP-glucosyltransferase UGT74E2 modulates Arabidopsis architecture and water stress tolerance. *The Plant Cell* 22(8):2660-2679.

287. Rampey RA, *et al.* (2004) A family of auxin-conjugate hydrolases that contributes to free indole-3-acetic acid levels during Arabidopsis germination. *Plant Physiology* 135(2):978-988.

288. Strader LC, Culler AH, Cohen JD, & Bartel B (2010) Conversion of endogenous indole-3-butyric acid to indole-3-acetic acid drives cell expansion in Arabidopsis seedlings. *Plant physiology* 153(4):1577-1586.

289. Yang Y, *et al.* (2008) Inactive methyl indole-3-acetic acid ester can be hydrolyzed and activated by several esterases belonging to the AtMES esterase family of Arabidopsis. *Plant physiology* 147(3):1034-1045.

290. Qin G, *et al.* (2005) An indole-3-acetic acid carboxyl methyltransferase regulates Arabidopsis leaf development. *The Plant Cell* 17(10):2693-2704.

291. Spiess GM, *et al.* (2014) Auxin Input Pathway Disruptions Are Mitigated by Changes in Auxin Biosynthetic Gene Expression in Arabidopsis. *Plant physiology* 165(3):1092-1104.

292. Zažímalová E, Murphy AS, Yang H, Hoyerová K, & Hošek P (2010) Auxin transporters—why so many? *Cold Spring Harbor perspectives in biology* 2(3):a001552.

293. Peer WA, Blakeslee JJ, Yang H, & Murphy AS (2011) Seven things we think we know about auxin transport. *Molecular Plant* 4(3):487-504.

294. Enders TA & Strader LC (2015) Auxin activity: Past, present, and future. *American journal of botany* 102(2):180-196.

295. Rakusová H*, et al.* (2011) Polarization of PIN3-dependent auxin transport for hypocotyl gravitropic response in Arabidopsis thaliana. *The Plant Journal* 67(5):817-826.

296. Band LR*, et al.* (2012) Root gravitropism is regulated by a transient lateral auxin gradient controlled by a tipping-point mechanism. *Proceedings of the National Academy of Sciences* 109(12):4668-4673.

297. Ding Z*, et al.* (2011) Light-mediated polarization of the PIN3 auxin transporter for the phototropic response in Arabidopsis. *Nature cell biology* 13(4):447-452.

298. Adamowski M & Friml J (2015) PIN-dependent auxin transport: action, regulation, and evolution. *The Plant Cell* 27(1):20-32.

299. Růžička K*, et al.* (2009) Cytokinin regulates root meristem activity via modulation of the polar auxin transport. *Proceedings of the National Academy of Sciences* 106(11):4284-4289.

300. Marhavý P*, et al.* (2011) Cytokinin modulates endocytic trafficking of PIN1 auxin efflux carrier to control plant organogenesis. *Developmental cell* 21(4):796-804.

301. Willige BC, Isono E, Richter R, Zourelidou M, & Schwechheimer C (2011) Gibberellin regulates PIN-FORMED abundance and is required for auxin transport–dependent growth and development in Arabidopsis thaliana. *The Plant Cell* 23(6):2184-2195.

302. Löfke C*, et al.* (2013) Asymmetric gibberellin signaling regulates vacuolar trafficking of PIN auxin transporters during root gravitropism. *Proceedings of the National Academy of Sciences* 110(9):3627-3632.

303. Du Y*, et al.* (2013) Salicylic acid interferes with clathrin-mediated endocytic protein trafficking. *Proceedings of the National Academy of Sciences* 110(19):7946-7951.

304. Shinohara N, Taylor C, & Leyser O (2013) Strigolactone can promote or inhibit shoot branching by triggering rapid depletion of the auxin efflux protein PIN1 from the plasma membrane. *PLoS Biol* 11(1):e1001474.

305. Paciorek T*, et al.* (2005) Auxin inhibits endocytosis and promotes its own efflux from cells. *Nature* 435(7046):1251-1256.

306. Baster P*, et al.* (2013) SCFTIR1/AFB-auxin signalling regulates PIN vacuolar trafficking and auxin fluxes during root gravitropism. *The EMBO journal* 32(2):260-274.

307. Mravec J*, et al.* (2009) Subcellular homeostasis of phytohormone auxin is mediated by the ER-localized PIN5 transporter. *Nature* 459(7250):1136-1140.

308. Bosco CD*, et al.* (2012) The endoplasmic reticulum localized PIN8 is a pollen-specific auxin carrier involved in intracellular auxin homeostasis. *The Plant Journal* 71(5):860-870.

309. Ding Z*, et al.* (2012) ER-localized auxin transporter PIN8 regulates auxin homeostasis and male gametophyte development in Arabidopsis. *Nature communications* 3:941.

310. Sawchuk MG, Edgar A, & Scarpella E (2013) Patterning of leaf vein networks by convergent auxin transport pathways. *PLoS Genet* 9(2):e1003294.

311. Barbez E*, et al.* (2012) A novel putative auxin carrier family regulates intracellular auxin homeostasis in plants. *Nature* 485(7396):119-122.

312. Remy E & Duque P (2014) Beyond cellular detoxification: a plethora of physiological roles for MDR transporter homologs in plants. *Frontiers in physiology* 5.

313. Yang H & Murphy AS (2009) Functional expression and characterization of Arabidopsis ABCB, AUX 1 and PIN auxin transporters in Schizosaccharomyces pombe. *The Plant Journal* 59(1):179-191.

314. Kamimoto Y*, et al.* (2012) Arabidopsis ABCB21 is a facultative auxin importer/exporter regulated by cytoplasmic auxin concentration. *Plant and Cell Physiology* 53(12):2090-2100.

315. Kubeš M*, et al.* (2012) The Arabidopsis concentration-dependent influx/efflux transporter ABCB4 regulates cellular auxin levels in the root epidermis. *The Plant Journal* 69(4):640-654.

316. Szemenyei H, Hannon M, & Long JA (2008) TOPLESS mediates auxin-dependent transcriptional repression during Arabidopsis embryogenesis. *Science* 319(5868):1384-1386.

317. Long JA, Ohno C, Smith ZR, & Meyerowitz EM (2006) TOPLESS regulates apical embryonic fate in Arabidopsis. *Science* 312(5779):1520-1523.

318. Krogan NT, Hogan K, & Long JA (2012) APETALA2 negatively regulates multiple floral organ identity genes in Arabidopsis by recruiting the co-repressor TOPLESS and the histone deacetylase HDA19. *Development* 139(22):4180-4190.

319. Wang L, Kim J, & Somers DE (2013) Transcriptional corepressor TOPLESS complexes with pseudoresponse regulator proteins and histone deacetylases to

regulate circadian transcription. *Proceedings of the National Academy of Sciences* 110(2):761-766.

320. Dharmasiri N, Dharmasiri S, & Estelle M (2005) The F-box protein TIR1 is an auxin receptor. *Nature* 435(7041):441-445.

321. Kepinski S & Leyser O (2005) The Arabidopsis F-box protein TIR1 is an auxin receptor. *Nature* 435(7041):446-451.

322. Chapman EJ & Estelle M (2009) Mechanism of auxin-regulated gene expression in plants. *Annu Rev Genet* 43:265-285.

323. Tan X*, et al.* (2007) Mechanism of auxin perception by the TIR1 ubiquitin ligase. *Nature* 446(7136):640-645.

324. Liscum E & Reed J (2002) Genetics of Aux/IAA and ARF action in plant growth and development. *Auxin Molecular Biology*, (Springer), pp 387-400.

325. Walsh TA*, et al.* (2006) Mutations in an auxin receptor homolog AFB5 and in SGT1b confer resistance to synthetic picolinate auxins and not to 2, 4-dichlorophenoxyacetic acid or indole-3-acetic acid in Arabidopsis. *Plant Physiology* 142(2):542-552.

326. Abel S, Oeller PW, & Theologis A (1994) Early auxin-induced genes encode short-lived nuclear proteins. *Proceedings of the National Academy of Sciences* 91(1):326-330.

327. Rouse D, Mackay P, Stirnberg P, Estelle M, & Leyser O (1998) Changes in auxin response from mutations in an AUX/IAA gene. *Science* 279(5355):1371-1373.

328. Nagpal P*, et al.* (2000) AXR2 encodes a member of the Aux/IAA protein family. *Plant physiology* 123(2):563-574.

329. Worley CK*, et al.* (2000) Degradation of Aux/IAA proteins is essential for normal auxin signalling. *The Plant Journal* 21(6):553-562.

330. Dreher KA, Brown J, Saw RE, & Callis J (2006) The Arabidopsis Aux/IAA protein family has diversified in degradation and auxin responsiveness. *The Plant Cell* 18(3):699-714.

331. Villalobos LIAC*, et al.* (2012) A combinatorial TIR1/AFB–Aux/IAA co-receptor system for differential sensing of auxin. *Nature chemical biology* 8(5):477-485.

332. Shimizu-Mitao Y & Kakimoto T (2014) Auxin Sensitivities of All Arabidopsis Aux/IAAs for Degradation in the Presence of Every TIR1/AFB. *Plant and Cell Physiology* 55(8):1450-1459.

333. Guilfoyle TJ & Hagen G (2007) Auxin response factors. *Current opinion in plant biology* 10(5):453-460.

334. Ulmasov T, Liu Z-B, Hagen G, & Guilfoyle TJ (1995) Composite structure of auxin response elements. *The Plant Cell* 7(10):1611-1623.

335. Ulmasov T, Murfett J, Hagen G, & Guilfoyle TJ (1997) Aux/IAA proteins repress expression of reporter genes containing natural and highly active synthetic auxin response elements. *The Plant Cell* 9(11):1963-1971.

336. Boer DR, *et al.* (2014) Structural basis for DNA binding specificity by the auxin-dependent ARF transcription factors. *Cell* 156(3):577-589.

337. Nanao MH, *et al.* (2014) Structural basis for oligomerization of auxin transcriptional regulators. *Nature communications* 5.

338. Korasick DA, *et al.* (2014) Molecular basis for AUXIN RESPONSE FACTOR protein interaction and the control of auxin response repression. *Proceedings of the National Academy of Sciences* 111(14):5427-5432.

339. Rademacher EH, *et al.* (2012) Different auxin response machineries control distinct cell fates in the early plant embryo. *Developmental cell* 22(1):211-222.

340. Guilfoyle TJ (2015) The PB1 domain in auxin response factor and Aux/IAA proteins: a versatile protein interaction module in the auxin response. *The Plant cell* 27(1):33-43.

341. Berleth T & Jurgens G (1993) The role of the monopteros gene in organising the basal body region of the Arabidopsis embryo. *Development* 118(2):575-587.

342. Przemeck GK, Mattsson J, Hardtke CS, Sung ZR, & Berleth T (1996) Studies on the role of the Arabidopsis gene MONOPTEROS in vascular development and plant cell axialization. *Planta* 200(2):229-237.

343. Sessions A, *et al.* (1997) ETTIN patterns the Arabidopsis floral meristem and reproductive organs. *Development* 124(22):4481-4491.

344. Hardtke CS & Berleth T (1998) The Arabidopsis gene MONOPTEROS encodes a transcription factor mediating embryo axis formation and vascular development. *The EMBO journal* 17(5):1405-1411.

345. Harper RM, *et al.* (2000) The NPH4 locus encodes the auxin response factor ARF7, a conditional regulator of differential growth in aerial Arabidopsis tissue. *The Plant Cell* 12(5):757-770.

346. Nemhauser JL, Feldman LJ, & Zambryski PC (2000) Auxin and ETTIN in Arabidopsis gynoecium morphogenesis. *Development* 127(18):3877-3888.

347. Li H, Johnson P, Stepanova A, Alonso JM, & Ecker JR (2004) Convergence of signaling pathways in the control of differential cell growth in Arabidopsis. *Developmental cell* 7(2):193-204.

348. Tian Ce*, et al.* (2004) Disruption and overexpression of auxin response factor 8 gene of Arabidopsis affect hypocotyl elongation and root growth habit, indicating its possible involvement in auxin homeostasis in light condition. *The Plant Journal* 40(3):333-343.

349. Reed JW (2001) Roles and activities of Aux/IAA proteins in Arabidopsis. *Trends Plant Sci* 6(9):420-425.

350. Tatematsu K*, et al.* (2004) MASSUGU2 encodes Aux/IAA19, an auxin-regulated protein that functions together with the transcriptional activator NPH4/ARF7 to regulate differential growth responses of hypocotyl and formation of lateral roots in Arabidopsis thaliana. *The Plant Cell* 16(2):379-393.

351. Yang X*, et al.* (2004) The IAA1 protein is encoded by AXR5 and is a substrate of SCFTIR1. *The Plant Journal* 40(5):772-782.

352. Hamann T, Mayer U, & Jurgens G (1999) The auxin-insensitive bodenlos mutation affects primary root formation and apical-basal patterning in the Arabidopsis embryo. *Development* 126(7):1387-1395.

353. Weijers D*, et al.* (2005) Developmental specificity of auxin response by pairs of ARF and Aux/IAA transcriptional regulators. *The EMBO journal* 24(10):1874-1885.

354. Guilfoyle TJ & Hagen G (2012) Getting a grasp on domain III/IV responsible for Auxin Response Factor–IAA protein interactions. *Plant science* 190:82-88.

355. Lamark T*, et al.* (2003) Interaction codes within the family of mammalian Phox and Bem1p domain-containing proteins. *Journal of Biological Chemistry* 278(36):34568-34581.

356. Rogg LE, Lasswell J, & Bartel B (2001) A gain-of-function mutation in IAA28 suppresses lateral root development. *The Plant Cell* 13(3):465-480.

357. Vieten A*, et al.* (2005) Functional redundancy of PIN proteins is accompanied by auxin-dependent cross-regulation of PIN expression. *Development* 132(20):4521-4531.

358. Sauer M, *et al.* (2006) Canalization of auxin flow by Aux/IAA-ARF-dependent feedback regulation of PIN polarity. *Genes & development* 20(20):2902-2911.

359. Ioio RD, *et al.* (2008) A genetic framework for the control of cell division and differentiation in the root meristem. *Science* 322(5906):1380-1384.

360. Wang D, Pajerowska-Mukhtar K, Culler AH, & Dong X (2007) Salicylic acid inhibits pathogen growth in plants through repression of the auxin signaling pathway. *Current Biology* 17(20):1784-1790.

361. Robert-Seilaniantz A, Navarro L, Bari R, & Jones JD (2007) Pathological hormone imbalances. *Current opinion in plant biology* 10(4):372-379.

362. Tiryaki I & Staswick PE (2002) An Arabidopsis mutant defective in jasmonate response is allelic to the auxin-signaling mutant axr1. *Plant Physiology* 130(2):887-894.

363. Nagpal P, *et al.* (2005) Auxin response factors ARF6 and ARF8 promote jasmonic acid production and flower maturation. *Development* 132(18):4107-4118.

364. Navarro L, *et al.* (2006) A plant miRNA contributes to antibacterial resistance by repressing auxin signaling. *Science* 312(5772):436-439.

365. Dardick CD, Golem S, & Culver JN (2000) Susceptibility and symptom development in Arabidopsis thaliana to Tobacco mosaic virus is influenced by virus cell-to-cell movement. *Molecular Plant-Microbe Interactions* 13(10):1139-1144.

366. Initiative AG (2000) Analysis of the genome sequence of the flowering plant Arabidopsis thaliana. *nature* 408(6814):796.

367. Lamesch P, *et al.* (2012) The Arabidopsis Information Resource (TAIR): improved gene annotation and new tools. *Nucleic acids research* 40(D1):D1202-D1210.

368. Heinlein M (2015) Plasmodesmata: channels for viruses on the move. *Methods in molecular biology* 1217:25-52.

369. Stadler R, *et al.* (2005) Expression of GFP-fusions in Arabidopsis companion cells reveals non-specific protein trafficking into sieve elements and identifies a novel post-phloem domain in roots. *The Plant journal : for cell and molecular biology* 41(2):319-331.

370. Ham BK & Lucas WJ (2014) The angiosperm phloem sieve tube system: a role in mediating traits important to modern agriculture. *J Exp Bot* 65(7):1799-1816.

371. Kehr J & Buhtz A (2008) Long distance transport and movement of RNA through the phloem. *J Exp Bot* 59(1):85-92.

372. Turgeon R & Wolf S (2009) Phloem transport: cellular pathways and molecular trafficking. *Annual review of plant biology* 60:207-221.

373. Fenczik CA, Padgett HS, Holt CA, Casper SJ, & Beachy RN (1995) Mutational Analysis of the Movement Protein of Odontoglossum Ringspot Virus to Identify a Host-Range Determinant. *Mol Plant Microbe In* 8(5):666-673.

374. Padmanabhan MS, Kramer SR, Wang X, & Culver JN (2008) Tobacco mosaic virus replicase-auxin/indole acetic acid protein interactions: Reprogramming the auxin response pathway to enhance virus infection. *J Virol* 82(5):2477-2485.

375. Calderon-Villalobos LI, Tan X, Zheng N, & Estelle M (2010) Auxin perception--structural insights. *Cold Spring Harb Perspect Biol* 2(7):a005546.

376. Salehin M, Bagchi R, & Estelle M (2015) SCFTIR1/AFB-based auxin perception: mechanism and role in plant growth and development. *Plant Cell* 27(1):9-19.

377. Reed JW (2001) Roles and activities of Aux/IAA proteins in Arabidopsis. *Trends in plant science* 6(9):420-425.

378. Piya S, Shrestha SK, Binder B, Stewart CN, Jr., & Hewezi T (2014) Protein-protein interaction and gene co-expression maps of ARFs and Aux/IAAs in Arabidopsis. *Front Plant Sci* 5:744.

379. Gray WM, Kepinski S, Rouse D, Leyser O, & Estelle M (2001) Auxin regulates SCF(TIR1)-dependent degradation of AUX/IAA proteins. *Nature* 414(6861):271-276.

380. Fleming AJ (2006) Plant signalling: the inexorable rise of auxin. *Trends Cell Biol* 16(8):397-402.

381. Hayashi K (2012) The interaction and integration of auxin signaling components. *Plant Cell Physiol* 53(6):965-975.

382. Knoblauch M & van Bel AJ (1998) Sieve tubes in action. *The Plant Cell* 10(1):35-50.

383. Hall GS & Little DP (2007) Relative quantitation of virus population size in mixed genotype infections using sequencing chromatograms. *J Virol Methods* 146(1-2):22-28.

384. Berardini TZ*, et al.* (2004) Functional annotation of the Arabidopsis genome using controlled vocabularies. *Plant physiology* 135(2):745-755.

385. Boyle EI*, et al.* (2004) GO:: TermFinder—open source software for accessing Gene Ontology information and finding significantly enriched Gene Ontology terms associated with a list of genes. *Bioinformatics* 20(18):3710-3715.

386. Robinson MD & Smyth GK (2008) Small-sample estimation of negative binomial dispersion, with applications to SAGE data. *Biostatistics* 9(2):321-332.

387. Mattsson J, Ckurshumova W, & Berleth T (2003) Auxin signaling in Arabidopsis leaf vascular development. *Plant Physiol* 131(3):1327-1339.

388. Mironova VV, Omelyanchuk NA, Wiebe DS, & Levitsky VG (2014) Computational analysis of auxin responsive elements in the Arabidopsis thaliana L. genome. *BMC genomics* 15(Suppl 12):S4.

389. Notaguchi M, Wolf S, & Lucas WJ (2012) Phloem-mobile Aux/IAA transcripts target to the root tip and modify root architecture. *Journal of integrative plant biology* 54(10):760-772.

390. Mustroph A*, et al.* (2009) Profiling translatomes of discrete cell populations resolves altered cellular priorities during hypoxia in Arabidopsis. *Proceedings of the National Academy of Sciences* 106(44):18843-18848.

391. Dorokhov YL*, et al.* (2012) Airborne signals from a wounded leaf facilitate viral spreading and induce antibacterial resistance in neighboring plants. *PLoS Pathog* 8(4):e1002640-e1002640.

392. Heinlein M (2002) The spread of tobacco mosaic virus infection: insights into the cellular mechanism of RNA transport. *Cellular and Molecular Life Sciences CMLS* 59(1):58-82.

393. Lucas WJ & Gilbertson RL (1994) Plasmodesmata in relation to viral movement within leaf tissues. *Annual review of phytopathology* 32(1):387-415.

394. Lionetti V, Raiola A, Cervone F, & Bellincampi D (2014) Transgenic expression of pectin methylesterase inhibitors limits tobamovirus spread in tobacco and Arabidopsis. *Mol Plant Pathol* 15(3):265-274.

395. White R (1979) Acetylsalicylic acid (aspirin) induces resistance to tobacco mosaic virus in tobacco. *Virology* 99(2):410-412.

396. Malamy J, Carr JP, Klessig DF, & Raskin I (1990) Salicylic acid: a likely endogenous signal in the resistance response of tobacco to viral infection. *Science* 250(4983):1002-1004.

397. Zhu F, *et al.* (2014) Salicylic acid and jasmonic acid are essential for systemic resistance against tobacco mosaic virus in Nicotiana benthamiana. *Molecular Plant-Microbe Interactions* 27(6):567-577.

398. Cui F, *et al.* (2013) The Pseudomonas syringae type III effector AvrRpt2 promotes pathogen virulence via stimulating Arabidopsis auxin/indole acetic acid protein turnover. *Plant physiology* 162(2):1018-1029.

399. Caarls L, Pieterse CM, & Van Wees SC (2015) How salicylic acid takes transcriptional control over jasmonic acid signaling. *Frontiers in plant science* 6.

400. Dong J, Chen C, & Chen Z (2003) Expression profiles of the Arabidopsis WRKY gene superfamily during plant defense response. *Plant molecular biology* 51(1):21-37.

401. Spoel SH, *et al.* (2009) Proteasome-mediated turnover of the transcription coactivator NPR1 plays dual roles in regulating plant immunity. *Cell* 137(5):860-872.

402. Gao Q-M, Venugopal S, Navarre D, & Kachroo A (2011) Low oleic acid-derived repression of jasmonic acid-inducible defense responses requires the WRKY50 and WRKY51 proteins. *Plant physiology* 155(1):464-476.

403. Ndamukong I, *et al.* (2007) SA-inducible Arabidopsis glutaredoxin interacts with TGA factors and suppresses JA-responsive PDF1. 2 transcription. *The Plant Journal* 50(1):128-139.

404. Chini A, *et al.* (2007) The JAZ family of repressors is the missing link in jasmonate signalling. *Nature* 448(7154):666-671.

405. Leon-Reyes A, *et al.* (2010) Salicylate-mediated suppression of jasmonate-responsive gene expression in Arabidopsis is targeted downstream of the jasmonate biosynthesis pathway. *Planta* 232(6):1423-1432.

406. Holsters M, *et al.* (1978) In vivo transfer of the Ti-plasmid of Agrobacterium tumefaciens to Escherichia coli. *Molecular and General Genetics MGG* 163(3):335-338.

407. Clough SJ & Bent AF (1998) Floral dip: a simplified method for Agrobacterium-mediated transformation ofArabidopsis thaliana. *The plant journal* 16(6):735-743.

408. Jefferson RA, Kavanagh TA, & Bevan MW (1987) GUS fusions: beta-glucuronidase as a sensitive and versatile gene fusion marker in higher plants. *The EMBO journal* 6(13):3901.

409. Holsters M*, et al.* (1978) Transfection and transformation of Agrobacterium tumefaciens. *Molecular and General Genetics MGG* 163(2):181-187.

410. Laemmli U (1970) Cleavage of structural proteins during the assembly of the head of bacteriophage T4 Nature 227: 680–685. *Find this article online*.

411. Zachgo S, Perbal MC, Saedler H, & Schwarz-Sommer Z (2000) In situ analysis of RNA and protein expression in whole mounts facilitates detection of floral gene expression dynamics. *The Plant Journal* 23(5):697-702.

412. Mortazavi A, Williams BA, McCue K, Schaeffer L, & Wold B (2008) Mapping and quantifying mammalian transcriptomes by RNA-Seq. *Nature methods* 5(7):621-628.

413. Yan T*, et al.* (2005) PatMatch: a program for finding patterns in peptide and nucleotide sequences. *Nucleic acids research* 33(suppl 2):W262-W266.

414. Schneider CA, Rasband WS, & Eliceiri KW (2012) NIH Image to ImageJ: 25 years of image analysis. *Nature methods* 9(7):671-675.

415. Raven JA (1984) Physiological correlates of the morphology of early vascular plants. *Botanical Journal of the Linnean Society* 88(1-2):105-126.

416. Kehr J & Buhtz A (2008) Long distance transport and movement of RNA through the phloem. *J Exp Bot* 59(1):85-92.

417. Turgeon R & Medville R (2004) Phloem loading. A reevaluation of the relationship between plasmodesmatal frequencies and loading strategies. *Plant Physiol* 136(3):3795-3803.

418. McGarry RC & Kragler F (2013) Phloem-mobile signals affecting flowers: applications for crop breeding. *Trends in plant science* 18(4):198-206.

419. Kim M, Canio W, Kessler S, & Sinha N (2001) Developmental changes due to long-distance movement of a homeobox fusion transcript in tomato. *Science* 293(5528):287-289.

420. Notaguchi M, Higashiyama T, & Suzuki T (2014) Identification of mRNAs That Move over Long Distances Using an RNA-Seq Analysis of Arabidopsis/Nicotiana benthamiana Heterografts. *Plant and Cell Physiology*:pcu210.

421. Thieme CJ*, et al.* (2015) Endogenous Arabidopsis messenger RNAs transported to distant tissues. *Nature Plants* 1(4).

422. Oparka KJ & Turgeon R (1999) Sieve elements and companion cells—traffic control centers of the phloem. *The Plant Cell* 11(4):739-750.

423. Santa Cruz S (1999) Perspective: phloem transport of viruses and macromolecules - what goes in must come out. *Trends Microbiol* 7(6):237-241.

424. Sjolund RD (1997) The phloem sieve element: a river runs through it. *The Plant Cell* 9(7):1137.

425. van Bel AJ (1996) Interaction between sieve element and companion cell and the consequences for photoassimilate distribution. Two structural hardware frames with associated physiological software packages in dicotyledons? *Journal of Experimental Botany* 47(Special Issue):1129-1140.

426. Ueki S & Citovsky V (2007) Spread throughout the plant: systemic transport of viruses. *Viral Transport in Plants*, (Springer), pp 85-118.

427. Gibbs A (1976) Viruses and plasmodesmata. *Intercellular communication in plants: studies on plasmodesmata*, (Springer), pp 149-164.

428. Creager AN, Scholthof K-BG, Citovsky V, & Scholthof HB (1999) Tobacco mosaic virus: pioneering research for a century. *The Plant Cell* 11(3):301-308.

429. Scholthof HB (2005) Plant virus transport: motions of functional equivalence. *Trends Plant Sci* 10(8):376-382.

430. Kay R, Chan A, Daly M, & McPherson J (1987) Duplication of CaMV 35S promoter sequences creates a strong enhancer for plant genes. *Science* 236(4806):1299-1302.

431. Takahashi H*, et al.* (2000) The roles of three functional sulphate transporters involved in uptake and translocation of sulphate in Arabidopsis thaliana. *The Plant Journal* 23(2):171-182.

432. Truernit E & Sauer N (1995) The promoter of the Arabidopsis thaliana SUC2 sucrose-H+ symporter gene directs expression of β-glucuronidase to the phloem: evidence for phloem loading and unloading by SUC2. *Planta* 196(3):564-570.

433. Zanetti ME, Chang F, Gong F, Galbraith DW, & Bailey-Serres J (2005) Immunopurification of polyribosomal complexes of Arabidopsis for global analysis of gene expression. *Plant Physiology* 138(2):624-635.

434. Baggerly KA, Deng L, Morris JS, & Aldaz CM (2003) Differential expression in SAGE: accounting for normal between-library variation. *Bioinformatics* 19(12):1477-1483.

435. Crevillén P*, et al.* (2005) Differential pattern of expression and sugar regulation of Arabidopsis thaliana ADP-glucose pyrophosphorylase-encoding genes. *Journal of Biological Chemistry* 280(9):8143-8149.

436. Singh KB, Foley RC, & Oñate-Sánchez L (2002) Transcription factors in plant defense and stress responses. *Current opinion in plant biology* 5(5):430-436.

437. Rushton PJ & Somssich IE (1998) Transcriptional control of plant genes responsive to pathogens. *Current opinion in plant biology* 1(4):311-315.

438. Stracke R, Werber M, & Weisshaar B (2001) The R2R3-MYB gene family in Arabidopsis thaliana. *Current opinion in plant biology* 4(5):447-456.

439. Eamens A, Wang M-B, Smith NA, & Waterhouse PM (2008) RNA silencing in plants: yesterday, today, and tomorrow. *Plant physiology* 147(2):456-468.

440. Zheng MS*, et al.* (2004) Up-regulation of Arabidopsis thaliana NHL10 in the hypersensitive response to Cucumber mosaic virus infection and in senescing leaves is controlled by signalling pathways that differ in salicylate involvement. *Planta* 218(5):740-750.

441. Ding S-W, Li H, Lu R, Li F, & Li W-X (2004) RNA silencing: a conserved antiviral immunity of plants and animals. *Virus research* 102(1):109-115.

442. Duan C-G, Wang C-H, & Guo H-S (2012) Application of RNA silencing to plant disease resistance. *Silence* 3(1):5.

443. Bouché N, Lauressergues D, Gasciolli V, & Vaucheret H (2006) An antagonistic function for Arabidopsis DCL2 in development and a new function for DCL4 in generating viral siRNAs. *The EMBO Journal* 25(14):3347-3356.

444. Baulcombe D (2004) RNA silencing in plants. *Nature* 431(7006):356-363.

445. Brosnan CA & Voinnet O (2011) Cell-to-cell and long-distance siRNA movement in plants: mechanisms and biological implications. *Current opinion in plant biology* 14(5):580-587.

446. Jiang Y, Liang G, Yang S, & Yu D (2014) Arabidopsis WRKY57 functions as a node of convergence for jasmonic acid–and auxin-mediated signaling in jasmonic acid–induced leaf senescence. *The Plant Cell* 26(1):230-245.

447. Olsen AN, Ernst HA, Leggio LL, & Skriver K (2005) NAC transcription factors: structurally distinct, functionally diverse. *Trends in plant science* 10(2):79-87.

448. Selth LA*, et al.* (2005) A NAC domain protein interacts with tomato leaf curl virus replication accessory protein and enhances viral replication. *The Plant Cell* 17(1):311-325.

449. Ren T, Qu F, & Morris TJ (2000) HRT gene function requires interaction between a NAC protein and viral capsid protein to confer resistance to turnip crinkle virus. *The Plant Cell* 12(10):1917-1925.

450. Korolev AV, Buschmann H, Doonan JH, & Lloyd CW (2007) AtMAP70-5, a divergent member of the MAP70 family of microtubule-associated proteins, is required for anisotropic cell growth in Arabidopsis. *Journal of cell science* 120(13):2241-2247.

451. Hajdukiewicz P, Svab Z, & Maliga P (1994) The small, versatilepPZP family ofAgrobacterium binary vectors for plant transformation. *Plant molecular biology* 25(6):989-994.

452. Knecht DA & Dimond RL (1984) Visualization of antigenic proteins on Western blots. *Analytical biochemistry* 136(1):180-184.

453. Yilmaz A*, et al.* (2011) AGRIS: the Arabidopsis gene regulatory information server, an update. *Nucleic acids research* 39(suppl 1):D1118-D1122.

454. De Schepper V, De Swaef T, Bauweraerts I, & Steppe K (2013) Phloem transport: a review of mechanisms and controls. *Journal of experimental botany* 64(16):4839-4850.

455. Mahajan SK, Chisholm ST, Whitham SA, & Carrington JC (1998) Identification and characterization of a locus (RTM1) that restricts long-distance movement of tobacco etch virus in Arabidopsis thaliana. *The Plant Journal* 14(2):177-186.

456. Decroocq V*, et al.* (2006) Multiple resistance traits control Plum pox virus infection in Arabidopsis thaliana. *Molecular plant-microbe interactions* 19(5):541-549.

457. Chisholm ST, Mahajan SK, Whitham SA, Yamamoto ML, & Carrington JC (2000) Cloning of the Arabidopsis RTM1 gene, which controls restriction of long-distance movement of tobacco etch virus. *Proceedings of the National Academy of Sciences* 97(1):489-494.

458. Whitham SA, Anderberg RJ, Chisholm ST, & Carrington JC (2000) Arabidopsis RTM2 gene is necessary for specific restriction of tobacco etch virus and encodes an unusual small heat shock–like protein. *The Plant Cell* 12(4):569-582.

459. Chisholm ST, Parra MA, Anderberg RJ, & Carrington JC (2001) Arabidopsis RTM1 and RTM2 genes function in phloem to restrict long-distance movement of tobacco etch virus. *Plant Physiology* 127(4):1667-1675.

460. Cosson P*, et al.* (2010) RTM3, which controls long-distance movement of potyviruses, is a member of a new plant gene family encoding a meprin and

TRAF homology domain-containing protein. *Plant physiology* 154(1):222-232.

461. Decroocq V*, et al.* (2009) The determinant of potyvirus ability to overcome the RTM resistance of Arabidopsis thaliana maps to the N-terminal region of the coat protein. *Molecular plant-microbe interactions* 22(10):1302-1311.

462. Bilgin DD, Liu Y, Schiff M, & Dinesh-Kumar S (2003) P58 IPK, a plant ortholog of double-stranded RNA-dependent protein kinase PKR inhibitor, functions in viral pathogenesis. *Developmental cell* 4(5):651-661.

463. Les Erickson F*, et al.* (1999) The helicase domain of the TMV replicase proteins induces the N-mediated defence response in tobacco. *The Plant Journal* 18(1):67-75.

464. Whalen MC (2005) Host defence in a developmental context. *Molecular plant pathology* 6(3):347-360.

465. Develey-Rivière MP & Galiana E (2007) Resistance to pathogens and host developmental stage: a multifaceted relationship within the plant kingdom. *New Phytologist* 175(3):405-416.

466. Carella P, Wilson DC, & Cameron RK (2014) Some things get better with age: differences in salicylic acid accumulation and defense signaling in young and mature Arabidopsis. *Frontiers in plant science* 5.

467. Kus JV, Zaton K, Sarkar R, & Cameron RK (2002) Age-related resistance in Arabidopsis is a developmentally regulated defense response to Pseudomonas syringae. *The Plant Cell* 14(2):479-490.

468. Carviel JL*, et al.* (2009) Forward and reverse genetics to identify genes involved in the age-related resistance response in Arabidopsis thaliana. *Molecular plant pathology* 10(5):621-634.

469. Carviel JL*, et al.* (2014) Investigation of intercellular salicylic acid accumulation during compatible and incompatible Arabidopsis-Pseudomonas syringae interactions using a fast neutron-generated mutant allele of EDS5 identified by genetic mapping and whole-genome sequencing. *PloS one* 9(3):e88608.

470. Cameron RK & Zaton K (2004) Intercellular salicylic acid accumulation is important for age-related resistance in Arabidopsis to Pseudomonas syringae. *Physiological and molecular plant pathology* 65(4):197-209.

471. Sunkar R & Zhu JK (2004) Novel and stress-regulated microRNAs and other small RNAs from Arabidopsis. *Plant Cell* 16(8):2001-2019.

472. Goodin MM, Zaitlin D, Naidu RA, & Lommel SA (2008) Nicotiana benthamiana: its history and future as a model for plant-pathogen interactions. *Molecular plant-microbe interactions* 21(8):1015-1026.

473. Bombarely A*, et al.* (2012) A draft genome sequence of Nicotiana benthamiana to enhance molecular plant-microbe biology research. *Molecular Plant-Microbe Interactions* 25(12):1523-1530.